

Multivalency, Cooperativity, Self-Assembly and Self-Sorting as Ordering Principles in Synthetic Supramolecular Architectures



Dissertation zur Erlangung des akademischen Grades des
Doktors der Naturwissenschaften (Dr. rer. nat.)

eingereicht im Fachbereich Biologie, Chemie, Pharmazie
der Freien Universität Berlin

vorgelegt von

Dipl.-Chem. Egor Vital'evic Dzyuba

aus Belojarski (Russische Föderation)

Oktober 2011

Die vorliegende Arbeit wurde unter Anleitung von Herrn Prof. Dr. C. A. Schalley am Institut für Chemie und Biochemie des Fachbereichs Biologie, Chemie, Pharmazie der Freien Universität Berlin in der Zeit von Juni 2008 bis Oktober 2011 angefertigt.

1. Gutachter: Prof. Dr. Christoph A. Schalley (Freie Universität Berlin)
 2. Gutachter: Prof. Stefan Hecht, PhD (Humboldt-Universität zu Berlin)
- Disputation am 05.12.2011

Erklärung

Hiermit versichere ich an Eides statt, dass diese Dissertation von mir persönlich, selbständig und ohne jede unerlaubte Hilfe angefertigt wurde. Aus fremden Quellen entnommene Gedanken und Daten sind als solche kenntlich gemacht. Die vorliegende Arbeit wurde an keiner anderen Hochschule als Dissertation eingereicht. Dies ist mein erster Promotionsversuch. Teile der Arbeit sind auszugsweise veröffentlicht worden; dies ist zu Beginn des jeweiligen Kapitels angegeben.

Berlin, 20.10.2011

Egor V. Dzyuba

Abstract (english)

The presented work deals with the investigation of the concepts “multivalency”, “cooperativity”, “self-assembly” and “self-sorting” that play a pivotal role in the research field of supramolecular chemistry. The aims and results of this work can be subdivided as follows:

- The studies of „multivalency“ and „cooperativity“ are based on the use of the Vögtle/Hunter-type tetralactam macrocycle (TLM) as the host component and different dicarbonyl compounds that were implemented into the corresponding guest molecules.
- At the beginning of this work the monovalent case was investigated using only one macrocycle and guest component. Thus, differently substituted guests bearing a diamide moiety (or station) as the binding motif were evaluated. Diamides that are substituted with simple alkyl chains bind stronger into the cavity of the macrocycle compared to their phenyl substituted analoga. In addition, substituents at the 4-position of the phenyl moiety have influence the binding behavior. Electron-withdrawing groups decrease the binding constant K_a while higher K_a values are observed for the phenyl substituted diamides bearing electron-donating groups. These observations were confirmed by both ^1H NMR titrations and Isothermal Titration Calorimetry (ITC).
- The ability of a similar binding motif to form host-guest complexes bearing a tetralactam macrocycle, the so-called diketopiperazine station, was also investigated. In addition, mechanically interlocked [2]rotaxanes were synthesized in good yields using the Cu^{I} -catalyzed [3+2]-cycloaddition (“click chemistry”). Herein, the spacer between the binding station and the stopper that prevents the deslipping of the axle compound from the macrocycle influences the hydrogen bonding between the axle and the macrocycle. Both (triazole) $\text{H}\cdots\text{O}=\text{C}(\text{TLM})$ und (diketopiperazine) $\text{C}=\text{O}\cdots\text{H}-\text{N}(\text{TLM})$ hydrogen bonds can be confirmed by ^1H and $^1\text{H}, ^1\text{H}$ -ROESY NMR in case of the [2]rotaxane bearing a triethylene glycol chain between the diketopiperazine station and the stopper. In case of the [2]rotaxane without this spacer only (diketopiperazine) $\text{C}=\text{O}\cdots\text{H}-\text{N}(\text{TLM})$ hydrogen bonds were observed.
- A broad series of multivalent molecules was synthesized. On the one hand, a novel tetralactam macrocycle bearing a phenanthroline moiety could be obtained. The attachment of this ligand allows the synthesis of di- and trivalent host molecules through coordination chemistry using metal centers such as Cu^{I} , $\text{Ru}^{\text{II}}\text{Cl}_2$ or Fe^{II} . On the

other hand, further multivalent host molecules were obtained using coupling reactions such as Suzuki or Sonogashira reaction. These molecules differ in the number and the position of the tetralactam macrocycles and allow therefore an extensive evaluation of “*multivalency*” in synthetical supramolecular systems. Additionally, the corresponding guests were obtained and first binding studies were performed using ^1H NMR. Moreover, multivalent studies can also be performed using gold surfaces or nanoparticles, for example by single molecule force spectroscopy. Hence, macrocycles and guest compounds containing sulfur were synthesized.

- The studies of „*self-assembly*“ and „*self-sorting*“ are based on two different systems: (1) metallo-supramolecular polygons, which can be obtained quantitatively using nitrogen-containing ligands and *cis*-blocked metal centers, and (2) hydrogen bonding-bridged dimeric capsules bearing resorcinarenes (or pyrogallarenes) that are able to bind cations in their inner spheres.
- Tetra- and bidentate ligands that were used for the synthesis of the metallo-supramolecular polygons bear a 2,2'-bipyridine skeleton (or biaryl in case of the bidentate ligands) that is substituted with 3- or 4-ethynylpyridinyl moieties at its 4,4'-positions. Taking this into account, these ligands differ in the position of the nitrogen atom in the pyridine moiety and therefore influence the thermodynamic minimum of the system if they form metallo-supramolecular polygons by mixing them with the *cis*-blocked metal center containing Pt^{II} in the right ratio. Smaller polygons could be observed exclusively using ^1H and ^{31}P NMR, and ESI MS if ligands with 4-ethynylpyridyl groups were used while the use of the ligands bearing 3-ethynylpyridyl groups results in equilibrium of smaller and bigger polygons. Corresponding tandem MS experiments lead to additional structural evidence. For example, some of the bigger polygons contract to the smaller ones in the gas phase in a specific way while several fragmentation pathways exist in case of other polygons.
- A tetradentate ligand containing a 2,2'-bipyridine skeleton substituted with 4-ethynylpyridines at its 4,4'-positions was used for the investigation into “*self-sorting*”. Herein, metal centers were used where the ligands that block the *cis*-position at the metal atoms were varied. Therefore, only one CH_2 group is crucial for the fact whether the coordination takes place exclusively at the pyridine site or at both pyridine and bipyridine site. By doing so, heterobimetallic polygons of defined position of the metal centers can be obtained.

- The hydrogen-bonded dimeric capsules bearing differently sized cations were investigated in the gas phase of a mass spectrometer using hydrogen/deuterium exchange (HDX). A different exchange behavior was observed depending on the size of the cation under study. Taking this into account, the HDX allows to view on the gas phase structure of these capsules as a fast exchange can only take place by an intact seam between the two halves of a capsule for mechanistic reasons. This is the case if smaller cations, e. g. Cs^+ are included. Bigger cations as for example $(\text{CH}_3\text{CH}_2)_4\text{N}^+$ results in a so-called PackMan-shaped structure. The mechanism of the exchange of labile hydrogen atoms against deuterium in an intact seam can be considered as a one-dimensional Grotthuss Mechanism of proton transfer through water.
- The use of this method in the research field of supramolecular chemistry was summarized in a review article.

Abstract (german)

Die vorliegende Arbeit beschäftigt sich mit der Erforschung von Konzepten „Multivalenz“, „Kooperativität“, „Selbstassemblierung“ und „Selbstsortierung“, welche eine bedeutende Rolle auf dem Gebiet der Supramolekularen Chemie spielen. Die Ziele sowie Ergebnisse dieser Arbeit lassen sich wie folgt gliedern:

- Als Grundlage für die Studien zur Untersuchung von „Multivalenz“ und „Kooperativität“ dienen der Tetralactam-Makrozyklus (TLM) nach Vögtle/Hunter als Wirtkomponente sowie verschiedene Dicarbonylverbindungen, welche in die entsprechenden Gastmoleküle implementiert wurden.
- Zu Beginn dieser Arbeit wurde der monovalente Fall erforscht, bei dem Einfädungsstudien von einem Makrozyklus und einer Gastkomponente durchgeführt wurden. Dabei wurden unterschiedlich substituierte Gäste, welche eine Diamid-Einheit (oder Station) als Bindungsmotiv enthalten, untersucht. Diamide, welche mit einfachen Alkylketten substituiert sind, binden stärker in den Makrozyklus als ihre phenylsubstituierten Analoga. Zusätzlich spielen die Substituenten an der 4-Position der Phenyleinheit eine Rolle. Elektronenziehende Reste setzten die Komplexbildungskonstante K_a herab, während höhere K_a -Werte bei phenyl-substituierten Diamiden mit elektronenschiebenden Resten beobachtet wurden. Diese Aussagen können auf der Basis von den Daten, welche aus ^1H NMR Titrations und Isothermaler Titrationskalorimetrie (ITC) gewonnen werden konnten, gemacht werden.
- Die Fähigkeit eines ähnlichen Bindungsmotives zur Bildung von Wirt-Gast-Komplexen mit dem Tetralactam-Makrozyklus, der so genannten Diketopiperazin-Station, wurde ebenfalls untersucht. Zusätzlich konnten mechanisch verriegelte [2]Rotaxane unter Einsatz von Cu^I -katalysierten [3+2]-Cycloaddition („Click-Chemie“) in guten Ausbeuten hergestellt werden. Dabei beeinflusst der Spacer zwischen der Bindungsstation und den Stoppnern, welche das Abfädeln der Achsenkomponente aus dem Makrozyklus verhindern, die Wasserstoffbrücken zwischen der Achsenkomponente und dem Makrozyklus. (Triazol) $\text{H}\cdots\text{O}=\text{C}(\text{TLM})$ - und (Diketopiperazin) $\text{C}=\text{O}\cdots\text{H}-\text{N}(\text{TLM})$ -Wasserstoffbrücken wurden auf Grundlage von ^1H und $^1\text{H},^1\text{H}$ -ROESY NMR bei dem [2]Rotaxan beobachtet, welches eine Triethylenglykol-Brücke zwischen der Diketopiperazin-Station und dem Stopper enthält. Bei dem [2]Rotaxan, welches diese Brücke nicht hat, wurden nur (Diketopiperazin) $\text{C}=\text{O}\cdots\text{H}-\text{N}(\text{TLM})$ -Wasserstoffbrücken beobachtet.

- Es wurde eine Serie an multivalenten Molekülen synthetisiert. Einerseits wurde ein neuartiger Tetralactam-Makrozyklus hergestellt, welcher mit einer Phenanthrolin-Einheit substituiert wurde. Dieser Ligand erlaubt es, di- und trivalente Wirte über Metallkoordination an unterschiedliche Metallzentren wie Cu^I , $\text{Ru}^{II}\text{Cl}_2$ oder Fe^{II} herzustellen. Andererseits wurden weitere multivalente Wirte über Kupplungsreaktionen wie Suzuki- oder Sonogashira-Reaktion erhalten. Diese unterschieden sich in Anzahl und Position des Tetralactam-Makrozyklus und gestatten so eine umfassende Evaluierung von „Multivalenz“ in synthetischen supramolekularen Systemen. Entsprechende Gäste konnten ebenfalls synthetisiert und erste Bindungsstudien mittels ^1H NMR durchgeführt werden. Ferner können Multivalenz-Studien auch auf Gold-Oberflächen oder -Nanopartikeln durchgeführt werden, zum Beispiel unter Einsatz von Einzelmolekülspektroskopie. Dafür wurden Schwefelhaltige Makrozyklen und Gastmoleküle hergestellt.
- Als Grundlage für die Studien zur Untersuchung von „Selbstassemblierung“ und „Selbstsortierung“ dienten zwei unterschiedliche Systeme: (1) Metallo-supramolekulare Polygone, welche quantitativ aus Stickstoffhaltigen Liganden und *cis*-blockierten Metallzentren resultieren, und (2) wasserstoffverbrückte dimere Kapseln bestehend aus Resorcinarenen (oder Pyrogalloarenen), welche in ihrem Inneren ein Kation binden können.
- Die vier- und zweizähligen Liganden, welche für die Synthese metallo-supramolekularer Polygone verwendet wurden, bestehen aus einem 2,2'-Bipyridin-Gerüst (oder Biphenyl, wenn der Ligand zweizählige ist), welches an den 4,4'-Positionen mit 3- oder 4-Ethynylpyridinen substituiert wurde. Somit unterscheiden sich diese Liganden in der Position der Stickstoffatome der Pyridin-Einheit und beeinflussen so das thermodynamische Minimum des Systems, wenn sie in einem bestimmten Verhältnis mit einem *cis*-blockierten Metallzentrum, welches Pt^{II} als Metallatom enthält, metallo-supramolekulare Polygone bilden. Ausschließlich kleinere Polygone werden bei Liganden mit 4-Ethylpyridin-Resten mittels ^1H und ^{31}P NMR, und ESI MS beobachtet, während bei Liganden mit 3-Ethylpyridin-Resten ein Gleichgewicht zwischen kleineren und größeren Polygonen resultierte. Entsprechende Tandem MS Experimente liefern weitere Strukturhinweise, beispielsweise zerfallen manche der größeren Polygone in der Gasphase hoch spezifisch zu kleineren, während andere dies über mehrere Fragmentierungswege tun.
- Ein vierzähliger Ligand, bestehend aus einem 2,2'-Bipyridin-Gerüst, welches mit 4-Ethynylpyridinen an den 4,4'-Positionen substituiert wurde, wurde zur Untersuchung

von „Selbstsortierung“ benutzt. Es wurden Metallzentren eingesetzt, bei denen der Ligand, welcher die *cis*-Position des Metallzentrums blockiert, variiert wurde. Dabei ist nur eine CH₂-Gruppe entscheidend, ob die Koordination an der Pyridin- und Bipyridin-Seite oder selektiv nur an der Pyridin-Seite stattfindet. Somit sind auch heterometallische Polygone mit definierter Position der Metallzentren erhältlich.

- Die wasserstoffverbrückten dimeren Kapseln, welche unterschiedlich große Kationen einlagern können, wurden mittels Wasserstoff/Deuterium-Austausch (Hydrogen/Deuterium Exchange, HDX) in der Gasphase eines Massenspektrometers untersucht. Dabei konnte festgestellt werden, dass ein unterschiedliches Austauschverhalten in Abhängigkeit von der Größe des Kations vorliegt. Somit kann mittels HDX Rückschlüsse auf die Gasphasenstruktur dieser Kapseln gezogen werden, da ein schneller Austausch aus mechanistischen Gründen nur dann vorliegt, wenn der Saum zwischen den beiden Hälften einer Kapsel intakt ist. Dies ist bei kleineren Kationen wie Cs⁺ der Fall, bei größeren wie (CH₃CH₂)₄N⁺ liegt eine so genannte PacMan-Struktur vor. Mechanistisch gesehen kann ein Austausch von labilen Wasserstoffen gegen Deuterium in einem intakten Saum als ein eindimensionaler Grotthuss-Mechanismus betrachtet werden, welche eine entscheidende Rolle bei Protonentransport in Wasser spielt.
- Über die Verwendung dieser Methode in der Supramolekularen Chemie wurde ein Review-Artikel verfasst.

Table of Contents

1	PREFACE	14
2	INTRODUCTION AND OBJECTIVES	15
3	THEORETICAL BACKGROUND	21
3.1.	Core Concept of Supramolecules: The Use of Non-Covalent Bonds	21
3.2.	The Role of Self-Assembly and Self-Sorting ...	33
3.3.	... and the Impact of Multivalency and Cooperativity	39
3.4.	A “Supramolecular Exception”: The Mechanical Bond in Interlocked Molecules	46
3.5.	Analytical Methods in Supramolecular Chemistry	58
4	RESULTS AND DISCUSSION	72
4.1.	Steric and Electronic Substituent Effects on Axle Binding in Amide Pseudorotaxanes: Comparison of NMR & ITC Titration Data	72
4.2.	Phenanthroline-Substituted Tetralactam Macrocycles: A Facile Route to Rigid Di- and Trivalent Receptors and Interlocked Molecules	73
4.3.	Synthesis of Multivalent Host and Guest Molecules for the Investigation in Multivalency and Cooperativity	74
4.4.	C-H...O Hydrogen Bonds in “Clicked” Diketopiperazine-Based Amide Rotaxanes	98
4.5.	Effects of Subtle Differences in Ligand Constitution and Conformation in Metallo-Supramolecular Self-Assembled Polygons	99
4.6.	Thermodynamically controlled Self-Sorting of Heterobimetallic Metallo-Supramolecular Macrocycles: What a Difference a Methylene Groups makes!	100
4.7.	Gas-phase H/D-exchange experiments in supramolecular chemistry	101
4.8.	A one-dimensional analogue to the Grothuss mechanism of proton transport through water: Gas-phase H/D-exchange reactions on resorcinarene and pyrogallarene capsules	102

5	CONCLUSION AND PERSPECTIVES	103
6	ACKNOWLEDGMENTS	111
7	APPENDIX	113
7.1.	Curriculum Vitae	113
7.2.	List of Publications	115

Diese Arbeit ist meiner Familie gewidmet.

Danke, dass Ihr für mich da seid!

1 PREFACE

How can chemists design and construct macromolecules with extraordinary functions quantitatively and exclusively? How can surfaces and polymers be modified with respect to their hydrophilicity or robustness? How can chemists obtain a great impact in catalysis and material science? And how supposable is our today's knowledge about biomacromolecules without their synthetic siblings? It is hardly possible to ignore the immense potential and influence of supramolecular chemistry, a field that has risen in the last decades. Nowadays, supramolecular concepts such as „reversible formation” or “switchable macromolecules” can be found in basically every research field of chemical research. Even though some concepts of supramolecular chemistry may be claimed to be fully explored, it remains certainty that a deep and profound understanding of some concepts is still not achieved.

This thesis tries to take a deeper dive into marvelous supramolecular concepts such as multivalency, cooperativity, self-assembly and self-sorting. At the beginning, a short introduction will be given, followed by the objectives that will be divided into two main parts: (i) the research performed in the field of multivalency and cooperativity and (ii) in self-assembly and self-sorting. Afterwards, some theoretical background about supramolecular chemistry will be presented in order to give the reader conditions and informations for understanding the results and discussion part of this work. First, the use of weak non-covalent reversible bonds will be illustrated. Then, the concepts mentioned above will be introduced and some literature-known examples will be presented. Subsequently, mechanically interlocked supramolecules will be discussed as they merges all four concepts studied during this work. An overview of analytical methods that are widely used in the supramolecular chemistry will complete the theoretical part and the results and discussion part will be follow.

Almost all of the results obtained during this thesis are publicated, accepted or submitted for publication as manuscripts as highlighted at the beginning of each chapter in the results and discussion part. However, most of them have their own short introduction, a result and discussion part, a conclusion and an experimental section. This thesis will be then summarized in the conclusion chapter. In addition, some perspectives will be presented that may add new insight into the research presented here. An appendix part including a CV and a list of publications will close this work.

Berlin, 2011-10-20

Egor V. Dzyuba

2 INTRODUCTION AND OBJECTIVES

Lately, since the Feynman's speech "There's Plenty of Room at the Bottom" (1959)^[1] and the Nobel Prize for Cram, Lehn and Pedersen (1987)^[2] supramolecular chemistry^[3] has been earned its well-deserved place as an important interdisciplinary research field in the natural sciences. While chemistry has a significant influence on adjacent research fields such as biology, physics or geography, supramolecular chemistry plays an important role in most of chemical branches of research. This fact can be illustrated by two main concepts that play a pivotal role in supramolecular chemistry: (i) molecular recognition and (ii) supramolecular functionality as mentioned by Lehn.^[2a] While molecular recognition is a key principle in biochemistry, for example in the design of novel targets for natural receptors or for simulation of biological processes, supramolecular functionality helps chemists to design e. g. novel artificial molecules, polymers or surfaces with made-to-order features. Simplified, supramolecular chemistry is an important area of chemistry that deals with weak reversible non-covalent association of two or more molecules to higher-ordered supramolecules. In the last decades, the concepts such as multivalency, cooperativity, self-assembly and self-sorting influenced significantly the supramolecular chemistry research. The different works presented here apply these concepts and can be divided into two main parts:

- (i) Investigation of multivalency and cooperativity in multivalent (pseudo)rotaxanes using different binding motifs

In order to obtain a clear picture of multivalency and cooperativity effects in synthetic supramolecular architectures, pseudorotaxanes and rotaxanes as their mechanically interlocked siblings will be evaluated comprehensively. Hence, a significant amount of studies with the Vögtle/Hunter-type tetralactam macrocycles (TLM)^[4] as host molecules and various dicarbonyl compounds as guests that are able to bind into a TLM's cavity under the formation of four (TLM)N-H...O=C(guest) hydrogen bonds will be performed (Figure 1).

An important aspect for multivalent research is the evaluation of monovalent systems that act as starting reference points. It is required to perform an initial study of a monovalent TLM and different substituted dicarbonyl guests investigated by a combination of modern analytical methods widely used in supramolecular chemistry, e. g. ¹H NMR titration and ITC (Isothermal Titration Calorimetry). This research is advantageous for two reasons. On the one hand, the best binding motif can be identified with the help of these experiments. On the other hand, monovalent systems are often simple to study compared to more complex multivalent molecules. This allows the exercise of the handling of different analytical

methods. Notably, ITC plays a pivotal role as all relevant thermodynamic values of a supramolecular system that are essential for its characterization can be obtained in only one experiment. A first example of an ITC investigation is given in case of the TLM/diamide binding motif (chapter 4.1) using monovalent host-guests pairs.

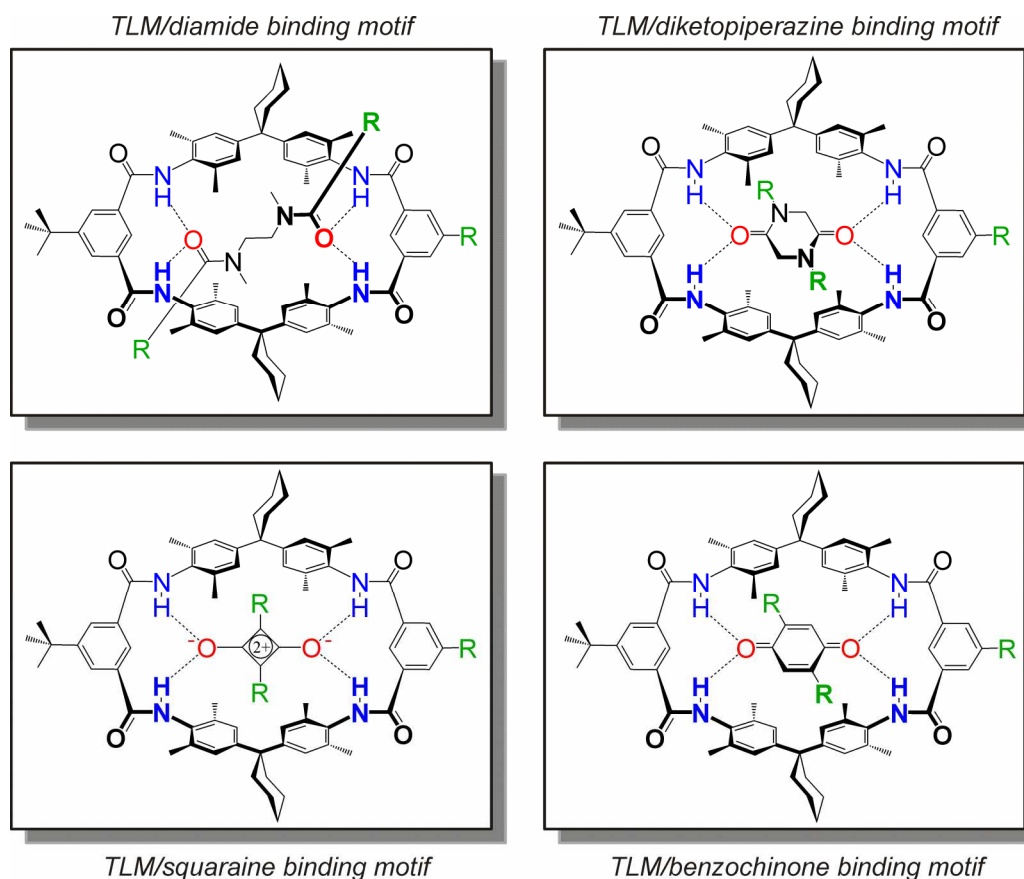


Figure 1. Structures of the TLM/dicarbonyl binding motifs used in this thesis. Green-colored substituents R highlight the possible connection to spacers resulting in multivalent architectures.

The next step would be the construction and evaluation of multivalent architectures bearing the described binding motifs. The “toolbox” approach^[5] described by Schalley *et al.* will be followed in order to obtain a broader assortment on multivalent hosts and guests, especially with the TLM/diamide binding motif (chapters 4.2 and 4.3). Different coupling approaches will be used. For example, ligand-decorated TLMs will be connected through metal coordination chemistry or coupling reactions such Sonogashira and appropriate ethyl-substituted linkers will be used. As analytical methods, the same combination of NMR and ITC would give the best opportunity. In addition, some sulfur-decorated supramolecules and their building blocks will be presented (chapter 4.4), e. g. for the use in SMFS (Single Molecule Force Spectroscopy) or in the LbL (Layer-by-Layer) self-assembly of supramolecules on gold nanoparticles.

The other binding motifs presented in Figure 1 are not just yet used in the multivalent molecules here besides of some exceptions as they should be evaluated first in monovalent pseudorotaxanes or rotaxanes. For example, the TLM/diketopiperazine motif will be evaluated using ^1H NMR and ITC, and used for the synthesis of [2]rotaxanes applying “click chemistry” for the formation of the mechanical bond (chapter 4.4) as the synthetic yields of the desired interlocked supramolecules also allow to estimate the potential of a binding motif. Moreover, reactions with high atom economy such as “click chemistry” might lead to an efficient synthesis of multithreaded mechanically interlocked polycatenanes and -rotaxanes.

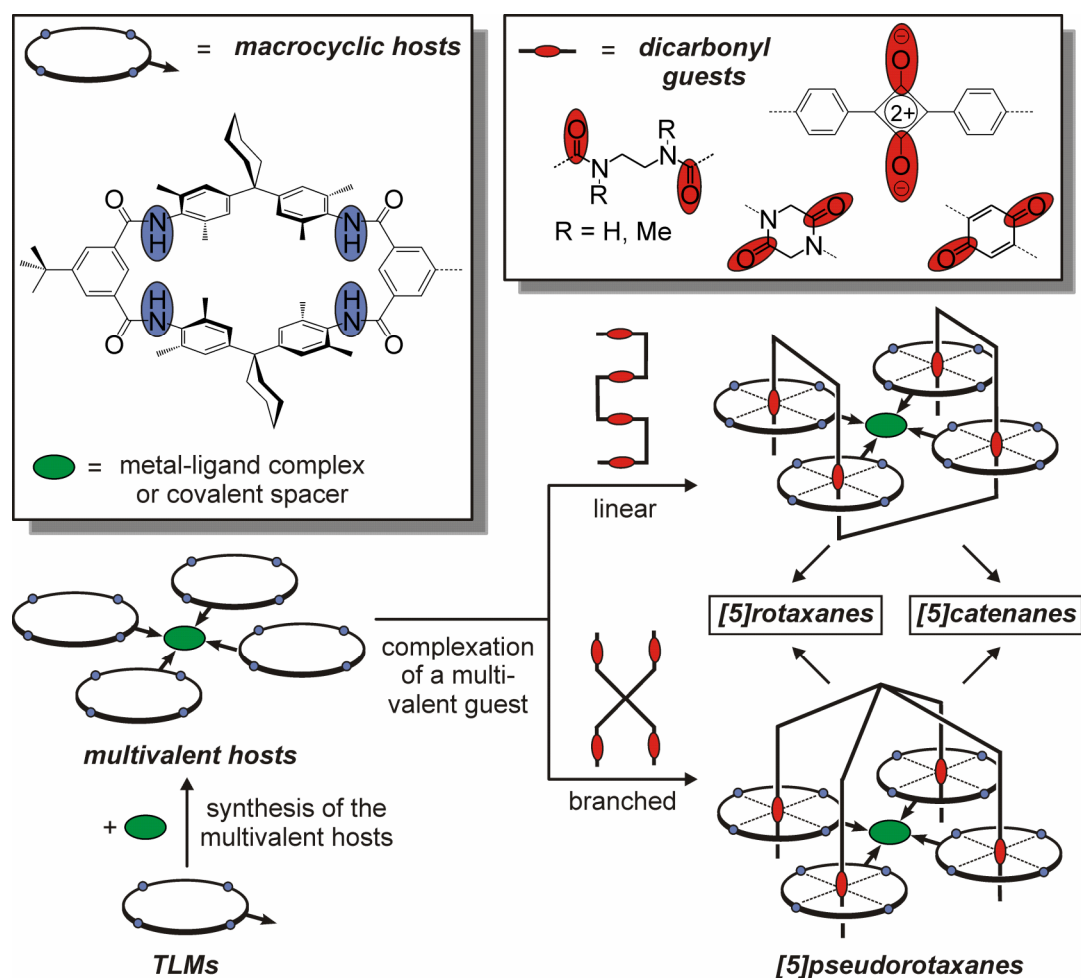


Figure 2. An overview of the multivalent research performed in this thesis shown exemplary on the tetravalent case. Different macrocyclic hosts containing TLMs and different dicarbonyl guests can form [5]pseudorotaxanes through hydrogen bond formation. These pseudorotaxanes can then result in catenanes (if the ends of the axle are cyclizing) or rotaxanes (by adding stopper groups).

The long-term objective of the first part of this work is to construct multivalent rotaxanes and catenanes (Figure 2) with special features such as motion processes of e. g. the macrocyclic compound under the influence of an external stimulus. Initially, multivalent host molecules can be formed using metal coordination chemistry (if macrocyclic hosts are decorated with ligands) or covalent bond formation through appropriate spacers. Afterwards,

a rigid or flexible guest (that can be obtained similarly through metal coordination of usual coupling chemistry) can be used for the construction of the desired multivalent pseudo-rotaxanes. These non-interlocked supramolecules can be locked mechanically (see chapter 3.4), and the desired rotaxanes and catenanes are result. However, the synthesis of such existing molecules has to be performed exclusively without significant byproduct formation and in high yields. Consequently, the studies of threading processes and stoppering reactions using powerful tools such as “click chemistry” or others are of great interest.

- (ii) Investigation of self-assembly and self-sorting in metallo-supramolecular polygons and hydrogen-bridged capsules

The second part of this thesis deals with the investigation of self-assembly and self-sorting processes that occur in two different systems. In the first ones, different di- and tetradentate ligands based on bipyridine/biaryl cores decorated with pyridine ethynyl moieties together with differently substituted metal centers are used in the construction of different homo- and heterometallic supramolecular polygons (Figure 3).

Recently, Brusilowskij and Schalley studied self-assembly events using a tetradentate ligand with the pyridine's nitrogen in *para* position to the ethynyl substituent and a 2,2'-bipyridine core (Figure 3, center left).^[5c,6] If using Pd^{II}(dppp)(OTf)₂ (dppp = 1,3-bis(diphenylphosphino)propane, OTf = trifluoromethanesulfonate or triflate) in metal M : ligand L ratio 1 : 1, a coordination takes place preferably at the pyridine site by stripping the weakly bonded triflate anions. This can be rationalized by the sterical demand of the dppp substituent at the Pd^{II} core. Using a higher ratio M : L of 2 : 1, M₄L₂ complexes are formed under thermodynamic control. However, the coordination of Pd^{II}(dppp) metal center is complete within minutes and no observation of intermediates forming under kinetic control is possible. Therefore, the kinetically more inert Pt^{II} center substituted also with dppp might lead to the observation of bigger polygons, e.g. M₆L₃ or M₈L₄. In addition, the influence of the position of the nitrogen (*para* or *meta* to the ethynyl substituents) and the presence/absence of the bipyridine core in the ligands have to be investigated (Figure 3, center right). Moreover, the observation that the coordination of the dppp-substituted metal centers take place at the pyridine moiety might lead to the observation of the self-sorting processes if metal centers substituted with dppe (1,2-bis(diphenylphosphino)ethane) are used (Figure 3, bottom). As analytical methods, NMR and electrospray ionization mass spectrometry (ESI MS) will be applied. Especially, tandem ESI MS as established in our research group lead to additional important structural information of the assembly ions under study.^[7]

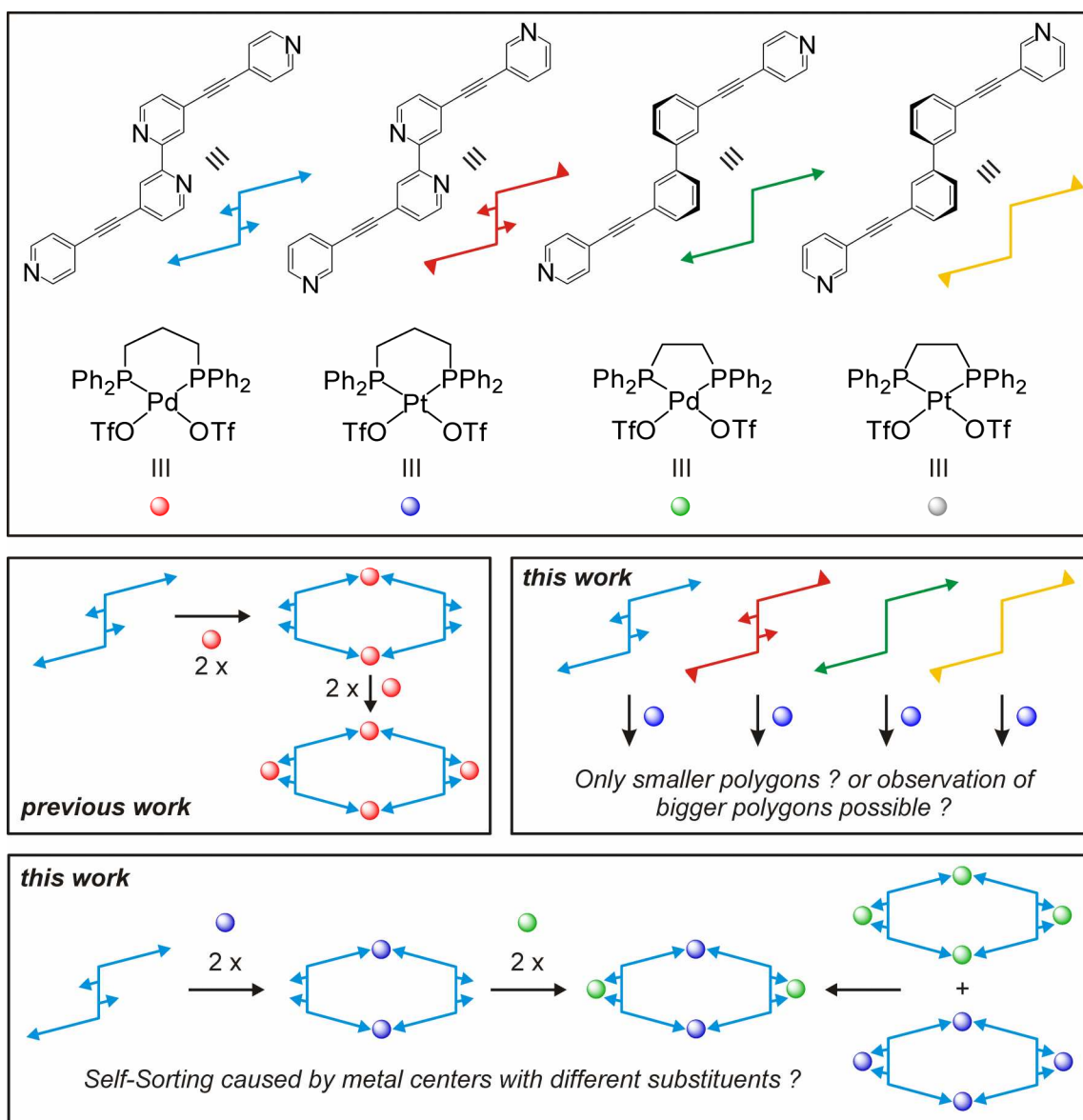


Figure 3. Previously, the self-assembly of a tetradentate ligand and $\text{Pd}(\text{dppp})(\text{OTf})_2$ to a M_4L_2 polygon (M = metal center, L = ligand) was evaluated.^[6] Herein, this study will be expanded to the self-assembly processes of different ligands (pyridine's nitrogen in *para* to the ethynyl substituent vs. *meta*, bipyridine vs. biphenyl) together with $\text{Pt}(\text{dppp})(\text{OTf})_2$. In addition, self-sorting processes using the same ligand as in the previous work and differently substituted metal centers can occur.

The second system studied during this work self-assembles under the formation of hydrogen bonds and cation- π interactions using resorcin[4]arene/pyrogall[4]arene molecules and differently sized cations in a capsular manner (Figure 4). An ESI MS technique will be used here for the investigation of their secondary structure based on the hydrogen/deuterium exchange (H/D-X) as bimodal exchange rates are often observable, e. g. labile hydrogen atoms involved in the hydrogen bonding networks exchange often slower than non-bonded ones. All mechanistic aspects, technical requirements and few examples of supramolecules where this method was used can be found in chapter 4.7.

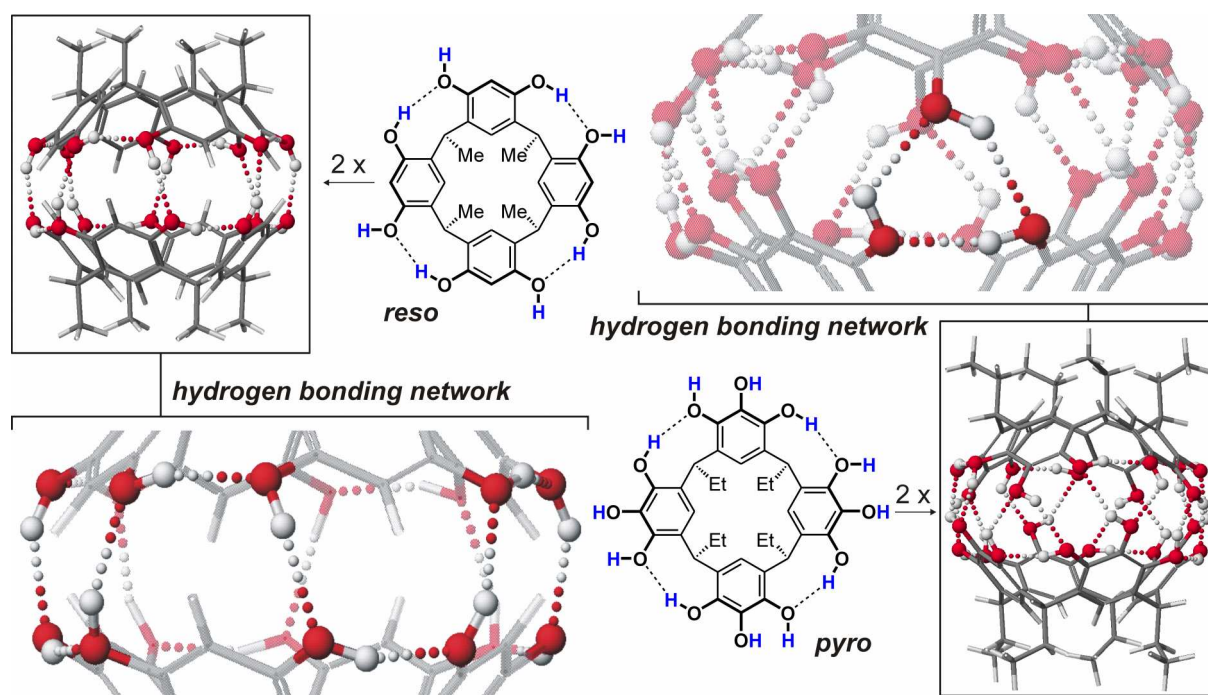


Figure 4. AM1 MOZYME-calculated structures of the capsule-shaped dimers of resorcin[4]arene **reso** and pyrogall[4]arene **pyro** (see chapter 4.8). The hydrogen bonding networks resulting from the presence of eight hydroxyl groups in case of **reso** and twelve in case of **pyro** are emphasized.

- [1] Feynman, R. P. *Eng. Sci.* **1960**, 23, 22.
- [2] (a) Lehn, J.-M. *Angew. Chem. Int. Ed. Engl.* **1988**, 27, 89. (b) Cram, D. J. *Angew. Chem. Int. Ed. Engl.* **1988**, 27, 1009. (c) Pedersen, C. J. *Angew. Chem. Int. Ed. Engl.* **1988**, 27, 1021.
- [3] (a) Lehn, J.-M. *Supramolecular Chemistry - Concepts and Perspectives*, Wiley-VCH, Weinheim, **1996**. (b) *Templated Organic Synthesis* (Eds.: Diederich, F.; Stang, P.), Wiley-VCH, Weinheim, **2000**. (c) Steed, J. W.; Turner, D. R.; Wallace, K. *Core Concepts in Supramolecular Chemistry and Nanochemistry*, Wiley, **2007**. (d) Atwood, J. L.; Steed, J. W. *Supramolecular Chemistry*, Wiley, **2009**.
- [4] (a) Hunter, C. A. *J. Am. Chem. Soc.* **1992**, 114, 5303. (b) Vögtle, F.; Meier, S.; Hoss, R. *Angew. Chem. Int. Ed. Engl.* **1992**, 31, 1619.
- [5] (a) Baytekin, B.; Zhu, S. S.; Brusilowskij, B.; Illigen, J.; Ranta, J.; Huuskonen, J.; Rissanen, K.; Kaufmann, L.; Schalley, C. A. *Chem.-Eur. J.* **2008**, 14, 10012. (b) Baytekin, B. *An easily accessible toolbox of functionalized macrocycles and rotaxanes and a (tandem) ESI-FTICR mass spectrometric study on Fréchet-type dendrimers with ammonium cores and hierarchical self-assembly of metallo-supramolecular nanospheres*, PhD thesis, Freie Universität Berlin, **2008**. (c) Brusilowskij, B. *Studien zur Entschlüsselung von Komplexität in supramolekularen Architekturen*, PhD thesis, Freie Universität Berlin, **2010**.
- [6] Brusilowskij, B.; Schalley, C. A. *Eur. J. Org. Chem.* **2011**, 469.
- [7] Schalley, C. A.; Springer, A. *Mass Spectrometry and Gas-Phase Chemistry of Non-Covalent Complexes*; Wiley, Hoboken/USA, **2009** and literature cited herein.

3 THEORETICAL BACKGROUND

3.1. Core Concept of Supramolecules: The Use of Non-Covalent Bonds

Supramolecular chemistry extends beyond the individual molecules and focuses on their inter- and/or intramolecular non-covalent interactions that result in the creation of organized assemblies or structures. In other words, non-covalent interactions lead to the formation of molecular clusters while covalent interactions lead to the formation of classical molecules. Lehn has defined supramolecular chemistry as the “the chemistry of molecular assemblies and of the intermolecular bond” or “the chemistry beyond the molecule”.^[1] Biological systems are often the inspiration for supramolecular research using molecular recognition, host-guest chemistry and molecular self-assembly.

Although typically energetically less robust by a factor of 10 in comparison to covalent bonds, non-covalent interactions are essential for the natural processes such as substrate binding to a receptor, the assembling of protein complexes, intermolecular reading of the genetic code or cellular recognition. In addition, they are of great interest for scientists who effort to mimic the natural systems by the design of artificial receptors/hosts capable of binding substrates/guests forming supramolecules with special features as their natural siblings.

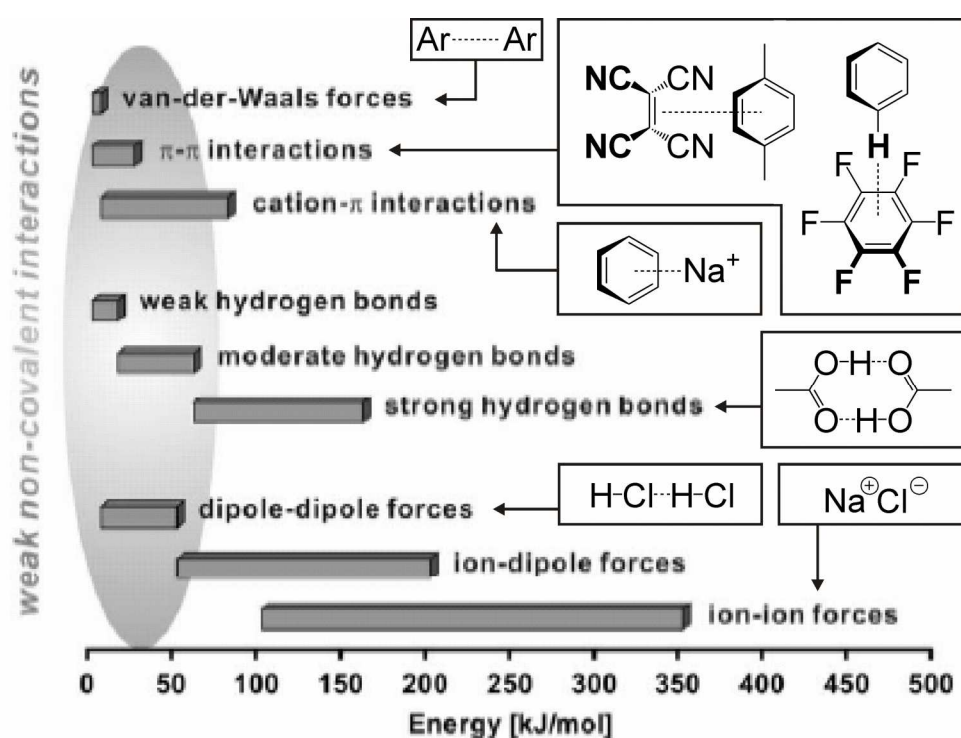


Figure 5. Stabilities of typical non-covalent interactions and examples for some of them (Ar = argon).^[1b]

The wide spreading of supramolecular chemistry is mostly due to the use of weak and reversible non-covalent bonds. This chapter summarizes the important characteristics of them (Figure 5) and focuses mainly on the hydrogen bonds, as they play an important role in the supramolecules presented within this work.

Noncovalent bonds range from ion (dipole) - ion (dipole) forces with a strength of several hundreds of kJ mol^{-1} to weak London dispersion interactions with a few kJ mol^{-1} . For example, strong electrostatical interactions occur between charged molecules or particles (ion-ion interactions) and/or between molecules with a permanent dipole moment (ion-dipole interactions). The force is acting simultaneously on different point charges (q_1) and (q_2) defined by Coulomb's law given by equation 1.

$$\text{(eq. 1)} \quad F = \frac{q_1 q_2}{4 \pi \epsilon_0 \epsilon_1 r^2}$$

(r is the distance between q_1 and q_2 , ϵ_0 is the vacuum permittivity and ϵ_1 is the dielectric constant of the environment in which the interaction occurs).

Hence, either molecules or particles can have similar charges (non-attractive interactions) or they are differently charged (attractive interactions). Oppositely charged ions attract one another. As a result, anions are more likely to be found near cations in solution, and vice versa. A significant role for the strength of electrostatically interactions plays the dielectric constant of the environment and the distance between both charges.

Other important non-covalent interactions are π - π interactions^[2] that refer to a stacked arrangement of molecules through interatomic interactions caused by intermolecular overlapping of p-orbitals in π -conjugated systems. Two common arrangements of π -interaction are face-to-face and edge-to-face. Such events contribute significantly to an overall stability of a supramolecule if large flat polycyclic aromatic hydrocarbons with a lot of delocalized π -electrons occur. Another special feature are π -donor- π -acceptor systems that can assemble into a charge-transfer complex.^[3] Herein, one aromatic moiety can be substituted with electron-donating groups and the other with electron-withdrawing substituent. The electron-rich aromatic compound donates electrons from its high energy filled orbitals to the electron-poor one in its low energy empty orbitals.

Related to this are cation- π forces, also known as the Dougherty effect, that act between an cation and the face of π -system, similar to a ion-dipole interaction described above.^[4] In comparison to molecules with a permanent dipole moment, aromatic moieties

such as a simple benzene have a permanent quadrupole moment. The electrostatic potential of benzene is negative at the surfaces of the aromatic ring and an interaction can occur only between the cation and these surfaces. The solvent also influences the relative strength of the bonding. Most data on cation- π interactions are acquired in the gas phase or in non-competitive solvents as the attraction becomes less pronounced with increasing solvent polarity. However, these interactions increase if the aromatic core is substituted with electron-donating groups. A further example of interactions with π -systems are anion- π interactions.^[5] They work in the reversible manner as compared to cation- π forces. Partial positively charged surface of an aromatic moiety is needed for such interactions and can be caused by strong electron-withdrawing substituents.

London dispersion interactions, a part of the Van der Waals forces, can be found between induced multipoles in molecules without permanent dipole moments. These interactions are described by the Lennard-Jones potential defined by equation 2.

$$\text{(eq. 2)} \quad V(r) = 4 \varepsilon \left[\left(\frac{\sigma}{r} \right)^{12} - \left(\frac{\sigma}{r} \right)^6 \right]$$

(ε is the polarizability of electron system of the interacting partners, σ is the distance where the potential of the interacting partners is zero and r is the distance between them).

The first term of this equation describes the non-attractive interactions, the second stands for attractive interactions. London dispersion forces define the chemical character of many organic compounds. They also define the solubility of organic substances.

The hydrophobic effect recently has become the focus of attention as it plays a pivotal role e.g. in the formation of micelles and membranes.^[6] In addition, applications have risen by utilizing hydrophobic effects in the field of supramolecular chemistry in water.^[7] These effects can be defined as the tendency of nonpolar substances to aggregate in aqueous solution and at the same time to exclude water molecules. A single unpolar molecule is solvated by a number of water molecules. The contribution of free enthalpy ΔH to this event is nearly zero, while this process is strongly discriminated with the focus on entropy ΔS contribution. Thus, if two unpolar molecules aggregate in water, they lose their solvation shell. Consequently, such interactions are entropy-driven but not attractive in a classical manner.

Since the role of the hydrogen bonds is essential for the research performed during this thesis as clearly shown in chapters 4.1 - 4.4, 4.7 and 4.8, their importance is notably

pointed out here. Hydrogen bonds are the most prominent non-covalent interactions as they can be found widely in nature. For example, the high boiling point of 100 °C of water, the contraction of it during the melting of ice and the density maximum at 4 °C is due to the H-O•••H bridges between single water molecules. Architectures of great biological relevance such as nucleobases in the DNA, amino acids in proteins or carbohydrates at cell surfaces rely significantly to the use of hydrogen bonds in natural systems.

A hydrogen bond is a particular kind of dipole-dipole interactions and is defined as a weak interaction between a hydrogen atom, which is attached to an electronegative element X and a second electronegative element Y that bears a free electron pair. The elements X and Y can be therefore N, O, F, P, S, Cl and Br. The part “X-H” of a molecule can be described as hydrogen bond donor (**D**) and Y is a hydrogen bond acceptor (**A**). Particularly strong hydrogen bonds occur if X is very electronegative (high polarity of the X-H bond) and Y is very basic (high acceptability of hydrogens). In addition, π -systems such as aromatic units or double and triple bonds can act as hydrogen bond acceptor. The binding energies of typical hydrogen bonds are shown in Table 1.^[8]

hydrogen bond	binding energies [kJ mol ⁻¹]	hydrogen bond	binding energies [kJ mol ⁻¹]
O-H•••N	30	N-H•••O	8-12
O-H•••O	25	N-H•••N	8-17
C-H•••O	8-12	N-H•••F	21
O-H••• π / N-H••• π	1-17	F-H•••F	155

Table 1. Binding energies of typical hydrogen bonds.^[8]

Hydrogen bonds can further be subdivided in very strong, strong and weak hydrogen bonds (Table 2).^[9] On the one hand, very strong hydrogen bonds have energies about 63 - 168 kJ mol⁻¹, typically a high covalent character and the bond lengths of H-X and H•••Y are nearly equivalent. On the other hand, strong hydrogen bonds are electrostatic in nature with binding energies in the range of 17 - 63 kJ mol⁻¹. However, these hydrogen bonds are those one that typically occurring in natural systems, e.g. DNA. Weak hydrogen bonds typically have binding energies < 17 kJ mol⁻¹ and includes e. g. interactions with π -systems.

Because hydrogen bonds are highly directed in comparison to for example London dispersion forces, they can be used both in natural and artificial systems for a specifically

interaction of one molecule to the other one. It is important to note that hydrogen bonds are enormously sensitive to the environment, especially to the temperature and solvent. Recently, Hunter investigated in the binding effects of different functional groups in different solvents.^[10] Two examples are shown in Figure 6.

characteristics	very strong	strong	weak
energy [kJ mol ⁻¹]	63 - 168	17 - 63	< 17
length	H-X ~ H...Y	H-X < H...Y	H-X << H...Y
distance X-H...Y	2.2 - 2.5 Å	2.5 - 3.2 Å	3.2 - 4.0 Å
elongation of X-H bond	0.05 - 0.2 Å	0.01 - 0.05 Å	≤ 0.01 Å
angle X-H...Y [°]	175 - 180	130 - 180	90 - 180
covalency	pronounced	weak	vanishing
electrostatic character	significant	dominant	moderate
examples	gas-phase dimers of strong acids / bases	biological molecules	X-H...π hydrogen bonds

Table 2. Characteristics of hydrogen bonds.^[9]

In Figure 6, possible favorable and unfavorable interactions are shown. For this, α and β are hydrogen-bond donor and hydrogen-bond acceptor constants for the solute molecules, and α_s and β_s are the corresponding hydrogen-bond donor and hydrogen bond acceptor constants for the solvent. The free energy of hydrogen bonding interactions can be calculated using equation 3.

$$(eq. 3) \quad \Delta\Delta G_{H-bond} = -(\alpha\beta + \alpha_s\beta_s) + (\alpha\beta_s + \alpha_s\beta) = -(\alpha - \alpha_s)(\beta - \beta_s)$$

Blue-colored space represents favorable interactions ($\Delta\Delta G_{H-bond} < 0$) and red-colored areas rely to unfavorable interactions ($\Delta\Delta G_{H-bond} > 0$). Such investigations help supramolecular chemists for several reasons. First, it contributes to template research. For example, it clearly shows that the use of O=PR'R'' or O=SR'R'' instead of O=NR'R'' (R' and R'' are

Theoretical Background

various substituents) would result in stronger binding affinities even in methanol. Furthermore, the functional group interaction profiles can provide some insight into the solubility properties of organic molecules. Functional groups that make favorable interactions in a given solvent are likely to reduce solubility, whereas unfavorable functional group interactions should lead to increased solubility.

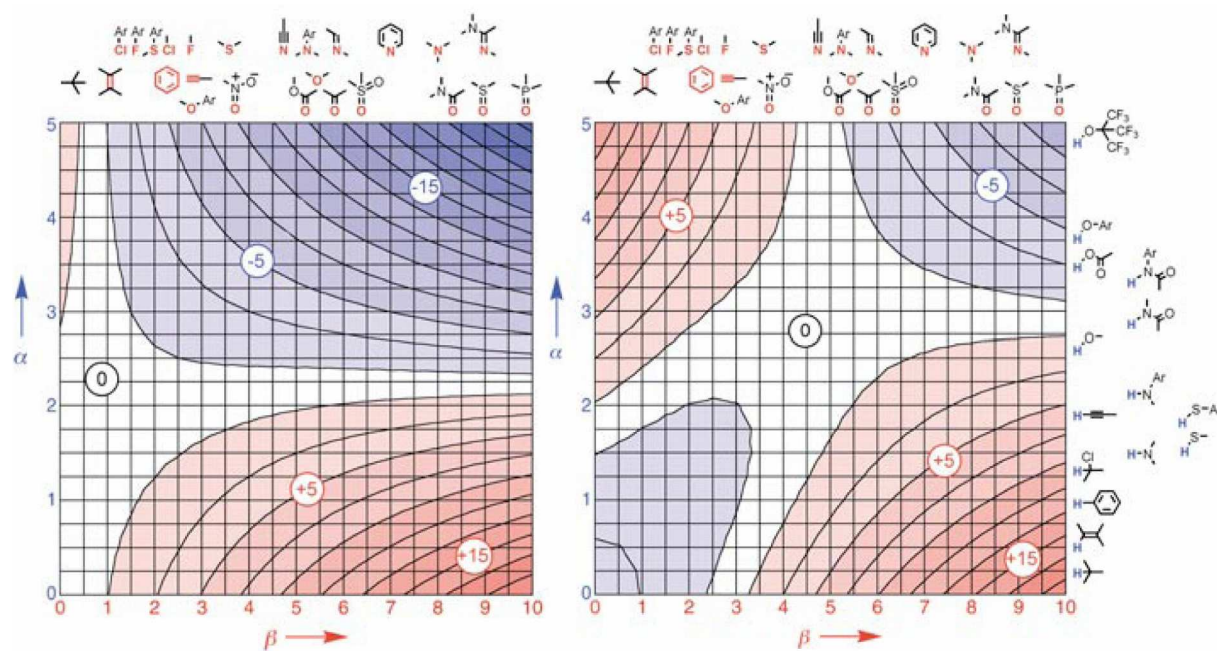


Figure 6. Functional group interaction profiles in chloroform (left, $\alpha_s = 2.2$, $\beta_s = 0.8$) and methanol (right, $\alpha_s = 0.9$ and 2.7 , $\beta_s = 5.8$). The free energy of hydrogen bonding interactions $\Delta\Delta G_{\text{H-bond}}$ [kJ mol^{-1}] is plotted against values α and β . The contour lines are drawn at 2 kJ mol^{-1} intervals.^[10]

The described effects are of great importance if host molecules such as the Vögtle/Hunter-type tetralactam macrocycles (TLM) are used for guest complexation (see e. g. chapter 2, Figure 1) as their hydrogen bond ability strongly depends on the solvent that has to have a non-competitive nature. Their synthesis and possible ways of modification and its binding behavior are discussed here. A typical synthetic pathway towards a TLM is shown in Figure 7. Initially, the synthesis starts with the so-called Hunter's diamine **3** that can be obtained from cyclohexanone **1** and 2,6-dimethylaniline **2** through condensation in a yield of typically 20 - 40%. Afterwards, the Hunter's diamine **3** reacts to the so-called extended diamine (EDA) in a typical yield of 20 - 60%. In this reaction, compound **3** is used in a huge excess in order to obtain as much as possible of the desired product and prevent the formation of oligo- or polymers. An introduction of solubilizing groups (e. g. *t*Bu) or groups that are required for coupling reactions are performed in this step. The acid chlorides can be obtained commercially or through the reaction of the corresponding acids with thionyl or oxalyl chloride. The second functional group can be then applied in the cyclisation step using

a second (or the same, if the TLM is symmetrical) acid chloride. Herein, the cyclisation proceeds under high dilution conditions. The yield of TLM is varying depending on the structure of EDA. An introduction of a nitrogen instead of the C(2) atom in the isophthaloyl moiety forces the EDA into its *cis* conformation as shown in Figure 7 by formation of two intramolecular hydrogen bonds of this nitrogen atom to the hydrogens of the amide moieties. Taking this into account, it is reasonable why the TLM can be isolated here with yields of approximately 80%.^[11] However, if this is not the case, a typical yield of this reaction is limited to only 10 - 30% since strong byproduct formation is often observed. Byproducts are the [2]catenane **8** or bigger oligomers, e. g. an octalactam macrocycle (OLM, not shown here).

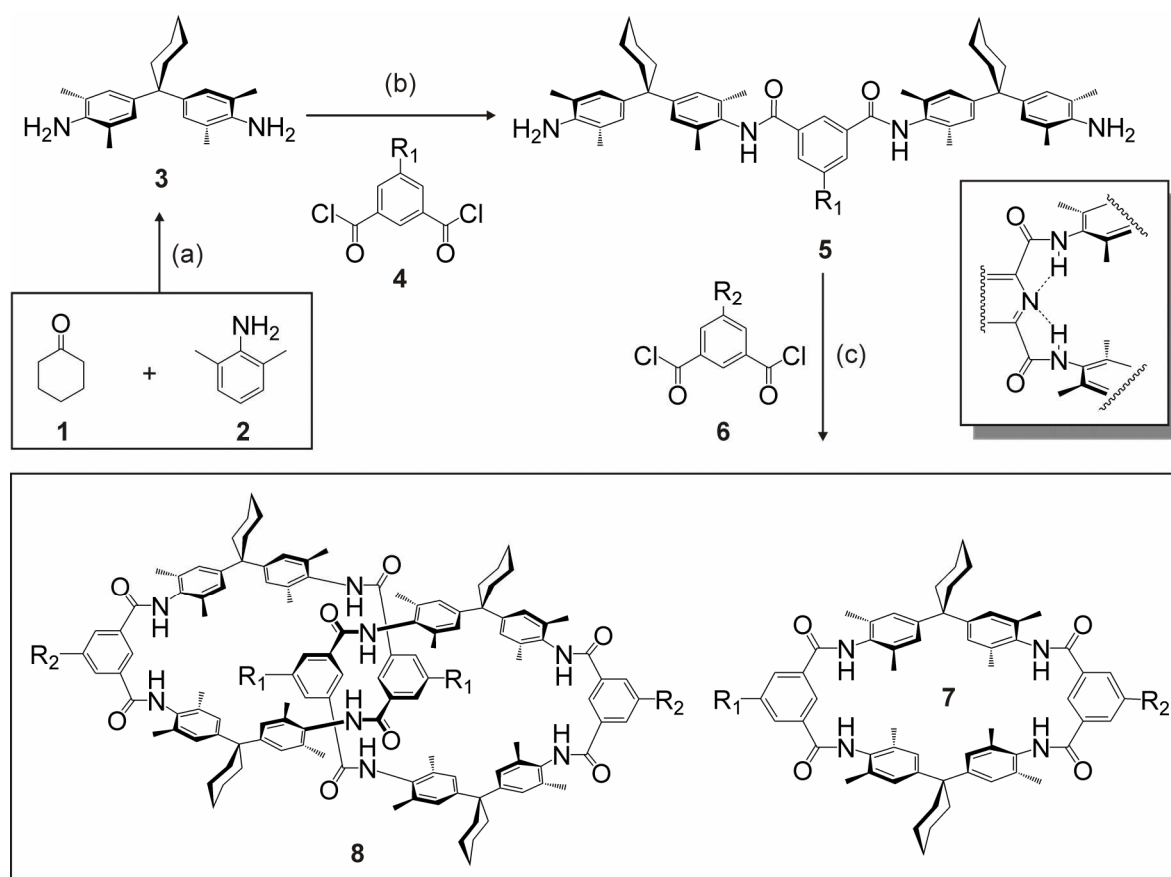


Figure 7. General view of the synthesis of a Hunter/Vögtle-type TLM: (a) HCl (37 wt%), EtOH, 80 °C, 5 - 7 days, 30 - 40%. (b) NEt₃, CH₂Cl₂, 25 °C, 18 hours, 20 - 80% (depending on the solubility of the resulting EDA). (c) NEt₃, CH₂Cl₂, 25 °C, 1 - 3 days, 10 - 80%. Besides the TLM and the [2]catenane, additional byproducts such as an octalactam macrocycle (OLM) or a [2]catenane consisting of an OLM and a TLM can be isolated. EDA **5** is shown in its *trans* conformation and only one isomer of the catenane **8** is shown here. Insert show the intramolecular hydrogen bonds that occur if the C(2) carbon is replaced against a N atom in the EDA **5**. Such pattern leads to a preorganization of **5** and the TLM yields in typically > 80 %. See text for different possibilities for R₁ and R₂.

A second possibility to perform the cyclisation step is the use of templates. Here, high concentrations are needed in order to form an EDA/template complex that, however, would

not be stable enough under high dilution conditions. Tatzke showed, that the use of glycine anhydride (or diketopiperazine) increase the yield of the TLM **11** up to 34% in this template-directed macrocyclization reaction.^[12] Probably, a glycine anhydride molecule preorganizes the EDA **9** in its *cis* conformation and then a successful cyclisation can take place. However, further investigations of this step using e. g. ¹H NMR or X-ray are still necessary in order to confirm the presence of the precursor/template complex as shown in Figure 8.

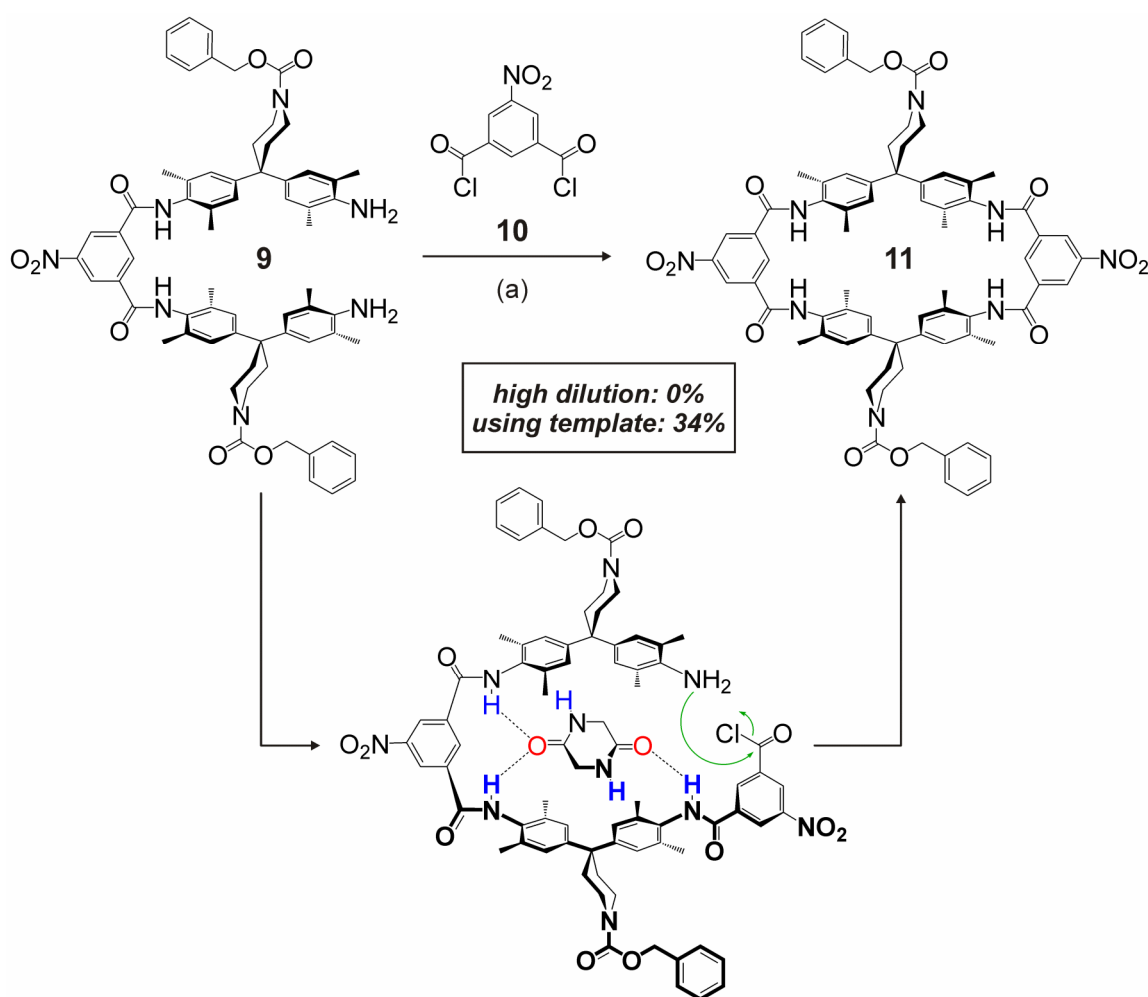


Figure 8. Synthesis of the TLM **11** using glycine anhydride as a template that probably preorganizes the EDA **9** by formation of hydrogen bonds. This TLM is the only example of Hunter/Vögtle-type TLM's so far where the template-directed synthesis was successful.

It is essential to have a possibility to modify these TLM for research presented here, e. g. by attaching ligands for metal coordination chemistry or connecting two or more TLM's to appropriate linker molecules in order to obtain multivalent hosts. This can be done by two approaches: (i) the group of interest is implemented in the acid chloride and is therefore introduced in the high dilution cyclisation step (Figure 9, pathway A). (ii) A group appropriate for coupling reactions is introduced in the high dilution cyclisation step and afterwards Suzuki, Sonogashira or amide coupling reactions are performed (pathway B). Both approa-

ches are demonstrated on EDA **12**, substituted with *t*Bu on the one side for a better solubility (Figure 9). On the one hand, a pyridine moiety can be introduced in the cyclisation step (pathway A). This approach allows the synthesis of a tetravalent host through coordination to a Pd^{II} metal core. On the other hand, introduction of I, Br or OTf allows the use of either Suzuki or Sonogashira coupling (Figure 9, pathway B). Ligands for coordination chemistry can be implemented or TLM's can be connected to each other covalently through linker molecules. Basically, this approach was used here (see chapters 4.2 and 4.3) and a comprehensive library of di- and trivalent hosts both through metal coordination and through covalent connection were synthesized and characterized underlying the “toolbox” approach.

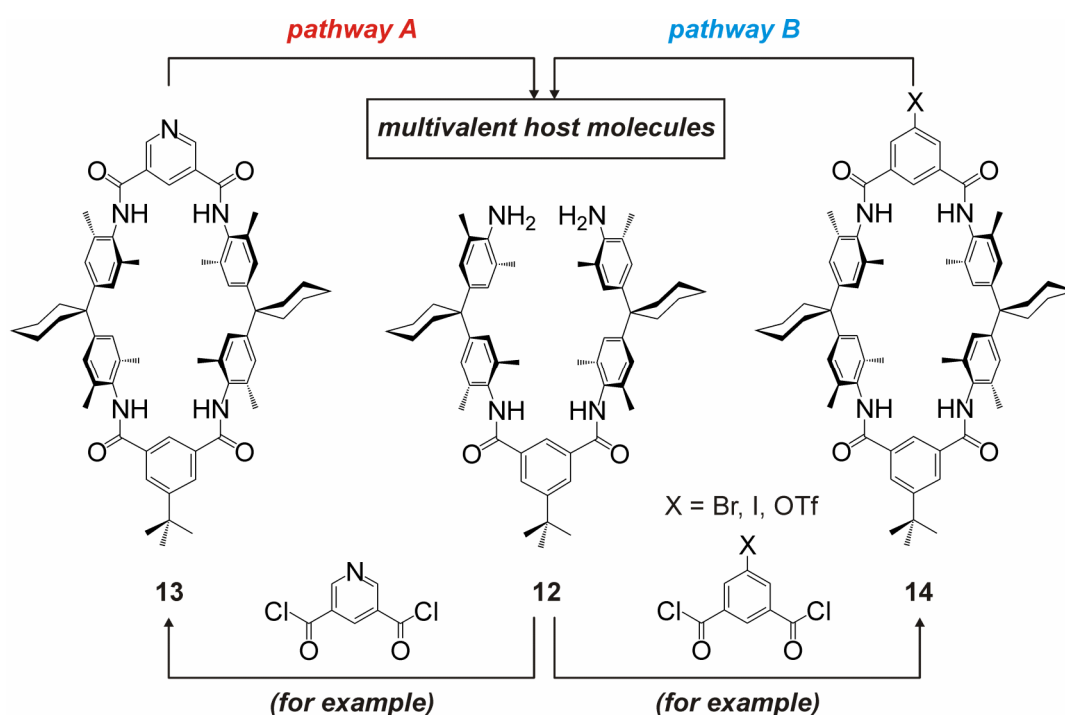


Figure 9. Different types of modification of a TLM demonstrated on the EDA **12**. On the one hand, introduction of functional groups in the cyclisation reaction is possible. On the other hand, TLM's can be decorated with groups such as Br, I, or OTf (= triflate) appropriate for coupling reactions.

This modular strategy is advantageous as it reduces the number of building blocks that are required for this research without restricting the structural diversity of the end products. For example, if using the iodo-substituted TLMs and different ethynyl-substituted spacer molecules, a variety of multivalent host molecules that differ in the number and the geometry of the TLM's can be obtained. Such “toolboxes” are essential for the investigation into e. g. multivalency and cooperativity in synthetic systems.

TLMs provide four converging hydrogen bonds for interaction with e. g. dicarbonyl guests.^[13] However, the energy for the rotation of a single amide bond in the TLM is ca. 10 kJ mol⁻¹ and the energy difference between the single conformers is ca. 5 kJ mol⁻¹. Thus,

different conformations of the TLM are possible (Figure 10). The 2-*in*-2-*out* conformation (two NH's in, two out) of the TLM was observed in the [2]rotaxane obtained through “click chemistry” (chapter 4.4). It consists of a di-*t*erbutyl-substituted TLM and a triazole-diketopiperazine-triazole axle center piece. If a chain is implemented between the axle center piece and the phenyl-trityl stoppers, (triazole)H•••O=C(TLM) and (diketopiperazine)C=O•••H-N (TLM) hydrogen bonds were confirmed by ^1H NMR. The first-mentioned hydrogen bonds can be formed through a rotation of the amide group in a fashion where the N-H is pointing out. However, if this chain is removed, the TLM can be fixed in its all-*in* conformation. Such binding motif can also be observed for other dicarbonyl guests (see chapter 2). If a mono-amide as a guest is complexed by the TLM, a 3-*in*-1-*out* conformation exists. Such binding motif was used e. g. in the rotaxane synthesis of diamide template reported by Vögtle *et al.*^[14]

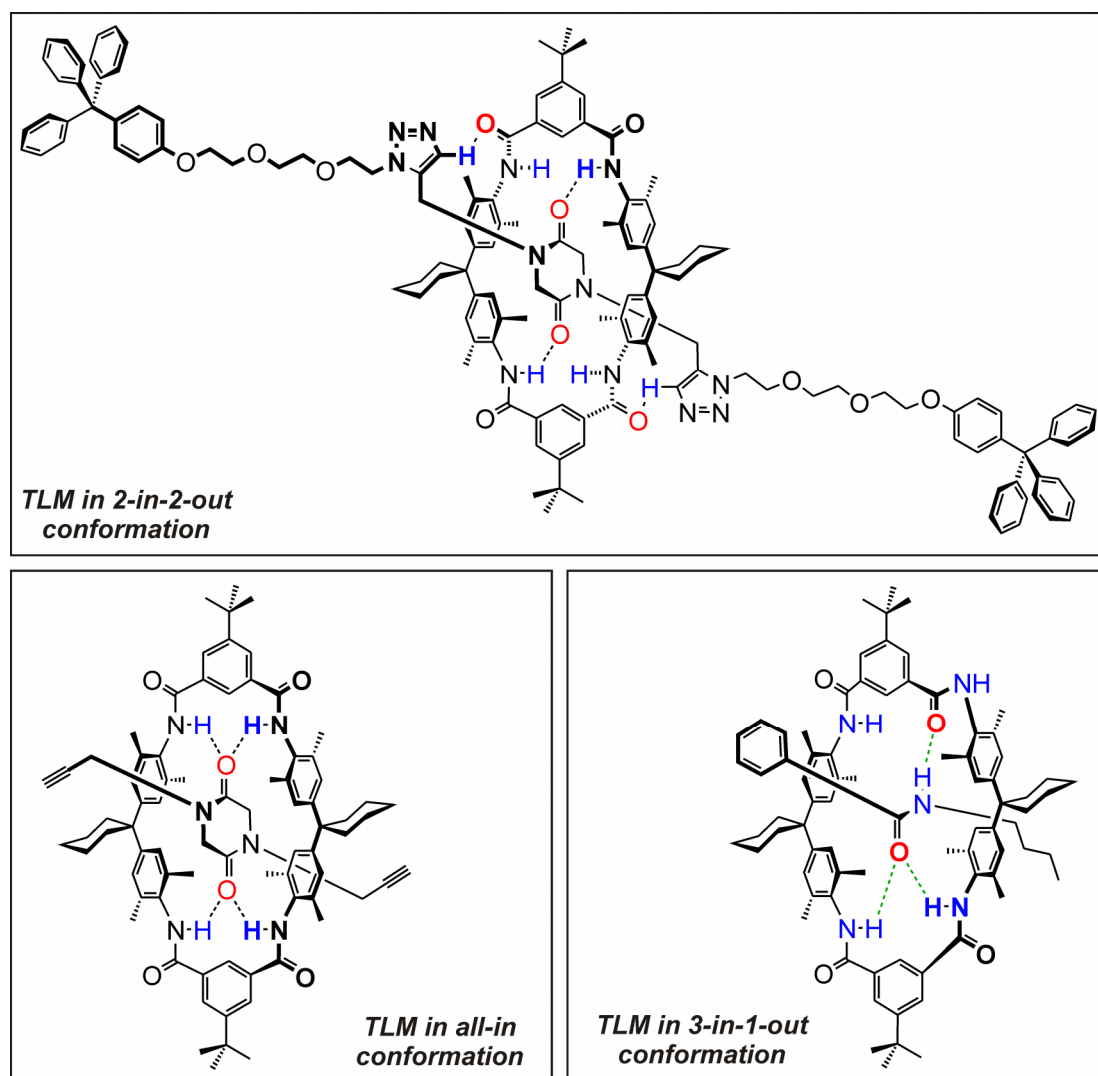


Figure 10. Rotaxanes and pseudorotaxanes bearing TLMs with different conformations: [2]rotaxane with triazole-diketopiperazine-triazole axle centerpiece bridged with a triethylene glycol chain to two phenyl-trityl stoppers (top); [2]pseudorotaxane bearing N,N'-dipropargyl diketopiperazine as the guest (left bottom). The [2]pseudorotaxane bearing N-butylbenzamide as the guest shown right down.^[13d]

The role of the hydrogen bonds in synthetic supramolecular systems can also be demonstrated on the phenomenon of hydrogen-bridged molecular capsules.^[15] In comparison to TLMs that bind the desired guest molecules in a 2D-shaped architecture, capsules can fully enclose guests and/or solvent molecules. As shown in chapter 2, resorcin[4]arenes and pyrogall[4]arenes are able to form capsules with suitable cationic species that form additional cation- π interactions to the aromatic walls.^[16] Moreover, hexameric capsules can be observed in the gas phase^[17] (see chapter 3.5). Recent studies from Pyrse *et al.* showed that the construction of such supramolecules is also possible in the solid and solution phase (Figure 11).^[18] If first heat as solids and then dissolve in CDCl_3 for NMR characterization, a hexamer of pyro-

gall[4]arene derivative self-assembles under encapsulation of three pyrene molecules. However, pyrene molecules are kinetically trapped inside this hexamer and are displaced after six hours against chloroform molecules. The resulted hexamer with six chloroforms can also be observed by dissolving pyrogall[4]arene first in CDCl_3 and then heat. No encapsulation of pyrene molecules is observed in this case.

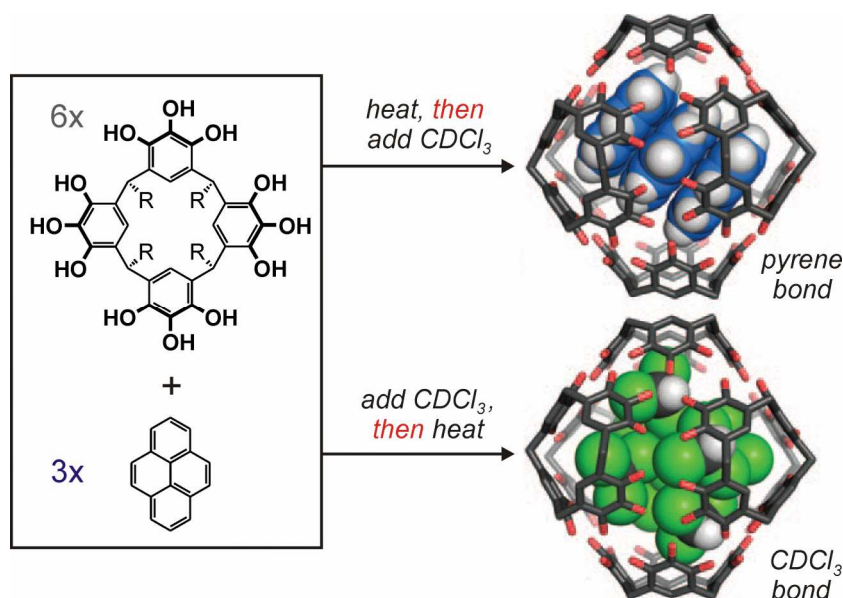


Figure 11. Pyrogallol[4]arene derivative self-assembles to form a hexameric capsule enclosing three molecules of pyrene when heated first and then dissolved in solvent and forms a hexameric capsule containing CDCl_3 when dissolved first and then heated. Molecular models were energy-minimized using HyperChem and PM3 ($\text{R}=\text{C}_{10}\text{H}_{21}$).^[18]

- [1] (a) Lehn, J.-M. *Supramolecular Chemistry - Concepts and Perspectives*, Wiley-VCH, Weinheim, **1996**. (b) Schalley, C. A., *Introduction*, in: *Analytical Methods in Supramolecular Chemistry* (Ed.: Schalley, C. A.), Wiley-VCH, Weinheim, **2007**, pp 1-16.
- [2] (a) Hunter, C. A.; Sanders, J. K. M. *J. Am. Chem. Soc.* **1990**, *112*, 5525. (b) Hunter, C. A.; Singh, J.; Thornton, J. M. *J. Mol. Biol.* **1991**, *218*, 837. (c) Meyer, E. A.; Castellano, R. K.; Diederich, F. *Angew. Chem. Int. Ed.* **2003**, *42*, 1210.
- [3] (a) Vogler, A.; Kunkely, H. *Coord. Chem. Rev.* **2000**, *208*, 321. (b) Ko, Y. H.; Kim, E.; Hwang, I, Kim, K. *Chem. Commun.* **2007**, 1305.

- [4] (a) Kumpf, R. A.; Dougherty, D. A. *Nature* **1993**, *261*, 1708. (b) Mecozzi, S.; West, A. P.; Dougherty, D. A. *J. Am. Chem. Soc.* **1996**, *118*, 2307. (c) Dougherty, D. A. *Nature* **1996**, *271*, 163. (d) Ma, J. C.; Dougherty, D. A. *Chem. Rev.* **1997**, *97*, 1303.
- [5] (a) Quiñonero, D.; Garau, C.; Rotger, C.; Frontera, A.; Ballester, P.; Costa, A.; Deyà, P. M. *Angew. Chem. Int. Ed.* **2002**, *41*, 3389. (b) de Hoog, P.; Gamez, P.; Mutikainen, I.; Turpeinen, U.; Reedijk, J. *Angew. Chem. Int. Ed.* **2004**, *43*, 5815. (c) Gamez, P.; Mooibroek, T. J.; Teat, S. J.; Reedijk, J. *Acc. Chem. Res.* **2007**, *40*, 435. (d) Schottel, B. L.; Chifotides, H. T.; Dunbar, K. R. *Chem. Soc. Rev.* **2008**, *37*, 68.
- [6] Tanford, C. *The Hydrophobic Effect: Formation of Micelles & Biological Membranes*, Wiley, New York, **1980** and literature cited herein.
- [7] Oshovsky, G. V.; Reinhoudt, D. N.; Verboom, W. *Angew. Chem. Int. Ed.* **2007**, *46*, 2366.
- [8] Rademacher, P. *Strukturen organischer Moleküle*, VCH, Weinheim, New York, **1987**.
- [9] (a) Desiraju, G. R. *Encyclopedia of Supramolecular Chemistry*, New York, Marcel Dekker Inc., **2004**. (b) Grabowski, S. J. *Chem. Rev.* **2011**, *111*, 2597. (c) Winkler, H. D. F. *Gasphasen-H/D-Austausch in der Supramolekularen Massenspektrometrie*, PhD thesis, Freie Universität Berlin, **2011**.
- [10] Hunter, C. A. *Angew. Chem. Int. Ed.* **2004**, *43*, 5310.
- [11] Braun, O.; Hüntten, A.; Vögtle, F. *J. prakt. Chem.* **1999**, *341*, 542.
- [12] Tatzke, M. *Synthese substituierter Tetralactam-Amidrotaxane*, Master thesis, Freie Universität Berlin, **2011**.
- [13] (a) Schalley, C. A.; Reckien, W.; Peyerimhoff, S.; Baytekin, B.; Vögtle, F. *Chem.-Eur. J.* **2004**, *10*, 4777. (b) Spickermann, C.; Felder, T.; Schalley, C. A.; Kirchner, B. *Chem.-Eur. J.* **2008**, *14*, 1216. (c) Zhu, S. S.; Nieger, M.; Daniels, J.; Felder, T.; Kossev, I.; Schmidt, T.; Sokolowski, M.; Vögtle, F.; Schalley, C. A. *Chem.-Eur. J.* **2009**, *15*, 5040. (d) Kirchner, B.; Spickermann, C.; Reckien, W.; Schalley, C. A. *J. Am. Chem. Soc.* **2010**, *132*, 484.
- [14] Händel, M.; Meier, S.; Hildebrandt, S. O.; Ott, F.; Schimdt, T.; Vögtle, F. *Liebigs Ann.* **1995**, 739.
- [15] (a) Conn, M. M.; Rebek Jr., J. *Chem. Rev.* **1997**, *97*, 1647. (b) Rebek Jr.; J. *Acc. Chem. Res.* **1999**, *32*, 278. (c) Warmuth, R.; Yoon, J. *Acc. Chem. Res.* **2001**, *34*, 95. (d) Hof, F.; Craig, S. L.; Nuckolls, C.; Rebek, Jr.; J. *Angew. Chem. Int. Ed.* **2002**, *41*, 1488. (e) Rebek, Jr.; J. *Acc. Chem. Res.* **2009**, *42*, 1660.
- [16] (a) Mansikkamäki, H.; Nissinen, M.; Schalley, C. A.; Rissanen, K. *New J. Chem.* **2003**, *27*, 88. (b) Mansikkamäki, H.; Schalley, C. A.; Nissinen, M.; Rissanen, K. *New J. Chem.* **2005**, *29*, 116.
- [17] Beyeh, N. K.; Kogej, M.; Åhman, A.; Rissanen, K.; Schalley, C. A. *Angew. Chem. Int. Ed.* **2006**, *45*, 5214.
- [18] Kvasnica, M.; Chapin, J. C.; Purse, B. W. *Angew. Chem. Int. Ed.* **2011**, *50*, 2244.

3.2. The Role of Self-Assembly and Self-Sorting...

This chapter discusses some fundamental concepts in supramolecular chemistry with the focus on (metallo-supramolecular) self-assembly and self-sorting. In principle, supramolecular chemistry is based on the molecular recognition approach, first mentioned by Fischer using his lock-and-key model in the enzyme-substrate chemistry.^[1] Nowadays, host-guest chemistry is more or less the consequence of the understanding of molecular recognition processes and the use of non-covalent bonds presented in chapter 3.1. Moreover, it combines these principles with other concepts such as self-assembly, self-sorting and template chemistry. Herein, molecular complementarity of the different non-covalent interactions in additive and/or cooperative manner is the most important factor in order to obtain an efficient synthesis and binding behavior of supramolecules. In addition to the complementarity of binding sites that leads to a sufficient binding effect, molecular preorganization might help to overcome some entropic costs that normally results from the host-guest interplay (and are normally overruled by enthalpy increase). A host that is designed to display the binding sites in a conformationally fixed way, perfectly complementary to the guest's needs, will bind much more strongly than a flexible host that needs to be rigidified in the binding event.^[2]

Supramolecular chemists have demonstrated that synthetic systems can be designed exhibiting molecular recognition. Two types of molecular recognition exist, static molecular recognition and dynamic molecular recognition.^[3] Static molecular recognition is simplified a 1:1-type complexation reaction between a host and a guest to form a host-guest complex through highly specific binding pathways. Some examples for this are already shown previously, e. g. different dicarbonyl compounds form host-guest complexes with TLMS or resorcin[4]arene-based capsules include a cation by formation of cation- π interactions. In comparison, dynamic molecular recognition proceeds through a two- (or more) step procedure where the binding of the first guest affects the association constant of a second guest with a second binding site and so on. This mode involves multivalency and cooperativity effects in order to provide a mechanism to regulate binding in biological systems as dynamic molecular recognition may enhance the ability to discriminate between several competing targets through conformational adjustment. Such recognition can be further useful for synthetic multivalent complexes that are one of the objectives of this work.

Self-assembly is an important concept as it leads to the reduction of the number of the building blocks needed for the formation of a supramolecule.^[4] Self-assembly is defined by Lehn as "the spontaneous association of either a few or many components resulting in the generation of either discrete oligomolecular supermolecules or extended polymolecular

assemblies such as molecular layer, films or membranes".^[5] Taking this into account, simple programmable building blocks with suitably positioned binding sites spontaneously self-assemble into the desired supramolecules under thermodynamic control. The last-mentioned fact leads to error correction during the assembly process and the products of interest can be obtained more or less quantitatively as they have lower Gibbs energies as their building blocks. Nature often utilizes this principle to construct very large architectures without significant loss of efficiency as can be seen in case of the tobacco mosaic virus, multienzyme complexes, the formation of cell membranes or molecular motors such as ATP synthase.^[6]

Supramolecular chemistry often points out the self-assembly approach to be useful in synthetic systems. As already mentioned in the chapter where hydrogen bonds are discussed, hydrogen-bonded capsules can spontaneously self-assemble by encapsulation of a guest and/or solvent molecules. Such capsules are quite versatile e. g. for supramolecular catalysis as reactions can take place efficiently inside their cavity, that are not possible in normal environment.^[7] However, especially coordination-driven self-assembly is in focus and can provide 2D- and 3D-shaped metallo-supramolecular polygons that can act as molecular container catalysators too. Fujita *et al.*^[8] and Stang *et al.*^[9] developed the use of metal coordination chemistry in combination with self-assembly in order to obtain the described supramolecules. As example, metallo-supramolecular squares are shown in Figure 12, both reported initially in the early 1990s.^[10]

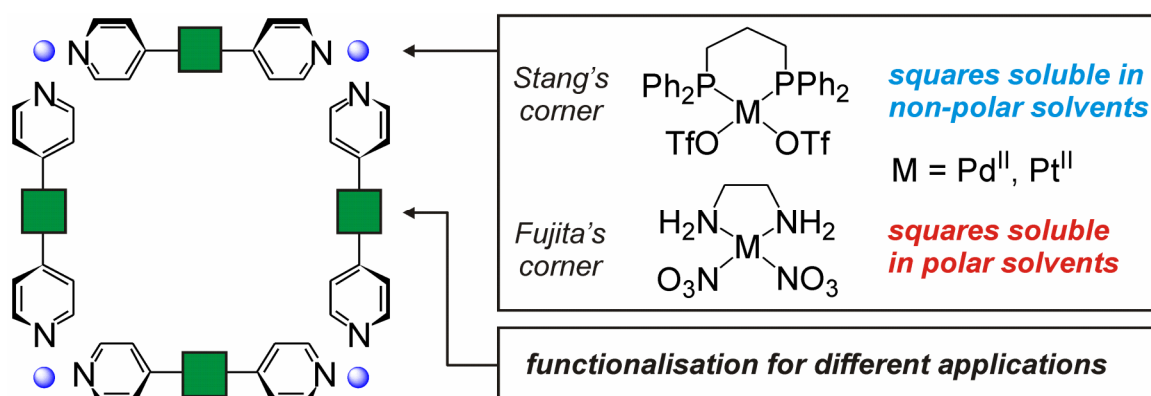


Figure 12. Schematic representation of metallo-supramolecular squares bearing either Fujita- or Stang-type metal corners. First squares were published without any functionality between the two pyridine moieties.

Such squares consists of a 4,4'-bipyridine (derivatives) as the ligand part and d⁸-square-planar Pd^{II} or Pt^{II} metal centers. One side of such metal species is blocked by different ancillary substituents; the other is occupied by weak bonded anions such as triflate or nitrate. At this side, coordination of e. g. pyridine-containing ligands can take place. While the so-called Stang's corner bears a dppp ancillary substituent and OTf as weak coordinating

anions, the so-called Fujita's corner is substituted by en (ethylene diamine) and NO_3^- as weak-coordinating counteranions. In addition, spacer groups can be implemented into the 4,4'-bipyridine core and the resulted squares can be functionalized with a wide arsenal of groups for supramolecular chemistry research. Interestingly, the solubility of such supramolecules depends on the metal center that is applied in the self-assembly process. If Stang's corner is used, the resulted assembly products are soluble in non-polar solvents such as CH_2Cl_2 . In comparison, the use of Fujita's corner leads to metallo-supramolecular polygons soluble in polar solvents, e.g. methanol or even water. This is, however, not general as the nature of the ligand must be taken into account.








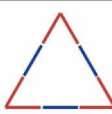


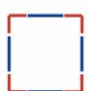

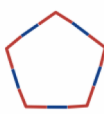









	 60°	 90°	 109,5°	 120°	 180°
 60°					
 90°					
 109,5°					
 120°					
 180°					

Figure 13. Metallo-supramolecular polygons that may result from the angles programmed into their building blocks (blue or red). Both can be either ligand molecules or metal species.^[11c]

In conclusion, the solubility of these molecules can be programmed in order to use an environment of interest, e. g. supramolecular catalysis in water. Another possibility to program supramolecules of interest is the angle between the binding sites in the desired ligand and/or metal corner. From this, the consistence of the metallo-supramolecular polygons can be estimated as shown in Figure 13.^[11] A similar table can be assembled for 3D-shaped metallo-supramolecular polygons.^[11b]

In addition to the metallo-supramolecular squares and other 2D-shaped metallo-supramolecules, the formation of 3D-shaped polygons was investigated. An example for this was reported by Schalley *et al.*^[12] Using the tridentate pyridine-terminated ligand and the Stang's $(\text{dppp})\text{Pd}^{\text{II}}(\text{OTf})_2$ metal center an equilibrium between a large bowl-shaped polygon and a small cage was observed (Figure 14). Moreover, the conversion of the large bowl-shaped polygon to a smaller cage was verified by tandem ESI MS experiments. Such contraction proceeds through a “backside attack” mechanism recently developed by Schalley *et al.* for squares that can contact to triangles in the gas phase in the same manner.^[13] This is a supramolecular analogue of a neighbor group effect. The mechanism developed after performing tandem ESI MS takes place under charge separation. Initially, a loss of a singly charged $(\text{dppp})\text{Pd}^{\text{II}}(\text{OTf})$ fragment occurs. The resulting unoccupied pyridine moiety attacks intramolecularly and the doubly charged (smaller) bowl is formed. The loss of a neutral ligand and opening of this bowl initializes the second bowl contraction through a similar attack. Such contractions can only be observed in the gas phase as the environment; especially the solvent might disturb them. However, they seem to occur quite often in supramolecular systems as observed for the metallo-supramolecular polygons discussed in chapter 4.5.

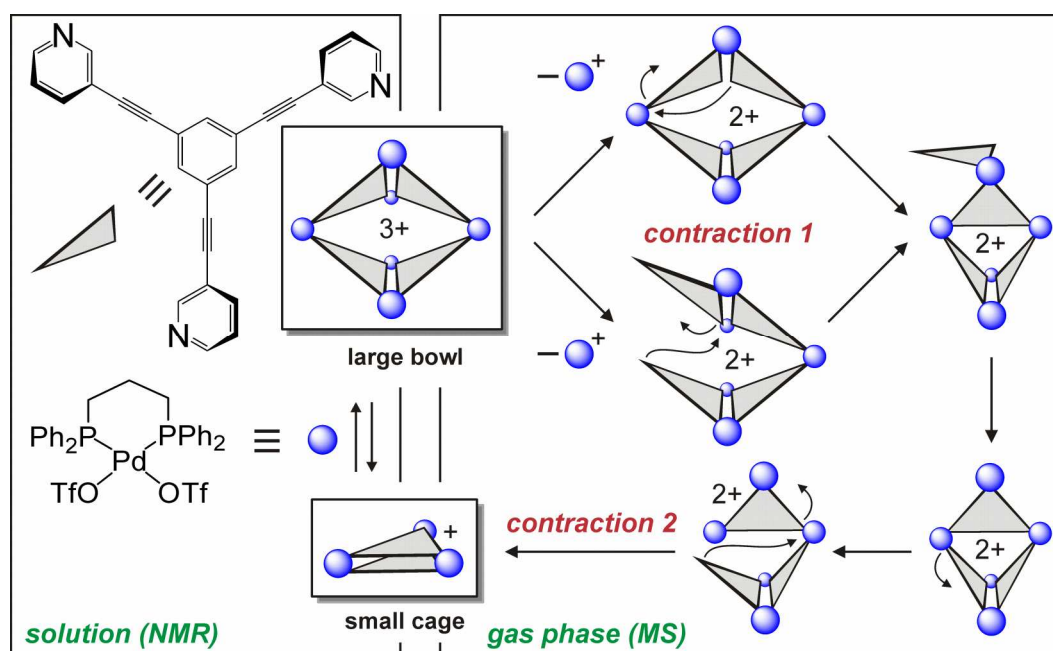


Figure 14. Equilibrium between the two possible structures formed from the tridentate ligand and $(\text{dppp})\text{Pd}^{\text{II}}(\text{OTf})_2$ in solution and the contraction pathway of the triply charged bowl ions that can be confirmed by tandem ESI MS.

A quite recent approach to introduce even more complexity into the supramolecules of interest is the concept of self-sorting developed first by Lehn *et al.*^[14] As mentioned for self-assembly, self-sorting also uses programmable building blocks and was defined by Isaacs *et al.* as “high fidelity recognition between molecules (and ions) within complex

mixtures".^[15] In principle, self-sorting means that only few structures (or even binding events) are observed instead of all possible because of discrimination occurs at some steps.

Generally, self-sorting systems can be subdivided into those that have reached under thermodynamic control or those that are trapped kinetically. Most examples operate under thermodynamic control.^[16] In addition, it can be differentiated between nonintegrative systems where more than one final structure result, and integrative systems that lead to one global complex bearing all elements of the mixture.^[17] The second-mentioned is the chief goal of research interest of a supramolecular chemists as it operates efficiently and under high atom/molecule economy. Taking this into account, the interplay of approaches such as size and shape, steric factors, hydrogen bond complementary and coordination sphere contributes significantly to the molecular codes that can be implemented by using self-sorting.

The ability of metal ions to coordinate strongly to ligands with different geometries is a powerful tool to force self-sorting processes. The coordination number and geometry of a metal ion depends fundamentally on its size, charge and electronic configuration, and the availability of properly matched ligands. Different metal ions can coordinate to ligands with diverse geometries that might become an increasingly relevant molecular code in the pursuit of systems with high complexity.^[16]

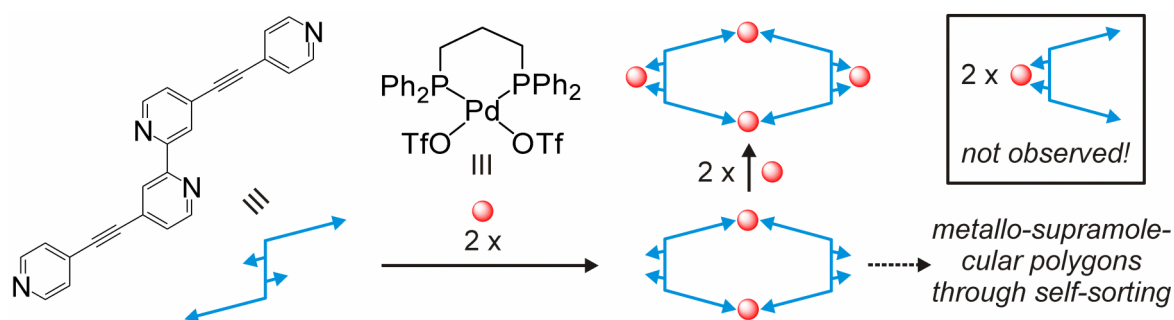


Figure 15. A 1:1 mixture of the tetradentate ligand and (dppp)Pd^{II}(OTf)₂ leads to an exclusive coordination at the pyridine site of the ligand under the formation of a M₂L₂ macrocycle. This can lead to further metallo-supramolecular polygons through self-sorting.

One of such metallo-supramolecular systems is described in chapter 4.6. It is based on the research recently discovered by Brusilowskij and Schalley.^[18] Here, a tetradentate ligand consisting of a 2,2'-bipyridine core substituted with 4-ethynylpyridine at the 4,4'-position is used (Figure 15). Upon mixing it with the (dppp)Pd^{II}(OTf)₂ metal center in 1 : 1 ratio in CD₂Cl₂, the pyridine site is occupied first and only a further addition of the metal leads to the coordination at the bipyridine. This can be rationalized by the fact that this coordination site is sterically more demanding due to repulsion between the bipyridine and the phenyl of the dppp at the Pd^{II} core. Thus, the coordination of (dppp)Pd^{II} to the bipyridine site is discriminated compared to the pyridine moiety of the ligand under study.

- [1] Fisher, E. *Ber. Deutsch. Chem. Ges.* **1894**, *27*, 2985.
- [2] Schalley, C. A., *Introduction*, in: *Analytical Methods in Supramolecular Chemistry* (Ed.: Schalley, C. A.), Wiley-VCH, Weinheim, **2007**, pp 1-16.
- [3] Roy, D. K.; Balanarayan, P.; Garde, S. R. *J. Chem. Sci.* **2009**, *121*, 815.
- [4] (a) Lindsey, J. S. *New J. Chem.* **1991**, *15*, 153. (b) Whitesides, G. M.; Mathias, J. P.; Seto, C. T. *Science* **1991**, *254*, 1312. (c) Philp, D.; Stoddart, J. F. *Angew. Chem. Int. Ed.* **1996**, *35*, 1154. (d) Schalley, C. A.; Lützen, A.; Albrecht, M. *Chem. Eur. J.* **2004**, *10*, 1072.
- [5] Lehn, J.-M. *Supramolecular Chemistry - Concepts and Perspectives*, Wiley-VCH, Weinheim, **1996**.
- [6] (a) Lindoy, L. F.; Atkinson, I. M. *Self-Assembly in Supramolecular Chemistry*, Royal Society of Chemistry, Cambridge, **2000** and literature cited herein. (b) Hamilton, T. D., *Self-Assembly in Biochemistry* in: *Encyclopedia of Supramolecular Chemistry* (Eds.: Atwood, J. L.; Steed, J. W.), Dekker, New York, **2004**, p 1257.
- [7] (a) *Supramolecular Catalysis* (Ed.: van Leeuwen, P. W. N. M.), Wiley-VCH, Weinheim, **2008** and literature cited herein. (b) Meeuwissen J.; Reek, J. N. H. *Nature Chem.* **2010**, *2*, 615.
- [8] (a) Fujita, M. *Chem. Soc. Rev.* **1998**, *27*, 417. (b) Fujita, M. *Acc. Chem. Res.* **1999**, *32*, 53. (c) Fujita, M.; Tominaga, M.; Hori, A.; Therrien, B. *Acc. Chem. Res.* **2005**, *38*, 371. (d) Klosterman, J. K.; Yamauchi, Y.; Fujita, M. *Chem. Soc. Rev.* **2009**, *38*, 1714.
- [9] (a) Stang, P. J.; Olenyuk, B. *Acc. Chem. Res.* **1997**, *30*, 502. (b) Seidel, S. R.; Stang, P. J. Stang, P. J.; Olenyuk, B. *Acc. Chem. Res.* **2002**, *35*, 972. (c) Northrop, B. H.; Yang, H.-B.; Stang, P. J. *Chem. Commun.* **2008**, 5896.
- [10] (a) Fujita, M.; Yazaki J.; Ogura, K. *J. Am. Chem. Soc.* **1990**, *112*, 5645. (b) D. H. Cao, P. J. Stang, *J. Am. Chem. Soc.* **1994**, *116*, 4981.
- [11] (a) Stang, P. J. *Chem. Eur. J.* **1998**, *4*, 19. (b) Leininger, S.; Olenyuk, B.; Stang, P. J. *Chem. Rev.* **2000**, *100*, 853. (c) Brusilowskij, B. *Studien zur Entschlüsselung von Komplexität in supramolekularen Architekturen*, PhD thesis, Freie Universität Berlin, **2010**. (d) Chakrabarty, R.; Mukherjee, P. S.; Stang, P. J. *Chem. Rev.* **2011**, DOI: 10.1021/cr200077m.
- [12] Brusilowskij, B.; Neubacher, S.; Schalley, C. A. *Chem. Commun.* **2009**, 785.
- [13] (a) Schalley, C. A.; Müller, T.; Linnartz, P.; Witt, M.; Schäfer, M.; Lützen, A. *Chem. Eur. J.* **2002**, *8*, 3538. (b) Engeser, M.; Rang, A.; Ferrer, M.; Gutierrez, A.; Baytekin, H. T.; Schalley, C. A. *Int. J. Mass Spectrom.* **2006**, *255*, 185.
- [14] Kramer, R.; Lehn, J.-M.; Marquisrigault, A. *Proc. Natl. Acad. Sci. USA* **1993**, *90*, 5394.
- [15] Wu, A. X.; Isaacs, L. *J. Am. Chem. Soc.* **2003**, *125*, 4831
- [16] Safont-Sempere, M. M.; Fernández, G.; Würthner, F. *Chem. Rev.* **2011**, DOI: 10.1021/cr100357h and literature cited herein.
- [17] Jiang, W.; Schalley, C. A. *Proc. Natl. Acad. Sci. USA* **2009**, *106*, 10425.
- [18] Brusilowskij, B.; Schalley, C. A. *Eur. J. Org. Chem.* **2011**, 469.

3.3. ... and the Impact of Multivalency and Cooperativity

The concept of multivalency denominates the phenomenon of simultaneous non-covalent binding event of multiple complementary functionalities on two (or more) entities, e. g. host-guest interactions (Figure 16).^[1] The resulting multivalent supramolecular complex is formed with binding affinities K_a and binding enthalpies ΔH often significantly higher than the sum of the corresponding monovalent interactions. This leads to higher thermodynamic (and kinetic) stability resulting in highly efficient molecular associations if requirements such as (i) preorganization of the binding partner through covalent linkage and/or (ii) introduction of a extensive number of binding actions are followed in order to overcome the significant loss of entropy. Taking this into account, multivalency is supposed to play a fundamental role in numerous biochemical processes, including signal transduction, pathogenic infection, and immune response and therefore gets an increased interest as a powerful tool for the development of synthetic receptors with high affinity and specificity for biological targets.^[2] An example for a typical multivalent interaction in nature for instance is the adhesion processes of viruses such as an influenza virus to the cell surface.^[3] Besides a binding energy increase, multivalency also affords control over the geometry of the interacting compounds through multi-point interaction. Viruses for example are able to change the cell surface to induce their endocytosis through multivalent interactions.

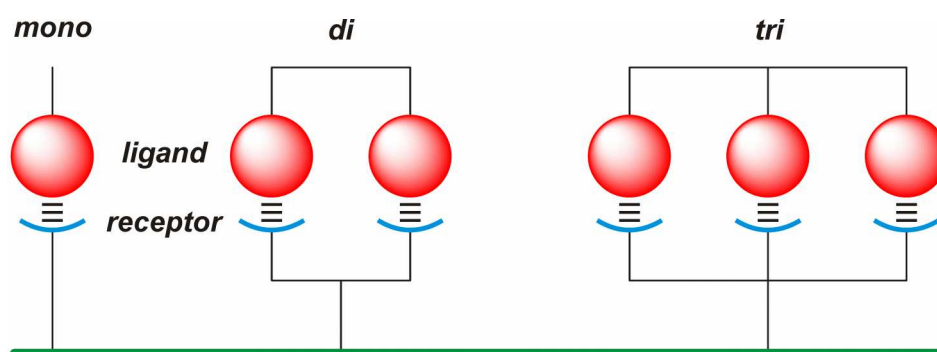


Figure 16. Schematic representation of mono-, di- and trivalent interactions between a ligand and a receptor. Such interactions can for example take place on a cell surface and play an important role by adhesion processes^[4] of viruses, bacteria or antibodies or the interaction between proteins^[5].

In addition, the use of multivalent effects promises supramolecular chemists to construct complex supramolecular architectures with new topologies and functionalities in a very efficient manner from suitably programmed building blocks.^[6] Their application might revolutionize the field of supramolecular chemistry. Multivalent studies on synthetic targets can mimic and therefore help to understand processes occur in nature where multivalency is under a cloud to be essential. A number of studies on multivalent interactions in synthetic

host-guest complexes have been realized, among using calixarenes,^[7] cyclodextrin complexes^[8] and multiply interlocked (pseudo)rotaxanes.^[9] Several multivalent complexes have been studied and reported in detail with respect to their individual binding inputs^[10] and numerous theoretical models exist to describe them so far.^[11]

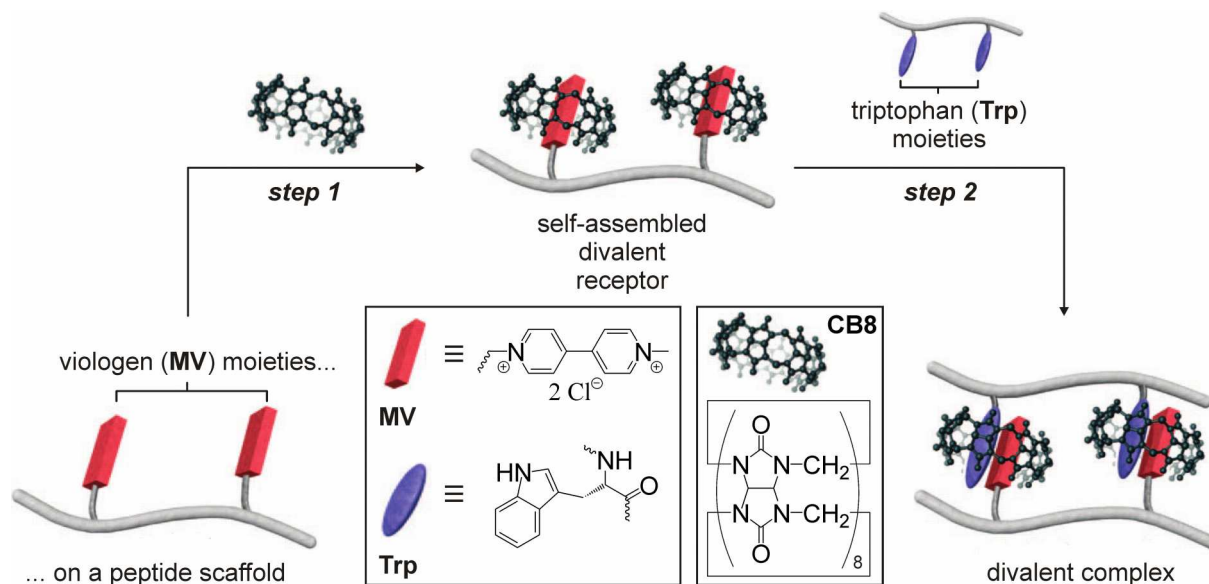


Figure 17. Schematic representation of the system adapted from Urbach *et al.* using viologen (**MV**) moieties on a peptide scaffold. They form the divalent receptors (**CB8•MV**)_n by adding cucurbit[8]uril (**CB8**) in aqueous solution and are then able to perform a multivalent interaction to the peptide scaffolds decorated with tryptophan (**Trp**) moieties.

A current study of Urbach *et al.*^[12] nicely underlines the relevance of multivalency in supramolecular chemistry. Herein, the viologen (**MV**)/cucurbit[8]uril (**CB8**) binding motif was introduced into a series of multivalent host-guest complexes and used for the evaluation of multivalent interactions in water (Figure 17). The final complexes are constructed from a peptide scaffold decorated on the one hand with doubly charged viologen guest molecules and on the other hand with tryptophan (**Trp**) units, also connected through a peptide backbone. Cucurbit[8]uril (**CB8**) is used as the connection-directed macrocyclic compound. The self-assembled mono-, di-, and trivalent receptors (**CB8•MV**)_n ($n = 1 - 3$) that are formed with viologen binding units deposited on the peptide backbone and **CB8** in a discrete fashion, bind to their target peptides containing 1 - 3 **Trp** scaffolds with 3 - 280-fold enhancements in affinity and additive enthalpies due to multivalency. The predictable behavior of this system make it well suited to serve as a model for multivalent binding: (i) the complete research can be performed in aqueous media and the results would therefore have an impact on biologically relevant complexes, (ii) the molecules can be easily obtained using an automatically peptide synthesizer in a likely “toolbox” manner as described for the TLM’s above and no significant differences in practicability are required and (iii) a striking

combination of ^1H NMR, UV-Vis and ITC was used in order to evaluate the multivalent binding. The last aspects mentioned here are important for this thesis as e. g. the compounds bearing the TLM/dicarbonyl binding motif that were used in the mono- and multivalent research rely on these characteristics. However, the supramolecules shown in Figure 17 were focused only related to their increasing in binding association constants (and energies) synchronistic to the increase in the additional binding sites and no further predication was made in order to explain what happen in the single binding states of for example a trivalent host-guest interaction.

On the contrary, cooperativity summarizes effects of the host-guest binding that influences the single steps in the formation of the complete host-guest architecture through further interactions.^[13] Consequently, the stepwise binding is in the focus and not the overall binding affinity. In principle, cooperativity can be divided into two types: (i) chelate cooperativity between multiple interaction sites and (ii) allosteric cooperativity. An example for the second type is the binding of oxygen molecules to hemoglobin, where the first binding event of oxygen leads to a reformation of the hemoglobin moieties in order to binding the second oxygen with higher affinity. Further classification of cooperativity can be done into three groups: (i) positive (synergistic), when the binding affinity of the subsequent binding event is higher than that for the previous one; (ii) negative (interfering), when the binding is lower, and (iii) noncooperative (additive), when the binding affinity is identical. It should be mentioned herein that multivalency and cooperativity do not exclude each other. In many cases, cooperative systems are also multivalent systems. However, in comparison to this only few multivalent systems show also positive cooperative behavior.^[14]

In order to describe and therefore understand the thermodynamic aspects of multivalent binding, an approach based on the additivity of the Gibbs free energies (ΔG) can be used as shown in equation 4.

$$\text{(eq. 4)} \quad \Delta G_{\text{multi}} = n \Delta G_{\text{mono}} + \Delta G_{\text{interaction}}$$

(ΔG_{mono} is the standard free binding energy of the corresponding monovalent interaction, n is the valency of the complex and $\Delta G_{\text{interaction}}$ is the balance between favorable and unfavorable effects of the binding event)

The binding (or affinity) constant K_{multi} of a multivalent interaction is selected as the binding strength of a multivalent interaction and summarizes all possible interactions between two or more entities. It is related to the Gibbs energy by equation 5.

$$(eq. 5) \quad \Delta G_{multi} = - RT \ln K_{multi}$$

Two parameters α and β were introduced by Whitesides *et al.*^[1a] in order to describe multivalent interactions more precisely. The value α is the cooperativity factor and leads to the prediction whether a binding is cooperative or not. It is defined by equation 6.

$$(eq. 6) \quad \alpha = \frac{\Delta G_{multi}}{n \Delta G_{mono}}$$

A positive cooperativity is observed if $\alpha > 1$; otherwise, a negative cooperative interaction can be postulated or the interaction is only pure additive if $\alpha = 1$. However, the determination of α values requires knowledge about the number of binding partners, which is not known in many instances, for example if synthetical or biological polymers are under study.

In addition, the contribution of the multivalency is often expressed with the enhancement factor β , also introduced also by Whitesides *et al.*^[1a] and defined as shown in equation 7. This parameter reflects the strength of a multivalent association compared to a monovalent one and is often used to compare the efficiency of guests bearing different structural characteristics with respect to its conformation or valency. Molecules with high β values are more efficient in their multivalent binding then compounds with a lower one.

$$(eq. 7) \quad \beta = \frac{K_{multi}}{K_{mono}}$$

An alternative model was specified by Reinhoudt *et al.*^[15] and takes both the effective concentration (C_{eff}) and effective molarity (EM)^[16] into account to describe a stepwise multivalent binding (Figure 18). These parameters can be illustrated by equations 8 and 9.

$$(eq. 8) \quad K_{multi} = \gamma (K_{mono})^n (C_{eff})^{n-1}$$

$$(eq. 9) \quad EM = \left[\frac{K_{multi}}{\gamma (K_{mono})^n} \right]^{\frac{1}{n-1}} = \frac{K_{intera}}{K_{intera}}$$

Herein, the value γ collects all statistical factors determining the numbers of possible association/dissociation pathways in the subsequent interaction steps.

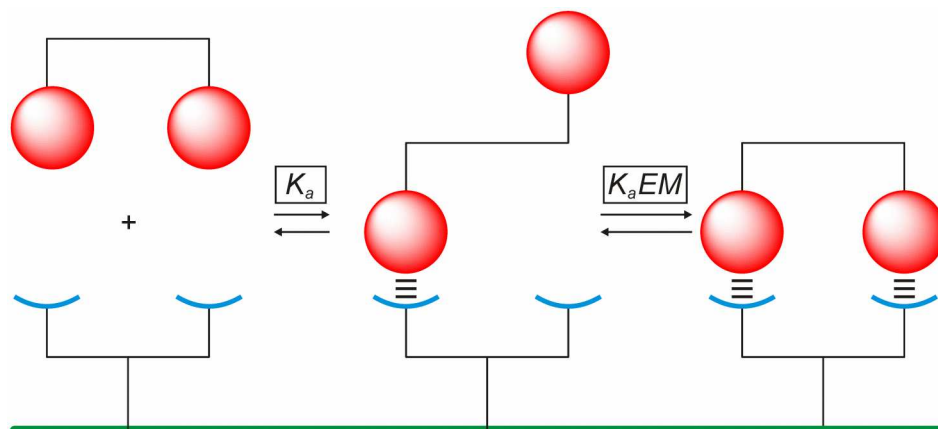


Figure 18. Schematic representation of a divalent cooperative binding interaction at a molecular recognition interface.^[17]

The effective concentration C_{eff} gives rise to a concentration-dependent binding mode for multivalent interactions. Intramolecular binding is favored at low concentrations and intermolecular binding at high concentrations. It is conceptually similar to the more generally used effective molarity (EM). On the one hand, C_{eff} is based on concentrations calculated or estimated from physical geometries of complexes such as spacer rigidity and length. Effective molarity EM on the other hand signifies the ratio of intra- and intermolecular binding affinities K_{intra} and K_{inter} (eq. 9) and can be measured directly in an experiment. High EM values emerge if intramolecular processes benefit over the corresponding intermolecular ones and therefore the knowledge of the EM value is of great interest for an accurate quantification of cooperativity and multivalency effects.

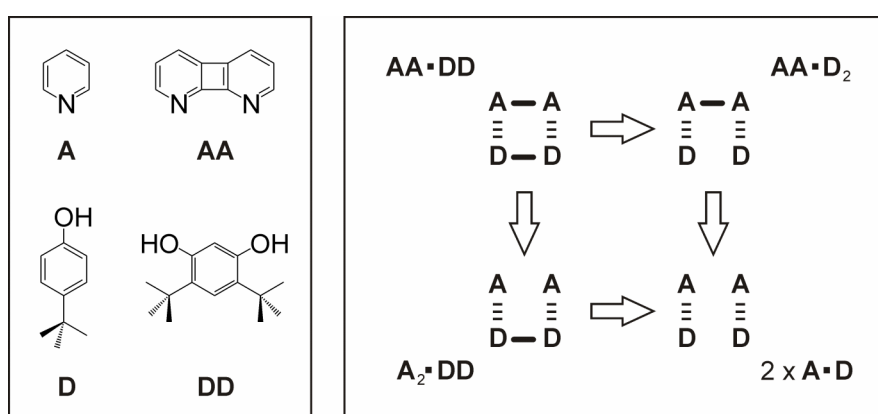


Figure 19. Double mutant cycle to quantify the free energy, the binding affinity and the effective molarity of a divalent hydrogen-bonded complex $AA\cdot DD$ (A = hydrogen-bond acceptor, D = hydrogen-bond donor).

In order to quantify the *EM* values in divalent hydrogen-bonded supramolecules experimentally, Hunter *et al.* introduced the use of the chemical double mutant cycle (Figure 19).^[18] Herein, the system consists of pyridine (**A**) and 1,8-diazabiphenylene (**AA**) as the mono- and divalent hydrogen bond acceptors on the one side and 4-tertbutylphenol (**D**) and diterbutyl-substituted resorcinol (**DD**) hydrogen bond donors on the other side. If using supramolecules interacting through hydrogen bonding, self-association phenomena can complicate the evaluation. However, this error can be minimized using this combination shown in Figure 19 because phenols are bad hydrogen acceptors but good hydrogen bond donors to for example the pyridine nitrogen atoms. Hence, by careful determination of the thermodynamic values of the hydrogen-bonded donor-acceptor pairs **AA•DD**, **AA•D₂**, **A₂•DD** and **A•D** by usual analytical methods (NMR, ITC, UV-Vis, see chapter 3.5), the *EM* value and the energy of the cooperativity $\Delta\Delta G^\circ$ can be estimated using equations 10 and 11.

$$(eq. 10) \quad 2 EM = K(\mathbf{AA}\cdot\mathbf{DD}) K^2(\mathbf{A}\cdot\mathbf{D}) / K(\mathbf{AA}\cdot\mathbf{D}_2) K(\mathbf{A}_2\cdot\mathbf{DD})$$

$$(eq. 11) \quad \Delta\Delta G^\circ = \Delta G^\circ(\mathbf{AA}\cdot\mathbf{DD}) - \Delta G^\circ(\mathbf{AA}\cdot\mathbf{D}_2) - \Delta G^\circ(\mathbf{A}_2\cdot\mathbf{DD}) - 2\Delta G^\circ(\mathbf{A}\cdot\mathbf{D}) = - RT \ln(2 EM)$$

Cooperative and multivalent effects can also influence the kinetic behavior of supramolecules. Thus, the trivalent elevator molecules described by Stoddart *et al.* are prominent examples (see also chapter 3.4).^[9a,b,c] While the first two threading processes of the ammonium-based guest into the cavities of two of three crown ether moieties of the trivalent host are fast and cannot be followed by ¹H NMR, the last step proceeds after approximately 7 days. By taking this into account, a clear two-step process of the threading of the trivalent guest into the trivalent host was observed with the first step being kinetically and the second one thermodynamically controlled.

-
- [1] (a) Mammen, M.; Choi, S.-K.; Whitesides, G. M. *Angew. Chem. Int. Ed.* **1998**, *37*, 2754. (b) Kiessling, L. L.; Gestwicki, J. E.; Strong, L. E. *Angew. Chem. Int. Ed.* **2006**, *45*, 2348. (c) Ludden, M. J. W.; Reinhoudt, D. N.; Huskens, *Chem. Soc. Rev.* **2006**, *35*, 1122. (d) Rehm, T.; Schmuck, C. *Chem. Commun.* **2008**, 801. (e) Ling, X. Y.; Reinhoudt, D. N.; Huskens, J. *Pure Appl. Chem.* **2009**, 2225. (f) Schneider, H.-J. *Angew. Chem. Int. Ed.* **2009**, *48*, 3924. (g) Uhlenheuer, D. A.; Petkau, K.; Brunsveld, L. *Chem. Soc. Rev.* **2010**, *39*, 2817.
- [2] (a) Chen, H.; Privalsky, M. L. *Proc. Natl. Acad. Sci. USA* **1995**, *92*, 422. (c) Connell, I.; Agace, W.; Klemm, P.; Schembri, M.; Mårild, S.; Svanborg, C. *Proc. Natl. Acad. Sci. USA* **1996**, *93*, 9827. (c) Sacchettini, J. C.; Baum, L. G.; Brewer, C. F. *Biochemistry* **2001**, *40*, 3009. (d) Lindhorst, T. K. *Top. Curr. Chem.* **2002**, *218*, 201.

- [3] Lees, W. J.; Spaltenstein, A.; Kingery-Wood, J. E.; Whitesides, G. M. *J. Med. Chem.* **1994**, *37*, 3419.
- [4] (a) Mager, M. D.; LaPointe, V.; Stevens, M. M. *Nature Chem.* **2011**, *3*, 582. (b) Li, L.; Klim, J. R.; Derda, R.; Courtney, A. H.; Kiessling, L. L. *Proc. Natl. Acad. Sci. USA* **2011**, DOI: 10.1073/pnas.1101454108.
- [5] Stites, W. E. *Chem. Rev.* **1997**, *97*, 1233.
- [6] (a) Röckendorf, N.; Lindhorst, T. K. *Top. Curr. Chem.* **2001**, *217*, 201. (b) Badjić, J. D.; Nelson, A.; Cantrill, S. J.; Turnbull, W. B.; Stoddart, J. F. *Acc. Chem. Res.* **2005**, *38*, 723.
- [7] (a) Casnati, A.; Sansone, F.; Ungaro, R. *Acc. Chem. Res.* **2003**, *36*, 246. (b) Sansone, F.; Baldini, L.; Casnati, A.; Ungaro, R. *New J. Chem.* **2010**, *34*, 2715.
- [8] (a) Nijhuis, C. A.; Yu, F.; Knoll, W.; Huskens, J.; Reinhoudt, D. N. *Langmuir* **2005**, *21*, 7866. (b) Liu, Y.; Chen, Y. *Acc. Chem. Res.* **2006**, *39*, 681. (c) Huskens, J. *Curr. Opin. Chem. Biol.* **2006**, *10*, 537.
- [9] (a) Badjić, J. D.; Balzani, V.; Credi, A.; Lowe, J. N.; Silvi, S.; Stoddart, J. F. *Chem.-Eur. J.* **2004**, *10*, 1926. (b) Badjić, J. D.; Cantrill, S. J.; Grubbs, R. H.; Guidry, E. N.; Orenes, R.; Stoddart, J. F. *Angew. Chem. Int. Ed.* **2004**, *43*, 3273. (c) Zhu, X.-Z.; Chen, C.-F. *J. Am. Chem. Soc.* **2005**, *127*, 13158. (d) Jiang, Y.; Zhu, X.-Z.; Chen, C.-F. *Chem.-Eur. J.* **2010**, *16*, 14285. (e) Chen, C.-F. *Chem. Commun.* **2011**, *47*, 1674.
- [10] (a) Bisson, A. P.; Carver, F. J.; Hunter, C. A.; Waltho, J. P. *J. Am. Chem. Soc.* **1994**, *116*, 10292. (b) Bisson, A. P.; Hunter, C. A. *Chem. Commun.* **1996**, 1723. (c) Adams, H.; Hunter, C. A.; Lawson, K. R.; Perkins, J.; Spey, S. E.; Urch, C. J.; Sanderson, J. M. *Chem.-Eur. J.* **2001**, *7*, 4863. (d) Ballester, P.; Oliva, A. I.; Costa, A.; Deyà, P. M.; Frontera, A.; Gomila, R. M.; Hunter, C. A. *J. Am. Chem. Soc.* **2006**, *128*, 5560.
- [11] (a) Kitov, P. I.; Bundle, D. R. *J. Am. Chem. Soc.* **2003**, *125*, 16271. (b) Ercolani, G. *J. Am. Chem. Soc.* **2003**, *125*, 16097. (c) Ercolani, G. *J. Phys. Chem. B* **2003**, *107*, 5052. (d) Huskens, J.; Mulder, A.; Auletta, T.; Nijhuis, C. A.; Ludden, M. J. W.; Reinhoudt, D. N. *J. Am. Chem. Soc.* **2004**, *126*, 6784. (e) Ercolani, G.; Schiaffino, L. *Angew. Chem. Int. Ed.* **2011**, *50*, 1762.
- [12] Reczek, J. J.; Kennedy, A. A.; Halbert, B. T.; Urbach, A. R. *J. Am. Chem. Soc.* **2009**, *131*, 2408.
- [13] (a) Hunter, C. A.; Anderson, H. L. *Angew. Chem. Int. Ed.* **2009**, *48*, 7488. (b) Ercolani, G.; Schiaffino, L. *Angew. Chem. Int. Ed.* **2011**, *50*, 1762.
- [14] (a) Shinkai, S.; Ikeda, M.; Sugasaki, A.; Takeuchi, M. *Acc. Chem. Res.* **2001**, *34*, 494.
- [15] Mulder, A.; Huskens, J.; Reinhoudt, D. N. *Org. Biomol. Chem.* **2004**, *2*, 3409.
- [16] Cacciapaglia, R.; Di Stefano, S.; Mandolini, L. *Acc. Chem. Res.* **2004**, *37*, 113.
- [17] Chekmeneva, E.; Hunter, C. A.; Packer, M. J.; Turega, S. M. *J. Am. Chem. Soc.* **2008**, *130*, 17718.
- [18] (a) Cockroft, S. L.; Hunter, C. A. *Chem. Soc. Rev.* **2007**, *36*, 172. (b) Camara-Campos, A.; Musumeci, D.; Hunter, C. A.; Turega, S. M. *J. Am. Chem. Soc.* **2009**, *131*, 18518.

3.4. A “Supramolecular Exception”: The Mechanical Bond in Interlocked Molecules

So far, approaches described above can be summarized as the use of more or less reversible non-covalent bonds to form molecules that can dissociate by breaking those bonds using light, temperature or chemical stimuli. The concept of mechanically interlocked supramolecular architectures differs significantly and features molecules that can only dissociate after breaking of covalent bonds in their topology. Consequently, the compounds linked in these supramolecules are not assembled in a classical reversible manner. Stoddart *et al.*^[1] therefore coined the term “the mechanical bond” in order to unify the special features of such molecules. The examples mostly accentuated in the literature are [n]catenanes and [n]rotaxanes schematically shown in Figure 20. The concepts of multivalency, cooperativity, self-assembly and self-sorting play an important role and lead to the research of powerful templates that can be used for the preorganization of the supramolecules before the formation of the mechanical bond. The mechanically interlocked supramolecules cannot then destroyed so easy as their non-covalent bonded siblings but still have their characteristics such as motion processes or response if using an input, e. g. light, electrons or chemicals.

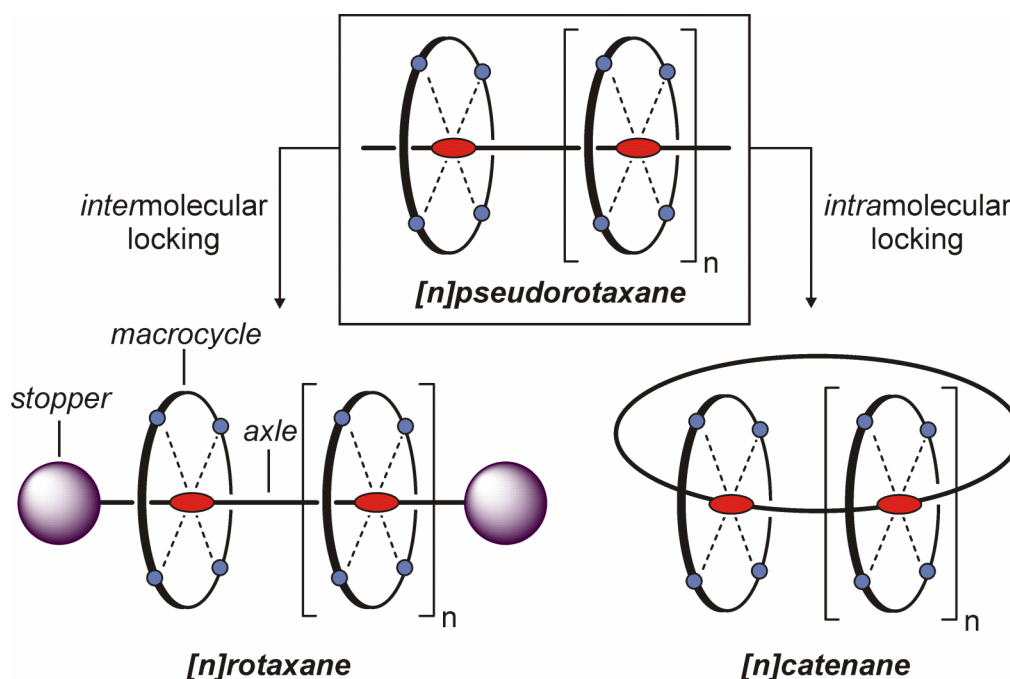


Figure 20. Schematic representation the formation of mechanically interlocked [n]rotaxanes or [n]catenanes from an [n]pseudorotaxane. The number $n = 0, 1, 2, 3 \dots$ denotes the number of macrocycles incorporated in these supramolecular species. The supramolecular concepts described above contribute to the formation of the [n]pseudorotaxanen in a reversible non-covalent manner.

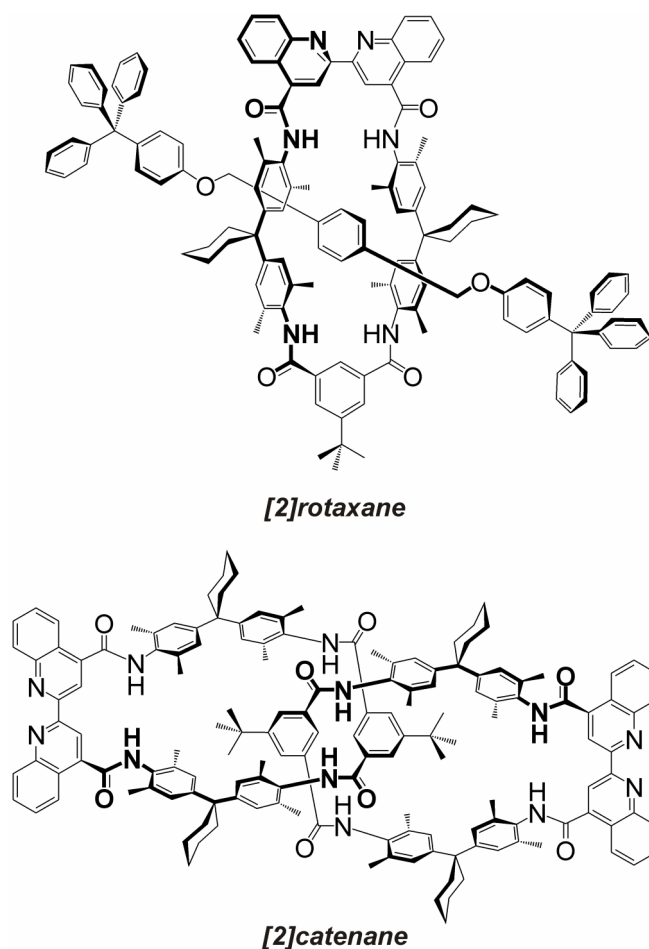


Figure 21. Two examples for mechanically interlocked molecules: [2]rotaxane consisting of a TLM and a bisether axle centerpiece and a [2]catenane bearing two intertwined TLM's.

An [n]rotaxane consists of three main components: (i) a macrocycle that acts as the host molecule for the (ii) linear-shaped axle compound incorporating the binding motif that forms non-covalent interactions to the macrocycle and (iii) bulky stopper groups that prevent the axle from deslipping. Consequently, the formation of the mechanical bond is caused by an intermolecular locking process. In contrary, an [n]catenane results from an intramolecular locking process, where both ends of the axle react with each other to a continuous centerpiece. Both types of mechanically bonded supramolecules can be initially formed from an [n]pseudorotaxane bearing a number n of macrocycles and a axle-type molecules both bond by non-covalent interactions after a reversible self-assembly process has taken place.

Examples for a [2]rotaxane and a [2]catenane are shown in Figure 21.^[2] Both compounds bear a TLM that is widely used in this thesis as described in chapter 3.1. While the [2]rotaxane is composed of a bisquinone-substituted TLM and a bisether axle end-capped with trityl phenyl stoppers synthesized via “anion template” (see below),^[3] the [2]catenane bears two identical TLMs in an intertwined manner. Such [2]catenanes are so-called homocircuit. It should be pointed out that catenanes are topological isomers of their mechanically non-interlocked components as they cannot be separated from each other without destroying one of the rings by breaking a covalent bond. In marked contrast, rotaxanes are topologically not isomeric to their non-interlocked components since an expansion of the macrocycle would lead to dissociation without breaking a covalent bond.

First interlocked supramolecules were initially obtained independently by Harrison *et al.* and Schill *et al.* who presented first [2]rotaxanes in the late 60s.^[4] However, their synthetical approach was statistical and therefore time-consuming, and the desired

molecules were only obtained in low yields.^[5] Nowadays, a better understanding of non-covalent interactions such as hydrogen bonding or the use metal coordination chemistry has led to a number of powerful templates with high affinities and discrete directional binding. Taking this into account, synthetic pathways exist for the introduction of mechanical bonds in [n]catenanes and [n]rotaxanes (Figure 22 and 23).^[6]

[n]Catenanes can be synthesized by so-called “clipping” approach using either a macrocycle and its linear precursor or two precursors of a macrocycle. Both combinations form in the first step preorganized pseudorotaxanes that can be then locked in the last step (Figure 22). The success of this approach strongly depends on the concentration and on the specificity of the reaction used for the ring-closing step. On the one hand, the non-covalent bonded pseudocatenane can dissociate at a too low concentration, on the other hand, polymer byproducts can be formed in the macrocyclization step. Therefore, the reaction conditions need to be controlled very accurately.

In comparison, [n]rotaxanes can be obtained by means of using three reaction procedures: (i) the “slipping” method (Figure 23) requires a macrocycle and an axle compound that already bears bulky stopper groups. If both were mixed, the increase of the temperature leads to the enlargement of the size of the macrocycle allowing it then to “slippage” over the stopper groups of the axle. After cooling down, the cavity size of the macrocycle decreases and no “slipping” back is therefore possible. Herein, the bulkiness of the stoppers is of great importance. If they are sterically too demanding, the macrocyclic compound has no chance to slip over them, not even at very high temperatures (which in addition can cause decomposition of the compounds). In contrast, too small groups would lead to a too low dissociation barrier between threaded and non-threaded compounds and equilibrium between them would be observable. Therefore, this synthetic approach is often challenging; (ii) the “clipping” method uses two non-cyclic precursors that form a preorganized complex bond through templating effects as shown for a [2]catenane above. One of those axles already bears stopper groups. After that, a cyclisation can take place and the [2]rotaxane is formed. This method is required if a very strong template effect is used and

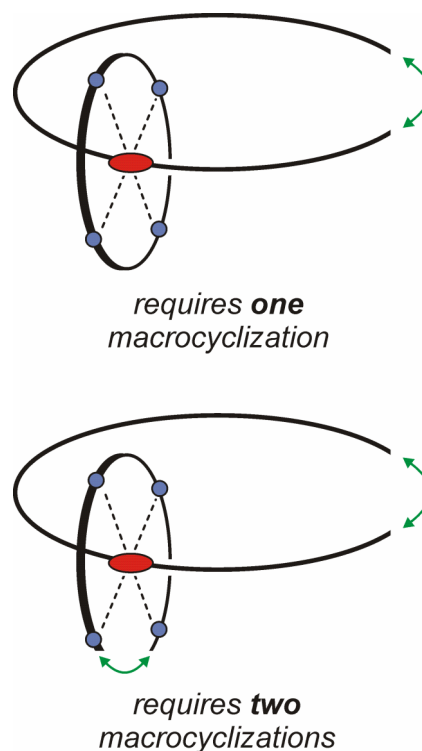


Figure 22. Schematical representation of two possible [2]pseudorotaxanes that can be locked to [2]catenanes after macrocyclization reaction (indicated by arrows).

polymer formation is suppressed. However, this is not always the case and this reaction leads often to yields about 30-50%; (iii) the “threading” or “trapping” approach is used most commonly in the synthesis of [2]rotaxanes. The axle (or semi-axle^[7]) bearing a binding motif (“template”) is enclosed by the macrocycle in the first step and after that, the stopper groups are attached in order to prevent a deslipping process. This method was used for the synthesis of [2]rotaxanes bearing diketopiperazine binding motif described in chapter 4.4.

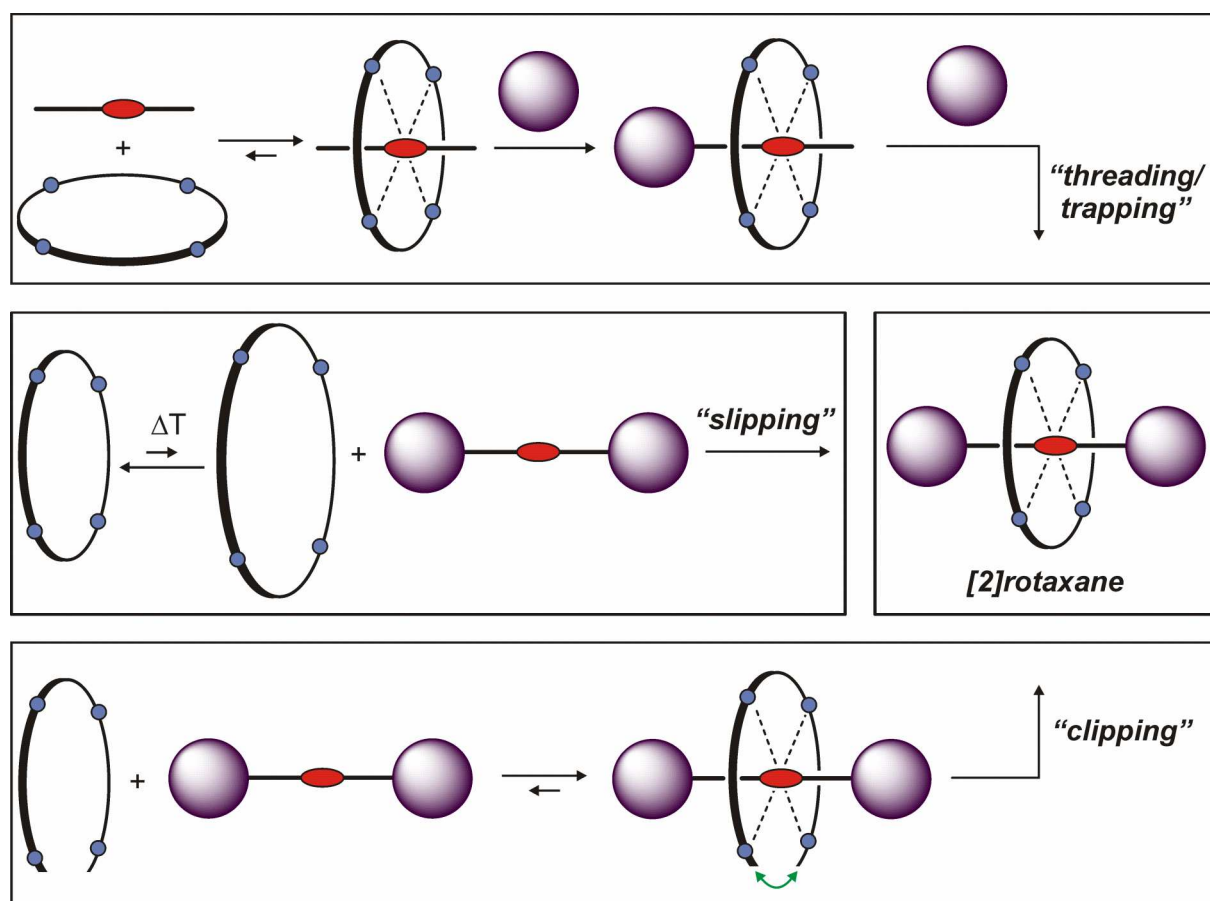


Figure 23. Schematic representation of the three different methods for the synthesis of [2]rotaxanes. Note that depending on the stoppering reaction (intermolecular vs. intramolecular locking), [2]catenanes can be formed in case of the use of “clipping” and “threading” method.

The choice of one of these three routes for the preparation of a rotaxane depends mainly on the chemical nature of the different components and the chemistry required establishing the interlocked molecule. A strong and directional interaction between the two individual components is therefore of great importance as the driving force in the synthesis of rotaxanes and catenanes. Herein, few examples of interlocked molecules (especially rotaxanes) should demonstrate their potential and focus on the remarkable features that can be introduced into them.

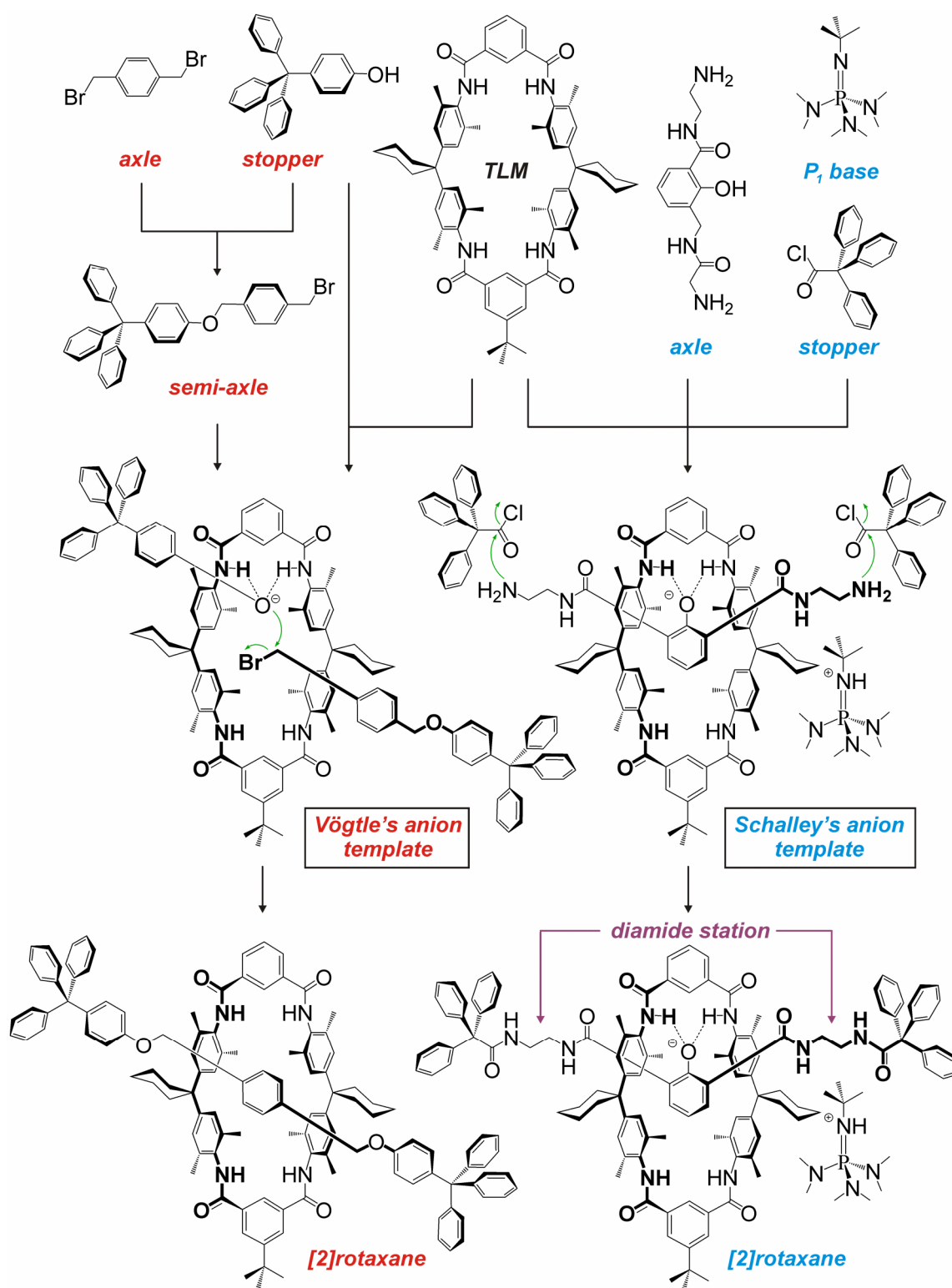


Figure 24. Synthetical approach towards [2]rotaxanes using Vögtle's (left, red-colored) and Schalley's anion template (right, blue-colored). Both routes require an addition of a base (see text) and are exemplary shown on one TLM with a hydrogen and a tertbutyl group as substituents at the isophthaloyl moiety. However, these substituents can be replaced in order to obtain e.g. multivalent architectures (see chapters 2, 3.1, 4.2 and 4.3). Arrows indicate the stopper attachments.

The first example presented here is related to the [2]rotaxanes already shown in Figure 24. It describes the synthesis of [2]rotaxanes through “anion template” initially reported by Vögtle *et al.* and Schalley *et al.*^[3,8] This approach is advantageous for two reasons: (i) the desired [2]rotaxanes can be obtained in high yields up to 95% and (ii) this template effect can be used for the construction of even more complex architectures related the investigations of e. g. multivalency effects from easily obtainable precursors as described in chapters 3.1 and 4.2. The Vögtle’s anion template synthesis of [2]rotaxanes^[3] uses a dibromo dibenzyl axle centerpiece, a TLM and a phenolic stopper. Initially, the reaction conditions used here (K_2CO_3 and dibenzo-24-crown-8 in CH_2Cl_2) lead to the deprotonation of the phenol to the phenolate, which after this is buried inside the wheel’s cavity by forming two hydrogen bonds to the amide hydrogens. The oxygen of the phenolate can then attack the benzylic position of the semi-axle, which is formed from the dibromo dibenzyl axle and one equivalent of the tritylphenolate stopper obtained after deprotonation. Note that the complete reaction proceeds in one-pot reaction, i. g. deprotonation, threading and formation of the semi-axle. In comparison, the Schalley’s anion template^[8] requires a phenol-centered axle end-capped with two diamide moieties. The diamide motif was recently investigated and discussed in chapter 4.1 and 4.3 on mono- and multivalent diamide guest molecules. However, after the deprotonation of the phenol centerpiece resulting in a phenolate, a threading process into the cavity of TLM occurs in analogy to the Vögtle’s anion template. As a base Schwesinger’s P_1 base^[9] was used that is sufficient for a complete deprotonation and provides good solubility of the resulting phenolate salt in non-competitive solvents. Adding the acid chloride stopper and NEt_3 as a base result in the formation of the desired [2]rotaxanes in yields of 20 - 30%. The special feature of this approach is that the site bond in the cavity of the TLM in the pseudorotaxane is not implemented in the reactive stoppering step as in case of the Vögtle’s anion template, where the phenolate forms an ether moiety after attacking the benzylic position of the semia-axle and loses the hydrogen bonding to the TLM. Thus, the structural and dynamic composition of the [2]rotaxane is not influenced.

The [2]rotaxane obtained from the use of Schalley’s “anion template” is interesting for a second reason. Besides a rotation of the TLM that normally occur a traveling of the TLM along the axle over the phenol between the two diamide stations is observed using 1H NMR experiments. Surprisingly, deprotonation of the phenol to the phenolate by the P_1 base does not lead to a complete suppression of this shuttling motion. The reason for this is due to the nature of the electrostatic interactions. The TLM is still able to pass through the phenolate/protonated P_1 moiety since its formation is reversible and only the motion rate was lowered. Consequently, the cation acts as a “brake” for the shuttling movement (Figure 25) and the shuttling speed can be modulated by addition of acid/base. Such processes play a pivotal role in the design of molecular mashines.

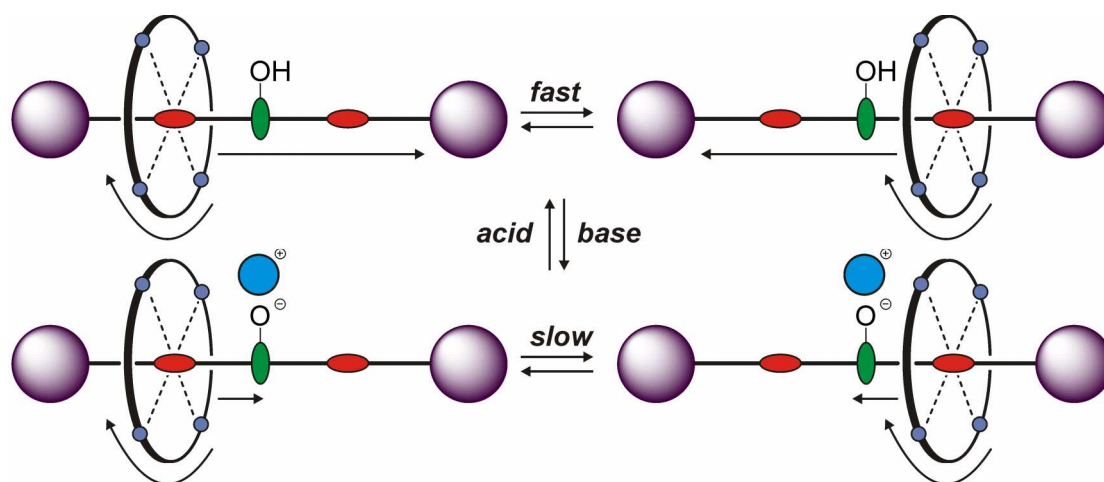


Figure 25. Schematic representation which summarizes the dynamic processes involved in the acid/base controlled switching of [2]rotaxanes obtained by using Schalley's anion template. The red station is standing for the diamide binding motif, the green station for the phenolate. The blue circuit represents the protonated P_1 base HP_1^+ as the cation "break".

Another interesting [2]rotaxane bearing a TLM is shown in Figure 26 and was investigated by Smith *et al.*^[10] This [2]rotaxane can be obtained by the "threading/trapping" method. It contains a squaraine^[11] binding motif and two triazole stations, which were introduced in this [2]rotaxane using "click chemistry". The use of squaraine is the special feature herein because of its shade resulting from its donor-acceptor-donor unit. Formally, the four-membered ring implies hückel aromaticity with two π -electrons. The electron-rich aryl substituents used in most cases donate electrons into this electron-poor moiety and a conjugation through the whole molecule takes place. However, the TLM binds to the squaraine with a binding constant $K_a = 5 \cdot 10^3 \text{ M}^{-1}$ (in $CDCl_3$) and protect this station from (i) nucleophilic attacks and (ii) from fluorescence emission if irradiated with 365 nm light. The addition of anions (e. g. chloride) force the TLM to leave the squaraine station due to the fact that chloride is able to bind into the isophthaloyl moiety of a TLM with $K_a > 10^5 \text{ M}^{-1}$ (in $CDCl_3$).^[3a] The TLM elongates to the triazole under the formation of (TLM)N-H \cdots Cl \cdots H-C(triazole) hydrogen bonds. In this state, the squaraine station both can be attacked by nucleophiles and also perform a fluorescence after irradiation with light with a wavelength of 365 nm as seen by "naked eye" ("turn-on" deep-red fluorescence as clearly visible in the photographs, Figure 26). The original state of this [2]rotaxane can be recovered by addition of a sodium salt causing a precipitation of NaCl and bearing a very bulky anion that is not able to bind into the isophthaloyl diamide of a TLM. Such an anion is e. g. $B[3,5-(CF_3)_2C_6H_3]_4^-$. In comparison to the [2]rotaxane obtained by Schalley's anion template, the shuttling can completely interrupted here by adding/removing an anion such as chloride.^[12] Moreover, the anion recognition of mechanically interlocked architectures such as [2]rotaxanes described here have a relevant importance in the field of anion recognition.^[13]

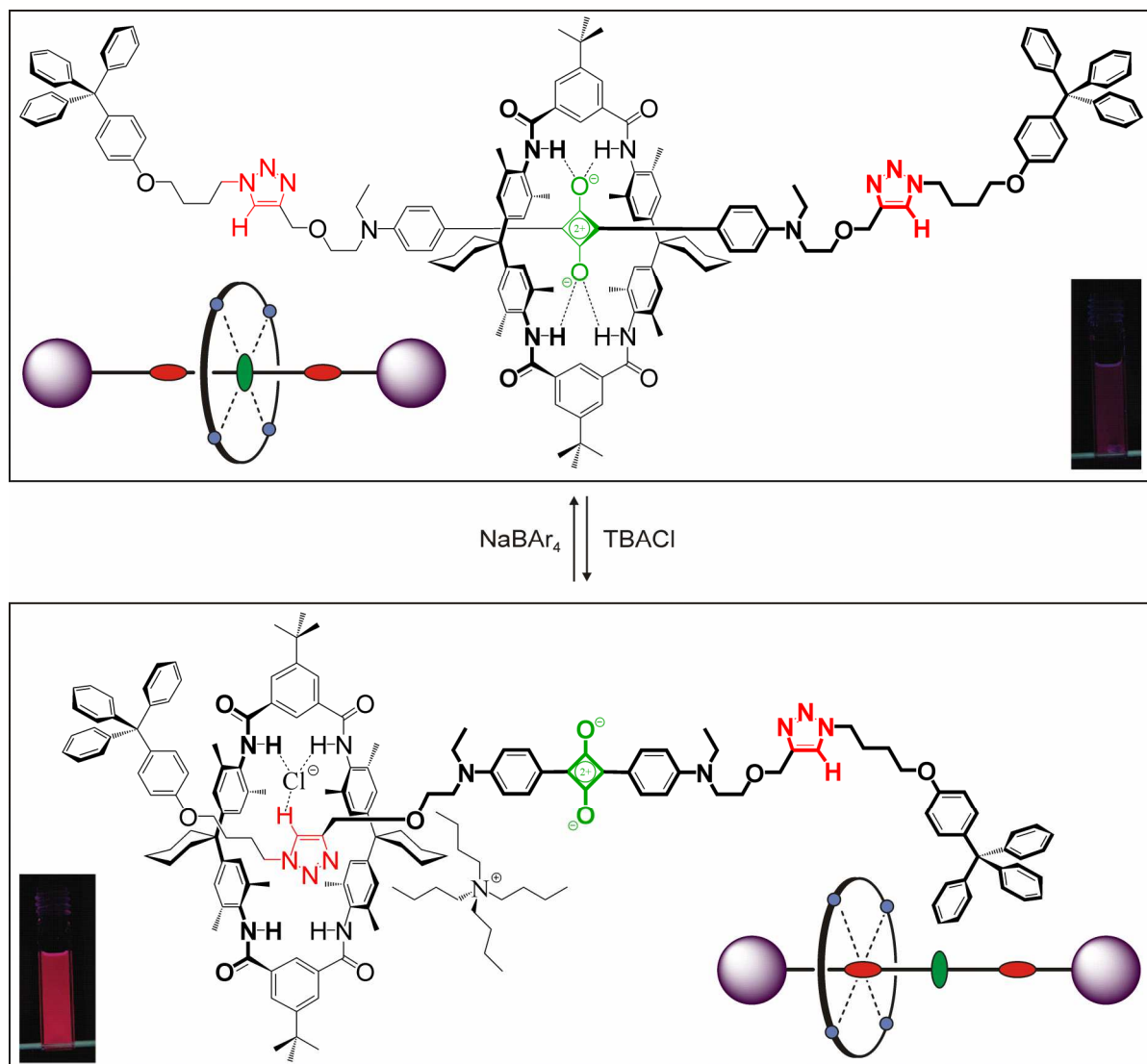


Figure 26. Structure of the [2]rotaxane without (top) and with (bottom) chloride. This switching process is shown schematically if an anion was added as TBA (tetra-*n*butyl) salt, e. g. TBACl, and can be induced by other anions, e. g. acetate. In this example, chloride can be removed by a sodium salt with a sterically demand anion that do not bind to the diamide isophthaloyl moiety of the TLM such as Ar (= B[3,5-(CF₃)₂C₆H₃]₄). Moreover, the switching can be followed by “naked eye” (see photographs) by irradiating the samples with UV light ($\lambda = 365 \text{ nm}$).

The [2]rotaxanes with squaraine as the axle center piece shows nicely which properties mechanically interlocked molecules can have. Thus, (i) the use of “click chemistry” for the stoppering had a significant influence on the [2]rotaxanes bearing N,N'-dipropargyl diketopiperazine moieties presented in chapter 4.4. The catalyst used here is (Ph₃P)₃CuBr that operates in non-competitive solvents essential for the formation of hydrogen-bonded rotaxanes and pseudorotaxanes; (ii) since ¹H NMR titrations and ITC did not result in a successful evaluation of the binding values of the multivalent architectures bearing TLM/diamide motif so far (see chapter 4.3), the squaraine axle can be used here as a support. On the one hand, it should form host/guest complexes with multivalent hosts consisting of two,

three or four TLM's and act as solubilizing component since these hosts are insoluble in non-competitive solvents. On the other hand, it can act as fluorescence marker as shown in Figure 27 due to the fact that the influence of the multivalent bond is assumed to lead to more stable complexes as in case of the monovalent squaraine axle. Again, this monovalent squaraine is useful here as it has completely different UV-Vis and fluorescent properties in its complexes state compared to the non-complexed one.

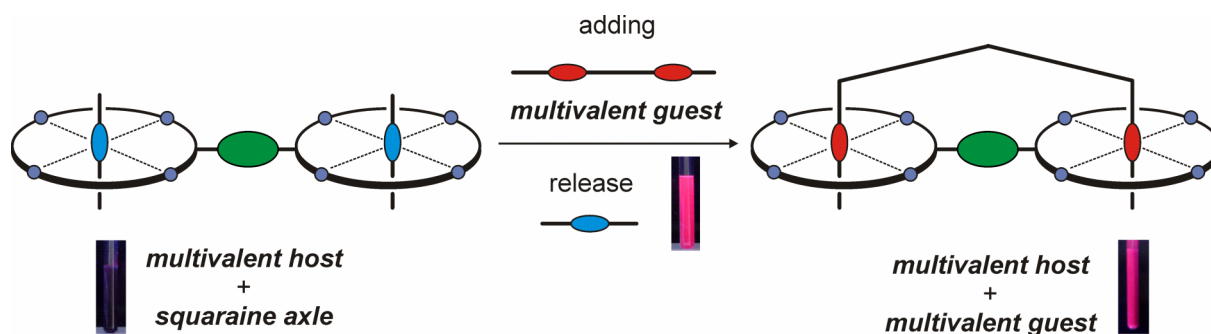


Figure 27. Schematical representation of the idea for performing the replace of the squaraine axle from the multivalent host by adding multivalent guest. In addition, photographs of NMR samples (CD_2Cl_2) irradiated with 365 nm light of squaraine (center), squaraine + TLM (left) and square + TLM + chloride as model compound for a multivalent guest (right) are shown.^[14]

The use of shuttling/switching processes of the macrocycles in the [n]rotaxanes caused by external stimuli, mainly light, redox or chemical compounds (e. g. acid/base, anions) as described on these few examples is believed to be the “golden way” towards synthetic molecular machines, one of the main goals of supramolecular chemists.^[15] Such machines are defined as “a mechanical device that performs a useful function using components of nanometer scale and defined structure” and thus can be found widely in nature.^[15] Prominent examples are ATP-synthase, myosin, kinesin, or dynein. Attempts to extend this concept from nature have yielded in complex synthetic supramolecular structures such as switches, tweezers, shuttles, and even molecular muscles, walkers and rotary motors. Each of these molecular machines has been designed specifically to perform particular functions upon application of an external energy input. An useful function can be a mechanical movement as shown above for [2]rotaxanes.

Another very famous example for such complex supramolecules is the nanoelevator synthesized by Stoddart *et al.*^[16], which can perform “elevating” process caused by adding acid/base (Figure 28). Herein, multivalency (described in the chapter 3.3) seems to be responsible for the efficient synthesis and high thermodynamic stability of this complex architecture. Moreover, such complexes significantly influences the research presented in this thesis, especially the multivalent pseudorotaxanes described in chapters 4.2 and 4.3. The molecular elevator shown in Figure 28 bears a trivalent trimer of DB24C8 as the host.

Two orthogonal binding sites were implemented in the guest, one of them is a dialkylammonium cation and the other one is a bipyridinium dication. In the acidic environment, the binding of the DB24C8 crown trimer takes place at the ammonium cations since this are the thermodynamically preferable binding stations ($K_a \sim 250 \text{ M}^{-1}$, in MeCN) in comparison to the bipyridinium dications ($K_a \sim 80 \text{ M}^{-1}$, in MeCN).^[17] Addition of a base leads to the deprotonation of the ammonium cations to the secondary amines. This results in the loss of hydrogen bonding and in the movement of the trivalent crown to the bipyridinium dications where it can acquire some stabilizing $\pi \cdots \pi$ stacking interactions. Addition of an acid leads to the protonation of the secondary amines to the ammonium cations, moving the crown back and finishing the cycle. This platform operates by taking three distinct steps associated with each of the three deprotonation/reprotonation processes, but it should be noted that the use of switching processes caused by chemical stimuli such as acid/base or adding/reversing of an anion as presented in all examples here is strongly limited to the salt formation that accumulates during the switching and needs to be removed at any time. However, as nature sets a good example, light should be the choice for inducing e. g. a motion process.

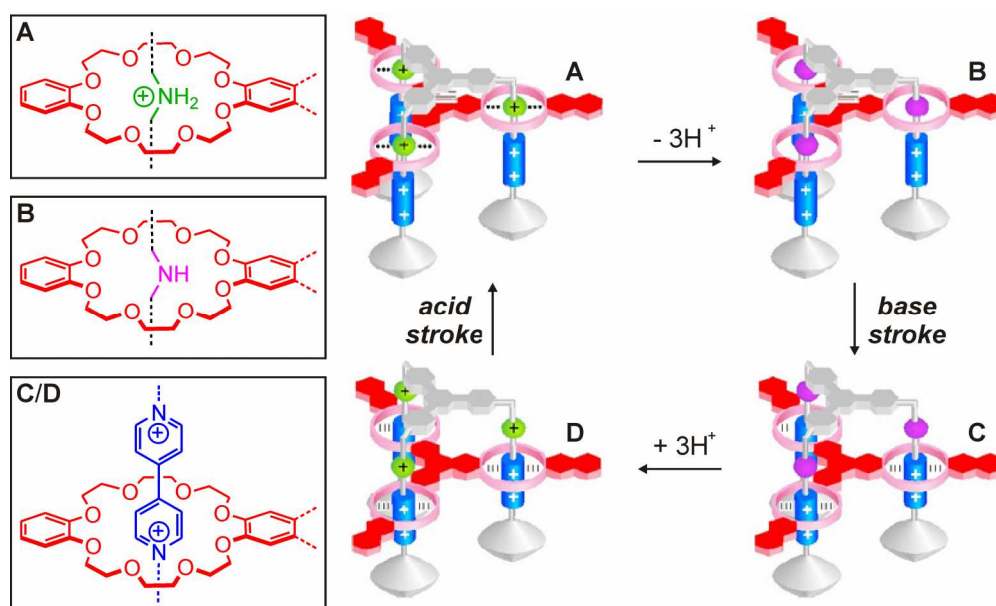


Figure 28. The base-acid controlled mechanical switching in a molecular elevator.

In order to complete this chapter, one characteristic of the synthetical features of mechanically interlocked molecules should be mentioned. By using the Dynamic Covalent Chemistry (DCC) approach described by Stoddart *et al.* the non-reversible formation of a mechanical bond can be canceled using reversible reactions such as Ru-catalyzed metathesis, Imine formation (Shiff's base) or S-S bond formation for the locking process.^[18] Therefore, locking and unlocking are in equilibrium and "error correction" can be introduced into synthetic processes where covalent chemistry is required.

- [1] (a) Amabilino, D. B.; Stoddart, J. F. *Chem. Rev.* **1995**, *95*, 2725. (b) Dichtel, W. R.; Miljanić, O. Š.; Zhang, W.; Spruell, J. M.; Patel, K.; Aprahamian, I.; Heath, J. R.; Stoddart, J. F. *Acc. Chem. Res.* **2008**, *41*, 1750. (c) Stoddart, J. F. *Chem. Soc. Rev.* **2009**, *38*, 1802.
- [2] Li, X.-y.; Illigen, J.; Nieger, M.; Michel, S.; Schalley, C. A. *Chem.-Eur. J.* **2003**, *9*, 1332.
- [3] (a) Hübner, G. M.; Gläser, J.; Seel, C.; Vögtle, F. *Angew. Chem. Int. Ed.* **1999**, *38*, 383; (b) Schmieder, R.; Hübner, G.; Seel, C.; Vögtle, F. *Angew. Chem. Int. Ed.* **1999**, *38*, 3528. (c) Seel, C.; Vögtle, F. *Chem.-Eur. J.* **2000**, *6*, 21. (d) Reuter, C.; Schmieder, R.; Vögtle, F. *Pure Appl. Chem.* **2000**, *72*, 2233. (e) Felder, T.; Schalley, C. A. *Angew. Chem. Int. Ed.* **2003**, *42*, 2258. (f) Schalley, C. A.; Silva, G.; Nising, C. F.; Linnartz, P. *Helv. Chim. Acta* **2002**, *85*, 1587. (g) Linnartz, P.; Bitter, S.; Schalley, C. A. *Eur. J. Org. Chem.* **2003**, 4819. (h) Linnartz, P.; Schalley, C. A. *Supramol. Chem.* **2004**, *16*, 263.
- [4] (a) Harrison, I. T.; Harrison, S. *J. Am. Chem. Soc.* **1967**, *89*, 5723. (b) Schill, G.; Zollenkopf, H. *Justus Liebigs Ann. Chem.* **1969**, *721*, 53.
- [5] Harrison, I. T. *J. Chem. Soc., Perkin Trans. 1* **1974**, 301.
- [6] (a) Raymo, F. M.; Stoddart, J. F.; *Chem. Rev.* **1999**, *99*, 1643. (b) Griffiths, K. E.; Stoddart, J. F. *Pure Appl. Chem.* **2008**, *80*, 485.
- [7] A discrete host-guest complex is formed if an axle and a macrocycle are mixed. However, the assembly/disassembly process is reversible while the stoppering reaction is not. Consequently, equilibrium is observable just as well after attaching one of the stopper groups leading to a semi-axle and no sharp borderline exists between “threading” and “trapping”.
- [8] (a) Ghosh, P.; Mermagen, O.; Schalley, C. A. *Chem. Commun.* **2002**, 2628. (b) Ghosh, P.; Federwisch, G.; Kogej, M.; Schalley, C. A.; Haase, D.; Saak, W.; Lützen, A.; Gschwind, R. M. *Org. Biomol. Chem.* **2005**, *3*, 2691.
- [9] Schwesinger, R.; Hasenfratz, C.; Schlemper, H.; Walz, L.; Peters, E.-M.; K. Peters, K.; von Schnering, H. G. *Angew. Chem., Int. Ed.* **1993**, *32*, 1361.
- [10] (a) Gassensmith, J. J.; Barr, L.; Baumes, J. M.; Paek, A.; Nguyen, A.; Smith, B. D. *Org. Lett.* **2008**, *10*, 3343. (b) Gassensmith, J. J.; Matthys, S.; Lee, J.-J.; Wojcik, A.; Kamat, P. V.; Smith, B. D. *Chem.-Eur. J.* **2010**, *16*, 2916.
- [11] (a) Xue, M.; Chen, C.-F. *Chem. Commun.* **2008**, 6128. (b) Gassensmith, J. J.; Baumes, J. M.; Smith, B. D. *Chem. Commun.* **2009**, 6329.
- [12] A shuttling process faster than the NMR time scale is not observable. However, a shuttling that proceeds only slightly faster or slower is indicated by observing broad signals in the ¹H NMR spectrum or different sets of signals. Broad signals were clearly visible in case of the [2]rotaxanes synthesized through Schalley's anion template. In case of the [2]rotaxanes bearing squaraine axle, one set of signal is observed indicating a discrete structure is obtained after addition of an anion. Otherwise, a very fast shuttling would be a reason for this observation. This cannot be the case because the presence of the squaraine binding motif would lower the shuttling process significantly.
- [13] (a) Beer, P. D.; Sambrook, M. R.; Curiel, D. *Chem. Commun.* **2006**, 2105. (b) Lankshear, M. D.; Beer, P. D. *Acc. Chem. Res.* **2007**, *40*, 657. (c) Steed, J. W. *Chem. Commun.* **2006**, 2637.

- (d) Vickers, M. S.; Beer, P. D. *Chem. Soc. Rev.* **2007**, *36*, 211. (e) Steed, J. W. *Chem. Soc. Rev.* **2009**, *38*, 506. (f) Juwarker, H.; Jeong, K.-S. *Chem. Soc. Rev.* **2010**, *39*, 3664. (g) Ballester, P. *Chem. Soc. Rev.* **2010**, *39*, 3810. (h) Mercer, D. J. *Chem. Soc. Rev.* **2010**, *39*, 3612. (i) Hua, Y.; Flood, A. H. *Chem. Soc. Rev.* **2010**, *39*, 1262. (j) Lau, Y. H.; Rutledge, P. J.; Watkinson, M.; Todd, M. H. *Chem. Soc. Rev.* **2011**, *40*, 2848.
- [14] Löw, N. L. *Synthese und Analyse von multivalenten supramolekularen Strukturen basierend auf Hunter/Vögtle Tetralactam-Makrozyklen*, Master thesis, Freie Universität Berlin, **2011**.
- [15] (a) Sauvage, J.-P. *Acc. Chem. Res.* **1998**, *31*, 611. (b) Blanco, M.; Consuelo Jiménez, M.; Chambron, J.-C.; Heitz, V.; Linke, M.; Sauvage, J.-P. *Chem. Soc. Rev.* **1999**, *28*, 293. (c) Balzani, V.; Credi, A.; Raymo, F. M.; Stoddart, J. F. *Angew. Chem. Int. Ed.* **2000**, *39*, 3348. (d) Schalley, C. A.; Beizai, K.; Vögtle, F. *Acc. Chem. Res.* **2001**, *34*, 465. (e) Ballardini, R.; Balzani, V.; Credi, A.; Gandolfi, M. T.; Venturi, M. *Acc. Chem. Res.* **2001**, *34*, 445. (f) Harada, A. *Acc. Chem. Res.* **2001**, *34*, 456. (g) Collin, J.-P.; Dietrich-Buchecker, C.; Gaviña, P.; Consuelo Jimenez-Molero, M.; Sauvage, J.-P. *Acc. Chem. Res.* **2001**, *34*, 477. (h) Clemente-León, M.; Credi, A.; Martínez-Díaz, M.-V.; Mingotaud, C.; Stoddart, J. F. *Adv. Mater.* **2006**, *18*, 1291. (i) Balzani, V.; Credi, A.; Silvi, S.; Venturi, M. *Chem. Soc. Rev.* **2006**, *35*, 1135. (j) Credi, A. *Angew. Chem. Int. Ed.* **2007**, *46*, 5472. (k) Leigh, D. A.; Zerbetto, F.; Kay, E. R. *Angew. Chem. Int. Ed.* **2007**, *46*, 72. (l) Mateo-Alonso, A.; Guldi, D. M.; Paolucci, F.; Prato, M. *Angew. Chem. Int. Ed.* **2007**, *46*, 8120. (m) Champin, B.; Mobian, P.; Sauvage, J.-P. *Chem. Soc. Rev.* **2007**, *36*, 358. (n) Bonnet, S.; Collin, J.-P. *Chem. Soc. Rev.* **2008**, *37*, 1207. (o) Silvi, S.; Venturi, M.; Credi, A. *J. Mater. Chem.* **2009**, *19*, 2279. (p) Bodis, P.; Panman, M. R.; Bakker, B. H.; Mateo-Alonso, A.; Prato, M.; Buma, W. J.; Brouwer, A. M.; Kay, E. R.; Leigh, D. A.; Woutersen, S. *Acc. Chem. Res.* **2009**, *42*, 1462. (q) Durot, S.; Reviriego, F.; Sauvage, J.-P. *Dalton Trans.* **2010**, *39*, 10557.
- [16] (a) Balzani, V.; Clemente-León, M.; Credi, A.; Lowe, J. N.; Badjić, J. D.; Stoddart, J. F.; Williams, D. J. *Chem.-Eur. J.* **2003**, *9*, 5348. (b) Badjić, J. D.; Cantrill, S. J.; Stoddart, J. F. *J. Am. Chem. Soc.* **2004**, *126*, 2288. (c) Badjić, J. D.; Balzani, V.; Credi, A.; Silvi, S.; Stoddart, J. F. *Science* **2004**, *303*, 1845. (d) Badjić, J. D.; Ronconi, C. M.; Stoddart, J. F.; Balzani, V.; Silvi, S.; Credi, A. *J. Am. Chem. Soc.* **2006**, *128*, 1489.
- [17] Braunschweig, A. B.; Ronconi, C. M.; Han, J.-Y.; Aricó, F.; Cantrill, S. J.; Stoddart, J. F. Khan, S. I.; White, A. P. J.; Williams, D. J. *Eur. J. Org. Chem.* **2006**, 1857.
- [18] (a) Rowan, S. J.; Cantrill, S. J.; Cousins, G. R. L.; Sanders, J. K. M.; Stoddart, J. F. *Angew. Chem. Int. Ed.* **2002**, *41*, 898. (b) Meyer, C. D.; Joiner, C. S.; Stoddart, J. F. *Chem. Soc. Rev.* **2007**, *36*, 1705. (c) Haussmann, P. C.; Stoddart, J. F. *The Chemical Record* **2009**, *9*, 136. (c) Au-Yeung, H. Y.; Cougnon, F. B. L.; Otto, S.; Dan Pantoş, G.; Sanders, J. K. M. *Chem. Sci.* **2010**, *1*, 567.

3.5. Analytical Methods in Supramolecular Chemistry

Structure determination still remains a major challenge in supramolecular chemistry. Two important aspects of supramolecules set limitations to the analytical methods which can be applied: (i) their reversible formation and (ii) the weak nature of their interactions.^[1] Besides NMR spectroscopy, which is the most important characterization tool not only for the supramolecular architectures but also for the characterization of organic and inorganic compounds, a variety of methods were invented in the last decades. They can be classified in methods for the investigation in solution (different NMR techniques, ITC, UV-Vis, CD), in the solid state (X-Ray, surface analysis) or in the gas phase (MS). For example, UV-Vis can be applied for the characterization of chromophores. Additional titration tools allow binding studies to determinate the binding constant K_a and other thermodynamical parameters. Circular dichroism (CD) spectroscopy can be used to analyze chiral compounds. Different techniques for investigations of supramolecules on solid support are available: atomic force microscopy (AFM), scanning electron microscopy (SEM), transmission electron microscopy (TEM), or scanning tunneling microscopy (STM), just to name a few.

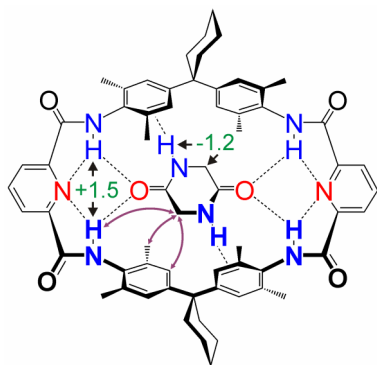


Figure 29. Host-guest complex bearing a pyridine-substituted tetralactam macrocycle (TLM) and glycine anhydride (or diketo-piperazine). Shifts of the proton signals (green) in the complex compared to their uncomplexed state are observed. The arrows indicate observed NOE contacts.

Therefore, strong signal shifts of the protons occur if they are involved in the hydrogen bonding and if they are located in the pocket of the guest molecule. Moreover, the guest can bear aromatic moieties, which are able to perform an anisotropic effect on the guest molecule.

The solution-phase method that has proved most useful for obtaining structural information on supramolecular complexes is ^1H NMR (Nuclear Magnetic Resonance) spectroscopy.^[2] For example, it often can lead to a sufficient portion of information about hydrogen atoms involved in the binding event between two or more supramolecules in solution or wherever a metal complexation to a ligand had take place. In addition, the comparison of the signals for the supramolecule and for the individual non-interacting precursors gains insight into the secondary structure (complexation induced changes in chemical shift, CIS). Such an event can be observed for instance by studying a guest molecule which binds into the cavity of a host

An example of a host-guest complex including its signal shifts in comparison to the non-complexed host and guest is shown in Figure 29.^[3] This complex is formed from a TLM, which bears two pyridine moieties with the nitrogen atom pointing into the cavity. These nitrogens form in sum four intramolecular hydrogen bonds to the amide hydrogens.^[4] Such binding event results in a preorganisation of the cavity of the TLM and a preferable binding of guests such as glycine anhydride (or diketopiperazine) can take place directed by the formation additional four intermolecular hydrogen bonds to the amide hydrogens. However, if comparing ^1H NMR spectra of glycine anhydride, TLM and their 1 : 1 complex in appropriate non-competitive solvent (e.g. CDCl_3), clear signal shifts occur indicating a complex formation had take place. The signal for the amide hydrogens shifts to the lower field of the ^1H NMR spectrum since these hydrogens are mostly affected by the presence of the guest molecule inside the cavity of the TLM. In comparison, the signals for the glycine anhydride hydrogens shift to the higher field, because they feel the anisotropy of the aromatic rings incorporated in the wheel's walls. These complexation-induced shifts confirm the axle to bind by four hydrogen bonds between the wheel's amide NH hydrogens and the guest's carbonyl oxygen atoms and also provide evidence for a threaded structure.

More detailed information on the binding can be collected from 2D NMR experiments. While $^1\text{H}, ^1\text{H}$ COSY and $^1\text{H}, ^{13}\text{C}$ HMQC/HMBC NMR experiments allow the assignment of the hydrogens (or carbons) to each other just from their different chemical covalent environment, $^1\text{H}, ^1\text{H}$ NOESY/ROESY NMR gain insight into inter- and intramolecular non-covalent interactions happen in the distance below approximately 4 Å.^[5] This can be clearly shown on the example of the host-guest complex discussed above (Figure 29), where NOE (Nuclear Overhauser Effect) contacts between the hydrogens of the CH_2 group of the glycine anhydride and the TLM's hydrogens occur. Another 2D NMR method, which can be useful especially for the differentiation of the size of a supramolecule, is the Diffusion Ordered Spectroscopy (DOSY). Herein, different compounds in a mixture can be assigned based on the differences in translation diffusion coefficients and meanderings in size and shape of the molecule as well as physical properties of the surrounding environment such as viscosity, temperature etc. can be obtained. For example, by mixing the bidentate 4,4'-bipyridine derivative ligand with the square-planar $(\text{dppp})\text{Pd}^{\text{II}}(\text{OTf})_2$ metal center, an equilibrium between metallo-supramolecular triangles and squares can be observed.^[6] In Figure 30, the signals for urea-NH and o-PyH with smaller intensity can be assigned to the square, while more intensive signals belong to the triangle. Furthermore, this method is advantageous especially for systems, which result in ^1H spectra with strong signal superposition. Such experiments were performed for the metallo-supramolecular polygons formed under kinetical control described in chapter 4.5, regrettably without success.

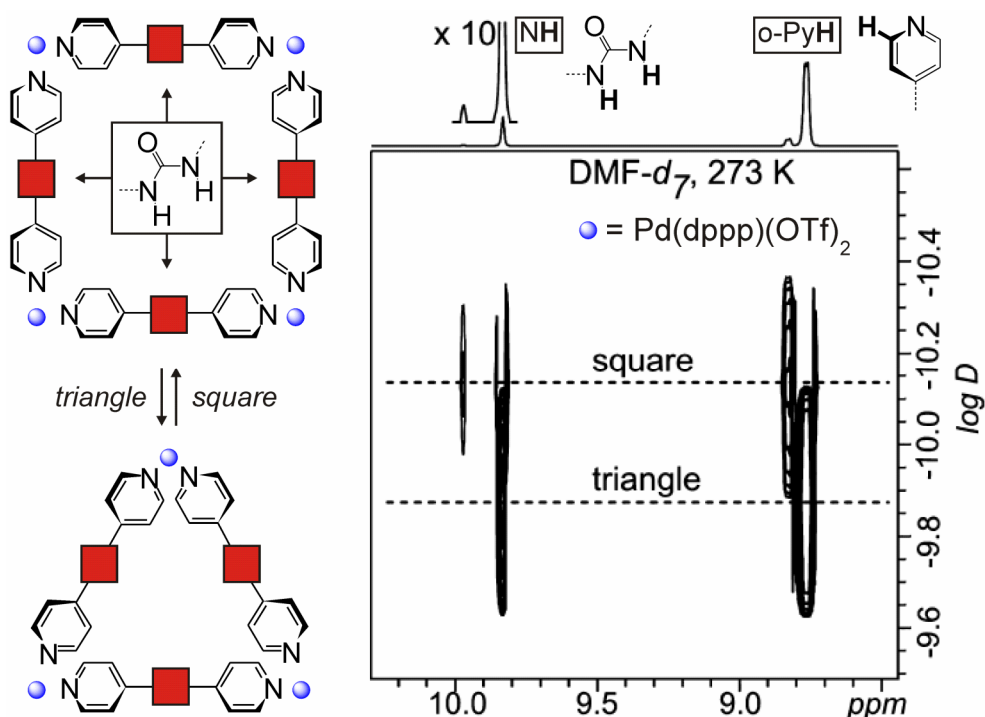


Figure 30. The equilibrium observed for the metallo-supramolecular self-assembled squares and triangles, and the DOSY NMR spectrum indicating that both species exist in solution.

As explained above, non-covalent binding processes play a pivotal role in the supramolecular chemistry. The ability to analyze the thermodynamic parameters such as the binding constant K_a , changes of enthalpy ΔH , free enthalpy (Gibbs energy) ΔG or entropy ΔS is indispensable. The knowledge of K_a can be used for a direct comparison of the strength of non-covalent interactions of different guests to a host and therefore defines specificity of a binding event. Knowing the values of ΔG , ΔH and ΔS allows in addition detailed insights into the fundamentals of the interactions.^[7] Bearing it in mind, ^1H NMR titrations (or in some cases dilution experiments^[8]) can help to obtain more or less directly the binding constant K_a and the changes of the free enthalpy ΔG by using the equation 12.

$$\text{(eq. 12)} \quad -RT \ln K_a = \Delta G = \Delta H - T \Delta S$$

(R is the universal gas constant, T the temperature, ΔG the change of free enthalpy, ΔH the change of enthalpy and ΔS the change of entropy).

One of the advantages of this method compared to e.g. UV-Vis titration is that no chromophores are required. Also, ^1H NMR titrations proceed mostly in a very simple manner. The NMR tube contains a solution of the host (or guest) molecule with a known concentration.

Various amounts of the guest solution (also of a known concentration) are added stepwise to the host (or guest) solution and a ^1H NMR spectrum is recorded immediately.

Since the binding of the guest is a reversible process that is in equilibrium with the release, two events can be distinguished: (i) the exchange of the guest in its complexed state against those in the uncomplexed one proceeds faster than the NMR time scale and averaged signals are visible in the spectra or (ii) the exchange proceeds slower than the NMR time scale and two or more sets of signals can be observed (for the protons of the guest complexed and not complexed).

For the first event, the binding constant K_a can be determined by a non-linear curve fitting based on equation 13. This equation is required for a 1 : 1 binding model as used for the TLM as the host and variously substituted diamide axle guests discussed in chapter 4.1.

$$(eq. 13) \quad \delta_{\text{obs}} = \delta_0 + \frac{\Delta\delta_{\text{max}}}{2[H]_0} \left[\frac{1}{K_a} + [H]_0 + [G]_0 - \sqrt{\left(\frac{1}{K_a} + [H]_0 + [G]_0 \right)^2 - 4[H]_0[G]_0} \right]$$

(δ_{obs} is the observed shift of the signals of the host (or guest) at each titration step as a function of the initial concentrations of host $[H]_0$ and guest $[G]_0$. δ_0 is the chemical shift of the signals of the free host (or guest). $\Delta\delta_{\text{max}}$ is the difference between the theoretical signal shift at 100% complexation and δ_0)

The second event, where different sets of signals occur, can be handled easier. By knowing that, the binding constant K_a can be expressed by the equation 14.

$$(eq. 14) \quad K_a = \frac{[HG]}{[H][G]}$$

($[H]$ is the concentration of the host, $[G]$ the concentration of the guest and $[HG]$ the concentration of the host-guest complex)

The binding constant K_a can be calculated simply by the integration of the signals for the complexed guest and the non-complexed one if the initial concentrations of the host and the guest are known. Such event was found in case of the diketopiperazine binding motif described in chapter 4.4.

It is required to use not only one method for the evaluation, because a comparison of the data obtained from different "analytical views" often leads to much more insight into the processes occur for example during the formation of supramolecules. Therefore, a second very useful method for the determination of the thermodynamics is Isothermal Titration Calorimetry (ITC).^[9] In this work, ITC was successfully used for evaluation of the monovalent pseudorotaxanes bearing the TLM/diamide binding motif (see chapter 4.1). In combination with ^1H NMR (titration), it is an immensely powerful technique for the evaluation of the binding behavior of these supramolecules in solution.

ITC is a calorimetric method based on the fact, that all non-covalent interactions are associated with changes of heat. These changes are independent of the size of the molecules and thus, all chemical or biochemical interactions (e.g. metal complexes, binding of small molecules to large macromolecules) can be evaluated.^[10] The use of ITC is strongly advantageous since all relevant thermodynamic parameters can be determined in only one experiment following equation 12 in comparison to the ^1H NMR and UV-Vis, where ΔH and ΔS are available only after temperature-dependent measurements. Also, the stoichiometry of the complexes is available, and the temperature-dependent assignment of ΔH if performing the ITC experiments at different temperatures would lead to the changes in heat capacity ΔC_p .^[11]

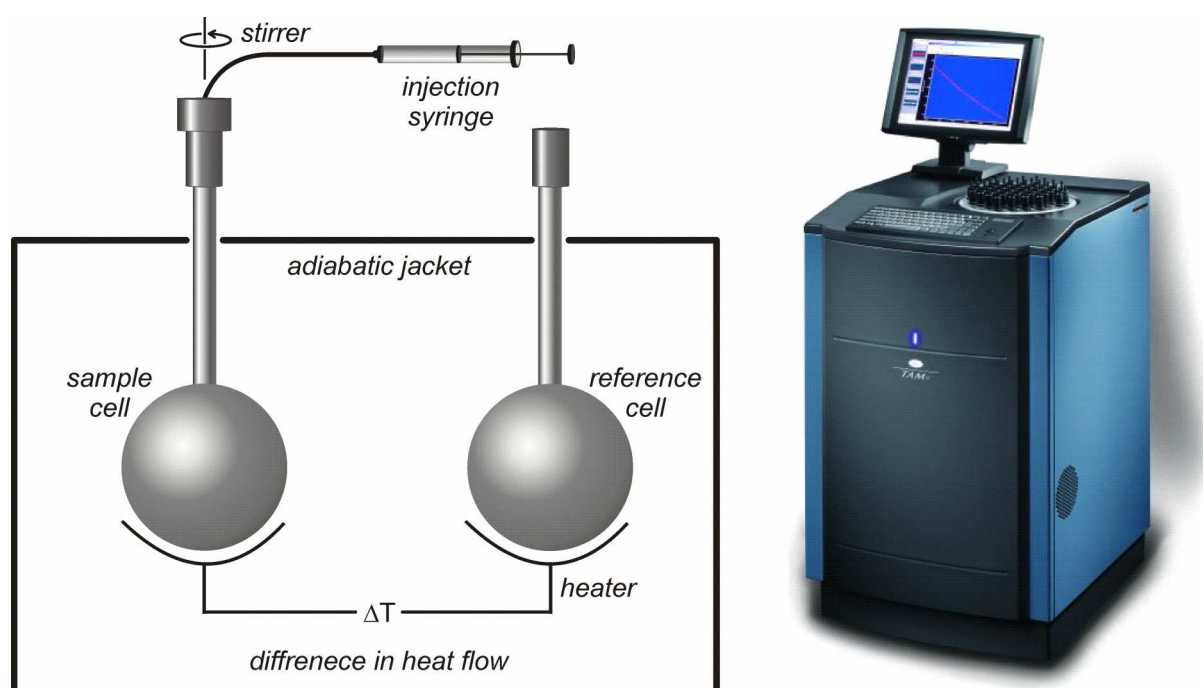


Figure 31. Schematic representation of the experimental setup of an isothermal titration calorimeter (left)^[12a] and a picture of the TAM III ITC used during this thesis.^[12b]

The basic experimental setup for an ITC experiment is shown in Figure 31. A commonly used titration calorimeter consists of two identical cells bearing a very heat

conducting material, the sample cell, where the titration experiment takes place and the reference cell. The sample cell is filled with the solution of the host in known concentration and appropriate solvent; the reference cell contains only the pure solvent. Both cells are enclosed by an adiabatic jacket and connected through a heater. Sensitive thermopile/thermocouple circuits detect temperature differences between the two cells and between the cells and the jacket.

At the beginning of the experiment, both cells have the same constant temperature saved by the heater. By injecting selected amounts of the solution of the guest molecule through a syringe pump system, heat is accommodated or devolved depending on whether the association reaction is endothermic or exothermic. For an exothermic reaction, the temperature in the sample cell will increase, and the feedback power will be deactivated to maintain equal temperatures between the two cells. For an endothermic reaction, the reverse process will occur: the feedback circuit will increase power to the sample cell to maintain the temperature. In both cases, the increase or decrease of the power can be detected and the raw data (so-called spike curve) can be obtained. The amount of heat Q evolved on addition of ligand can be expressed by the equation 15, which is required for a 1:1 binding model. For a more general model of binding, the multiple independent sites model, the host contains multiple ligand binding sites that are noninteracting.^[13]

$$(eq. 15) \quad Q = \frac{V_0 \Delta H [H]_t K_a [G]}{1 + K_a [G]}$$

(V_0 is the volume of the cell, ΔH the changes in enthalpy of binding, $[H]_t$ the total host concentration including bound and free fractions, K_a is the binding constant, and $[G]$ is the free guest concentration)

These data can be integrated and fitted, and a theoretically calculated curve can be obtained. This results in the availability of the binding constant K_a , the amount of energy ΔH , ΔG and the changes of entropy ΔS .

Another important parameter that is essential for an accurate ITC experiment is the Wiseman's parameter "c", defined as the product of the number n of binding events, the host concentration $[H]$ and the binding constant K_a as shown in the equation 16.

$$(eq. 16) \quad c = n K_a [H]$$

With equation 16, the experimental binding isotherm can be characterized by this parameter. For an accurate determination of K_a , it is often recommended that the value c is between 10 and 1000.^[14] Large values of c prohibit the determination of K_a since the transition is very sharp and too few points are collected near equivalence. Moreover, the saturation may be achieved in a single injection of ligand. In comparison, binding isotherms lose the characteristic sigmoidal shape with low values of c . Therefore, the equivalence point cannot be clearly identified. However, Turnbull and Daranas^[14] showed for crown ether/metal

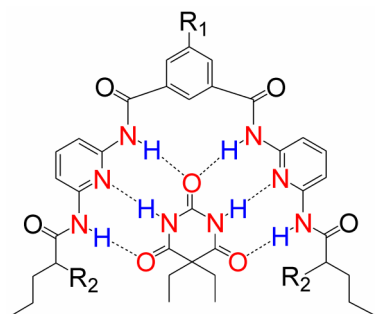


Figure 32. Structure of the hydrogen-bonded host-guest complex bearing differently substituted Hamilton receptors and barbital. In sum, six hydrogen bonds can be formed between both compounds.

complexes that the fact that “ c ” should be ideally above 10 is not true if some basic principles are assumed: (i) a sufficient portion of the binding isotherm is used for analysis, (ii) the binding stoichiometry is known, (iii) the concentrations of both ligand and receptor are known with accuracy, and (iv) there is an adequate level of signal-to-noise ratio in the data. Consequently, it is possible to study low affinity systems with ITC and the only limit of this method are host-guest interactions with high affinities (K_a higher than 10^7 M^{-1}).^[15] These difficulties in detection of high binding affinities also occur while varying the use of analytical methods mentioned above and therefore the investigation of systems with high binding affinities are still challenging.

The fact that all thermodynamic values can be determined in a single experiment allowed ITC to be used widely in supramolecular chemistry.^[16] Although some examples were presented in previous chapters, Lünig *et al.*^[17] investigated the hydrogen-bond formation between Hamilton receptors and barbital (Figure 32). This study shows successfully that a combination of different methods is essential for the characterization of a supramolecular system in complete manner. An important fact results here if comparing the ^1H NMR titration data with those obtained from ITC, where $\sim 30\%$ larger values were detected. This is not surprising since the shifts observed during a ^1H NMR titration only occur when the corresponding proton becomes part of a hydrogen bond. In contrast, ITC register any binding regardless whether this binding is caused by hydrogen bonds or by other interactions. The obtained data from ITC are similar to NMR, but ITC requires much greater accuracy in performing an experiment since large dilution enthalpies occur. These errors can affect strongly the enthalpies and should be eliminated by a blank titration of the guest into the blank solvent in a separate experiment. Nevertheless, calorimetry represents a powerful tool for the determination of the thermodynamics besides other methods such as NMR or UV/Vis.

In addition to the methods that are capable of analyzing supramolecules in solution, a series of methods for the characterization in the solid phase exist as well. The most prominent is definitely X-ray crystallography. It can determine the arrangement of atoms within a crystal. A beam of X-rays strikes a crystal and causes the beam of light to spread into many specific directions. From the angles and intensities of these diffracted beams, a three-dimensional picture of the density of electrons within the crystal can be obtained resulting in the availability of the mean positions of the atoms in the crystal as well as their chemical bonds or their disorder. Therefore, X-ray analysis is esteemed as the chief method for the determination of supramolecules.^[18] However, it is often challenging to crystallize weakly bound complexes. In addition, the solid-state structure may not always reflect the situation in solution, but often it is possible to compare solid with solution structures.

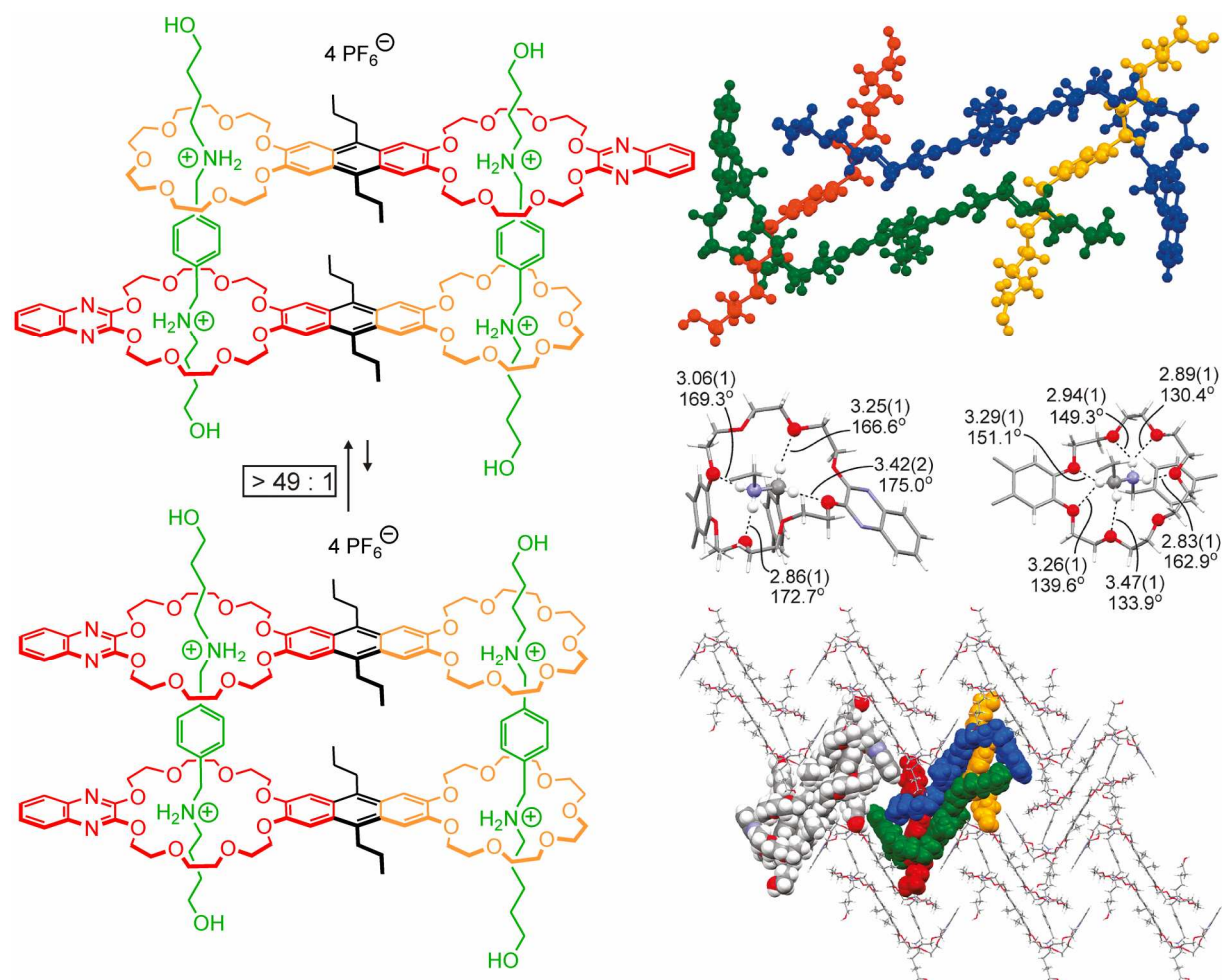


Figure 33. Structures of the two constitutional isomers of a pseudorotaxane in equilibrium (*anti/syn* > 49:1) in solution (left) and crystal structure confirming the presence of the excess of the *anti*-isomer (right): Top: Ball-and-stick representation with the pseudorotaxane components color-coded. Center: crown/ammonium binding motifs (left: 24-crown-8, right: 21-crown-7) with NH...O and CH...O hydrogen-bond lengths (in Å) and angles (in degrees). Bottom: Packing pattern with two complexes in space-filling representation. The building blocks of the central complex are color-coded for clarity.^[20]

Initially, the host-guest complex shown in Figure 29 was crystallized and the structure was confirmed as assumed from the ^1H NMR data.^[19] Another example is shown in Figure 33.^[20] The [4]pseudorotaxane described here consists of a divalent host bearing two differently sized crown ethers, and a divalent diammonium guest (green). The axle can penetrate dibenzo-24-crown-8 (DB24C8, red) easily, but the 21-crown-7 (21C7, orange) moiety is too narrow for the axle's central phenyl group to slip through and therefore the parallel or antiparallel arrangement of the host can occur. Since the [4]pseudorotaxane with the host molecules *anti* differs significantly from its *syn* conformer for symmetry reasons, a ration of > 49:1 *anti/syn* can be observed from a simple integration of signals using ^1H NMR spectroscopy. This result can be confirmed by X-ray, where only the structure of the *anti* isomer was obtained. Moreover, both binding events (DB24C8 vs. 21C7) can be evaluated. It should be mentioned, that X-ray crystallography was successfully used for structure determination of the diketo-piperazine/TLM complex described in chapter 4.4.

Supramolecules can be deposited on surfaces or nanoparticles yielding an impact on material science including polymers, catalysis and magnetic media just to name a few.^[21] Thus, TLM's, dicarbonyl compounds and rotaxanes were synthesized during this thesis as described in chapter 4.3. Especially, multivalent systems are in focus using both gold surfaces and nanoparticles. While supramolecule-decorated nanoparticles can be in principle characterized with usual analytical methods operating in solution such as NMR or UV-Vis, an important method for the "surface-based supramolecular chemistry" mentioned here is Single Electron Force Spectroscopy (SMFS or AFM Force Spectroscopy).^[22] It allows the study of the mechanical properties of the individual chemical bonds of the molecules and measures the behavior of them under stretching or torsional mechanical force by performed by pulling on the system under examination with controlled forces. As a single-molecule technique, it also allows to obtain properties of the particular molecule under study. Therefore, rare events not visible in an ensemble such as conformational changes can be observed.

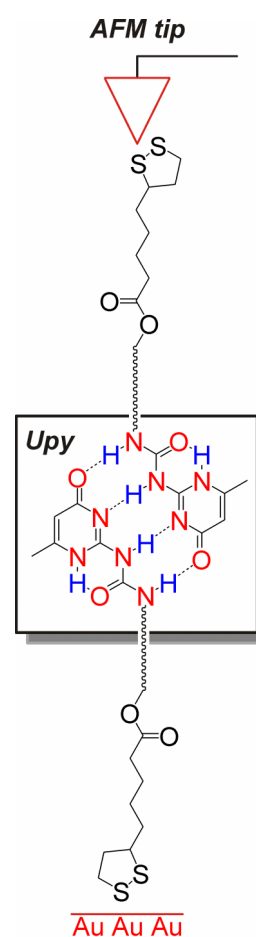


Figure 34. SFMS system consisting of two modified PEG polymers with end-capped **Ury** moieties. The dimer is obtained through the formation four hydrogen bonds. The wiggly line indicates the PEG polymer.

Common applications of force spectroscopy are measurements of polymer elasticity, especially biopolymers such as RNA, DNA, protein unfolding and the study of mechanical resistance of chemical bonds. This is of interest in particular for the molecules presented in this thesis. In order to account this method briefly, an AFM (Atomic Force Microscopy) tip is functionalized with a ligand (or guest) that binds to molecules (for example a host) deposited at the surface. The tip is pushed on the surface allowing for contact between the two interaction partners and then retracted until the newly formed non-covalent bonds are destroyed. Since this breaking is a kinetic stochastic process, the measured force at this event is not an absolute parameter, but it is a function of the pulling speed and by careful analysis at various pulling speeds, the energy landscape of the chemical bond under mechanical force can be mapped. One example is shown in Figure 34, where the quadruple hydrogen bonded ureido-4[1H]-pyrimidinone (**U_{py}**) dimer was successfully investigated using a gold-decorated AFM tip and surface.^[23] The PEG spacer is used because it efficiently decouples the complexation process from the surface and hence suppresses contributions resulting from secondary interactions.

Until now methods operating in solution, in solid state and accordingly on surfaces were described. Furthermore, it is possible to investigate supramolecules and their interaction behavior in the gas phase. Mass spectrometry (MS)^[24] provides the best possibilities to study such systems by offering a huge arsenal of gas-phase chemistry experiments that allow a much more detailed view on the structure of non-covalent complexes and their aspects such as molecular recognition or host-guest chemistry, self-assembly, self-sorting, or the structures of mechanically interlocked molecules.

Mass spectrometry is a technique that measures the mass-to-charge (m/z) ratio of charged species and is useful for the availability of masses of different molecules in simultaneous manner including the elemental composition and therefore the description of the chemical structures. It can be very helpful in the evaluation of the secondary structure of supramolecules if some preconditions are required.^[25] Notably, one of the unique MS instruments, the so-called Fourier Transform Electrospray Ionization Ion Cyclotron Resonance Mass Spectrometry (FT-ICR MS)^[26] was applied to investigate supramolecules such as hydrogen-bridged capsules or metallo-supramolecular polygons described in chapters 4.5 - 4.8 in a successful manner. It provides a very high resolution in combination with very high mass accuracy.

A mass spectrometer usually consists of an ion source, one or more mass analyzers and a detector. ESI FT-ICR MS is designed in a similar way: the ion source used here is the electrospray ionization technique (ESI) and Ion Cyclotron Resonance (ICR) cell as an analyzer. ESI is a very soft ionization method that transfers ions in a nondestructive way directly from solution into the gas phase. The sample dissolved in an appropriate (often more

polar) solvent is initially transferred through a metal capillary into a 2 to 5 kV electric field. The high voltage induces charge separation/repulsion at the capillary tip and a so-called Taylor cone is formed. From the tip of it, a jet of small droplets is ejected, that have a large excess of positive or negative charges depending on the voltage polarity. Solvent evaporation from the droplets is supported by a stream of heatable desolvation gas and the droplets contract concentrating the charges in a smaller and smaller volume until the Rayleigh limit is reached where the droplet cannot carry all charges anymore. The desolvated ions can be formed based on both the charge residue model, that suggests that the droplets undergo Coulomb repulsion at the Rayleigh limit and form a number of smaller droplets until only one ion is left in a nanodroplet, from which the residual solvent evaporates to yield the bare ion. The second ionization model is the ion evaporation model that takes into account that single ions can already be departed from multiply charged droplets still containing many ions. The finally produced single ions are then transferred into a mass analyzer, where they can study under environment-free conditions without any perturbing solvent or dissociation/reorganization processes (Figure 35).^[27]

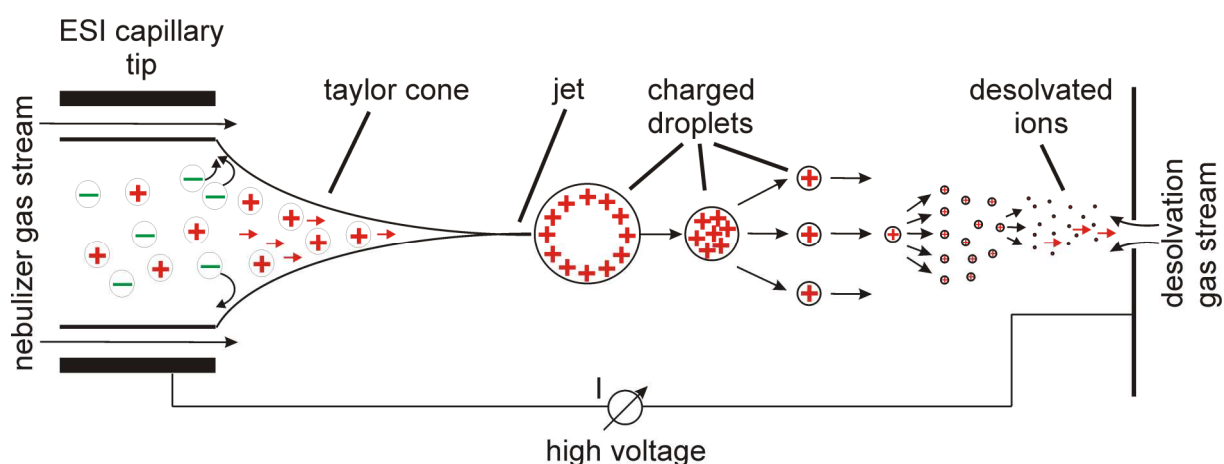


Figure 35. The principle of electro spray ionization technique (ESI).^[27]

The second important point of an ESI FT-ICR mass spectrometer is the IRC cell. It is located inside a spatial uniform static superconducting high field magnet operating typically at 4.7 to 13 T with pressures in the range of 10^{-10} to 10^{-11} mbar. When the ions pass along the magnetic field they are bent into a circular motion in a plane perpendicular to the field by the Lorentz Force (equation 17). Trapping plates at each end prevent the ions from precessing out of the cell.

(eq. 17) $F = z v B$

$$(eq. 18) \quad \omega_c = \frac{z B}{2 \pi m}$$

$$(eq. 19) \quad m/z = \frac{z B}{2 \pi \omega_c}$$

(F is the Lorentz force, v the incident velocity of the ion, z the charge on the ion, B the constant magnetic field strength, ω_c is the induced cyclotron frequency and m mass of the ion)

The frequency of the ions rotation depends on their m/z ratio (equations 18 and 19). Excitation of each individual m/z is achieved by a swept Radio Frequency (RF) pulse across the plates of the cell. Each individual excitation frequency will couple with the natural motion of the ions and raise them to a higher orbit where they induce an alternating current between the detector plates. The frequency related to this current is the same as the cyclotron frequency. When the RF goes off resonance for that particular m/z value, the ions relaxate to their original orbit and the next m/z packet is excited. Although the RF sweep is assembled of a series of stepped frequencies, it can be considered as all frequencies simultaneously. This results in the evaluation of all ions in one event producing a complex frequency vs. time spectrum that contains all the signals, the so-called FID (Free Induction Decay). Decon-volution of this signal by the FT method results in the frequency vs. intensity spectrum which is then converted to the mass vs. intensity spectrum.

One example of supramolecules investigated by ESI FTICR MS is shown in Figure 36.^[28] The formation of six **pyro**'s (pyrogall[4]arenes) to a hexameric architecture under enclosing a $Ru^{II}(bipy)_2^{2+}$ cation by formation weak cation- π bonds can be clearly observed in the high diluted gas-phase of a mass spectrometer. No evidence for this phenomenon occurring in solution was obtained with $Ru^{II}(bipy)_2^{2+}$ as guest molecule in comparison to biphenyl and pyrene that assemble into the hexamer by using heat (see chapter 3.2). This was rationalized with the quite strong cation-anion ion-pair interactions between the Ru^{II} core and PF_6^- as the counterion. Again, the gas phase provides the perfect environment and a deslipping of the conteranions is not prevented anymore.

A special feature of mass spectrometric experiments used for supramolecular systems is the hydrogen/deuterium exchange (H/D-X) of labile hydrogens involved (or not) in

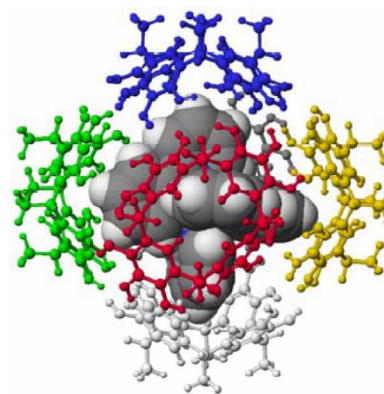


Figure 36. MM2-calculated structure of a **(pyro)₆** hexamer including a $Ru^{II}(bipy)_2^{2+}$ cation.

the formation of hydrogen bonds in between a supramolecule. This method was used during this thesis extensively for investigation of the **reso/pyro** dimers that include differently sized cations (chapter 4.8). Moreover, mechanistic aspects and examples of use in the research field of supramolecular chemistry were summarized in a perspective article (chapter 4.7).

-
- [1] Schalley, C. A. (Ed.), *Analytical Methods in Supramolecular Chemistry*, Wiley-VCH, Weinheim, **2006**.
- [2] Thordarson, P. *Chem. Soc. Rev.* **2011**, *40*, 1305.
- [3] Hunter, C. A.; Parker, M. J. *Chem.-Eur. J.* **1999**, *5*, 1891.
- [4] Carver, F. J.; Hunter, C. A.; Shannon, R. J. *J. Chem. Soc., Chem. Commun.* **1994**, 1277.
- [5] COSY = Correlated Spectroscopy; HMQC = heteronuclear multiple quantum coherence; HMBC = heteronuclear multiple bond coherence; NOESY = nuclear overhauser enhancement spectroscopy; ROESY = Rotating Frame Overhauser Effect Spectroscopy.
- [6] Weilandt, T.; Troff, R. W.; Saxell, H.; Rissanen, K.; Schalley, C. A. *Inorg. Chem.* **2008**, *47*, 7588.
- [7] Luque, I.; Freire, E. *Methods Enzymol.* **1998**, *295*, 100.
- [8] This method is somehow a reverse method compared to the titration and is used in cases, where the host and/or the guest are bad soluble in the solvent of choice, but the host-guest complex is good soluble, see Hunter, C. A.; Parker, M. J. *Chem.-Eur. J.* **1999**, *5*, 1891.
- [9] (a) Blandamer, M. J. In *Biocalorimetry: Applications of Calorimetry in the Biological Sciences*; Ladbury, J. E., Chowdhry, B. Z., Eds.; Wiley: Chichester, **1998**. (b) Holdgate, G. A. *BioTechniques* **2001**, *31*, 164. (c) O'Brien, R.; Ladbury, J. E.; Chowdhry, B. Z. In *Protein-Ligand Interactions: Hydrodynamics and Calorimetry. A Practical Approach*; Harding, S. E., Chowdhry, B. Z., Eds.; Oxford University Press: Oxford, **2001**. (d) Hansen, L. D.; Fellingham, G. W.; Russell, D. J. *Anal. Biochem.* **2011**, 220.
- [10] Praefcke, G. J. K.; Herrmann, C. *Biospektrum* **2005**, *11*, 44.
- [11] Pierce, M. M.; Raman, C. S.; Nall, B. T. *Methods* **1999**, *19*, 213.
- [12] (a) This schematic representation of an ITC experiment was made by Nora L. Löw for a presentation during a conference (SFB 765 "multivalency"). (b) <http://www.tainstruments.com>.
- [13] Indyk, L.; Fisher, H. F. *Methods Enzymol.* **1998**, *295*, 350.
- [14] Turnbull, W. B.; Daranas, A. H. *J. Am. Chem. Soc.* **2003**, *125*, 14859.
- [15] Sessler, J. L.; Gross, D. E.; Cho, W.-S.; Lynch, V. M.; Schmidtchen, F. P.; Bates, G. W.; Light, M. E.; Gale, P. A. *J. Am. Chem. Soc.* **2006**, *128*, 12281.
- [16] Schmidtchen, F. *Isothermal Titration Calorimetry in Supramolecular Chemistry*, in: *Analytical Methods in Supramolecular Chemistry* (Ed.: Schalley, C. A.), Wiley-VCH, Weinheim, **2006**.
- [17] Dethlefs, C.; Eckelmann, J.; Kobarg, H.; Weyrich, T.; Brammer, S.; Näther, C.; Lüning, U. *Eur. J. Org. Chem.* **2011**, 2066.
- [18] Aakeröy, C. B.; Champness, N. R.; Janiak C. *CrystEngComm* **2010**, *12*, 22.

- [19] (a) Adams, H.; Carver, F. J.; Hunter, C. A.; Osborne, N. J. *Chem. Commun.* **1996**, 2529. (b) Allot, C.; Adams, H.; Bernad, P. L., Jr.; Hunter, C. A.; Rotger, C.; Thomas, J. A. *Chem. Commun.* **1998**, 2449.
- [20] Jiang, W.; Sattler, D.; Rissanen, K.; Schalley, C. A. *Org. Lett.* **2011**, *13*, 4502-4505.
- [21] (a) Bonifazi, D.; Enger, O.; Diederich, F. *Chem. Soc. Rev.* **2007**, *36*, 390. (b) Corondao, E.; Gaviña, P.; Tatay, S. *Chem. Soc. Rev.* **2009**, *38*, 1674. (c) Davis, J. J.; Orłowski, G. A.; Rahman H.; Beer, P. D. *Chem. Commun.* **2010**, *46*, 54.
- [22] (a) Hugel, T.; Seitz, M. *Macromol. Rapid Commun.* **2001**, *22*, 989. (b) Neuman, K. C.; Nagy, A. *Nature Methods* **2008**, *5*, 491.
- [23] Zou, S.; Schönherr, H.; Vancso, G. J. *J. Am. Chem. Soc.* **2005**, *127*, 11230.
- [24] (a) Gross, J. H. *Mass Spectrometry*, Springer-Verlag Berlin Heidelberg/Germany, **2004**. (b) McIver, R. T.; McIver, J. R. *Fourier Transform Mass Spectrometry - Principles and Applications*, IonSpec Corporation, **2006**. (c) de Hoffmann, E.; Stroobant, V. *Mass Spectrometry: Principles and Applications*, Wiley, Chichester/England, **2007**.
- [25] (a) Schalley, C. A.; Martín, T.; Obst, U.; Rebek, J., Jr. *J. Am. Chem. Soc.* **1999**, *121*, 2133. (b) Schalley, C. A.; Castellano, R. K.; Brody, M. S.; Rudkevich, D. M.; Siuzdak, G.; Rebek, J., Jr. *J. Am. Chem. Soc.* **1999**, *121*, 4568. (c) Schalley, C. A.; Rivera, J. M.; Martín, T.; Santamaría, J.; Siuzdak, G.; Rebek, J., Jr. *Eur. J. Chem.* **1999**, 1325. (d) Schalley, C. A. *Int. J. Mass Spectrom.* **2000**, *194*, 477. (e) Schalley, C. A. *Mass Spectrom. Rev.* **2001**, *20*, 253. (f) Schalley, C. A.; Müller, T.; Linnartz, P.; Witt, M.; Schäfer, M.; Lützen, A. *Chem.-Eur. J.* **2002**, *8*, 3538. (g) Schalley, C. A.; Hoernschemeyer, J.; Li, X.; Silva, G.; Weis, P. *Int. J. Mass Spectrom.* **2003**, *228*, 373. (h) Schalley, C. A.; Ghosh, P.; Engeser, M. *Int. J. Mass Spectrom.* **2004**, *232*, 249. (i) Baytekin, B.; Baytekin, H. T.; Schalley, C. A. *Org. Biomol. Chem.* **2006**, *4*, 2825. (j) Engeser, M.; Rang, A.; Ferrer, M.; Gutiérrez, H. T. Baytekin, Schalley, C. A. *Int. J. Mass Spectrom.* **2006**, *255-256*, 185. (k) Schalley, C. A.; Springer, A. *Mass Spectrometry and Gas-Phase Chemistry of Non-Covalent Complexes*; Wiley, Hoboken/USA, **2009**. (l) Jiang, W.; Schalley, C. A. *J. Mass. Spectrom.* **2010**, *45*, 788. (m) Jiang, W.; Schäfer, A.; Mohr, P. C.; Schalley, C. A. *J. Am. Chem. Soc.* **2010**, *132*, 2309.
- [26] (a) Marshall, A.G. *Acc. Chem. Res.* **1985**, *18*, 316. (b) Marshall, A.G. *Acc. Chem. Res.* **1996**, *29*, 307. (c) Marshall, A. G.; Hendrickson, C. L.; Jackson, G. S. *Mass Spectrom. Rev.* **1998**, *17*, 1.
- [27] Dzyuba, E. V.; Poppenberg, J.; Richter, S.; Troff, R. W.; Schalley, C. A. "Mass Spectrometry and Gas-Phase Chemistry of Supramolecules: A Primer, in: *Supramolecular Chemistry - From Molecules to Nanomaterials*", Steed, J. W.; Gale, P. (eds.), John Wiley & Sons, Chichester, *accepted*.
- [28] Beyeh, N. K.; Kogej, M.; Åhman, A.; Rissanen, K.; Schalley, C. A. *Angew. Chem. Int. Ed.* **2006**, *45*, 5214.

4 RESULTS AND DISCUSSION

4.1. Steric and Electronic Substituent Effects on Axle Binding in Amide Pseudorotaxanes: Comparison of NMR & ITC Titration Data[†]

Abstract: A combination of ¹H NMR titrations and ITC experiments was used for the investigation of the binding behavior of differently substituted monovalent diamide axle molecules to the Hunter/Vögtle tetralactam macrocycle (TLM, Figure 37). The presented results influence the design of (multivalent) (pseudo)rotaxanes and their synthetic pathways using template effects. Differences in substitution at the diamide axle change the binding properties significantly. Guests with alkyl or alkenyl chains attached to the diamide carbonyl groups have a significantly higher binding affinity to the macrocycle than guests with

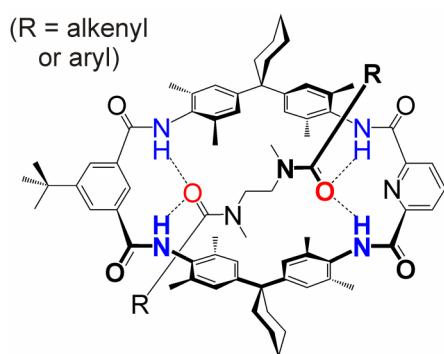


Figure 37. Structure of a pseudorotaxane consisting of a TLM and different diamide axles. These supramolecules were studied by ¹H NMR titration and ITC in order to obtain all relevant thermodynamic values in solution.

benzoyl amides and their substituted analogs. While the binding on these benzoyl and alkenyl substituted axles is driven by enthalpic effects, the binding in case of the guest with more flexible alkyl chains is mainly due to positive binding entropies.

The electronic effects of substituents at the benzoyl positions *para* to the amides also have a significant influence on the binding affinities. Electron-donating substituents increase the binding energy, whereas electron-withdrawing substituents decrease it. This can be explained by the electron density differences, strongly depend on the substitution of the diamide axle. Consequently, electron-withdrawing groups reduce the electron density in the binding motif and no or only weak hydrogen bonding occurs to the TLM and vice versa. The tendency of binding energies thus nicely follows the Hammett substituent parameters.

[†] Dzyuba, E. V.; Kaufmann, L.; Malberg, F.; Löw, N. L.; Groschke, M.; Brusilowskij, B.; Huuskonen, J.; Rissanen, K.; Kirchner, B.; Schalley, C. A. *Chemistry - An European Journal*. The original article will be online available at [http://onlinelibrary.wiley.com/journal/10.1002/\(ISSN\)1521-3765](http://onlinelibrary.wiley.com/journal/10.1002/(ISSN)1521-3765). Please contact the corresponding author (Egor V. Dzyuba) for reprint or pdf request.

4.2. Phenanthroline-Substituted Tetralactam Macrocycles: A Facile Route to Rigid Di- and Trivalent Receptors and Interlocked Molecules[†]

Abstract: A novel TLM bearing a phenanthroline moiety was prepared and investigated (Figure 38). Two synthetic routes were chosen to obtain the desired macrocycle. No product was obtained in case of the Miyaura borylation of the bromo-substituted TLM to the corresponding pinacol boronic acid ester TLM and subsequent Suzuki coupling with a bromophenyl substituted imidazolated phenanthroline compound. The desired phenanthroline-substituted TLM was obtained by using the Suzuki coupling of a 4-formyl-phenyl pinacol boronic acid ester leading to an aldehyde moiety and subsequently an imidazole formation with 1,10-phenanthroline-5,6-dione.

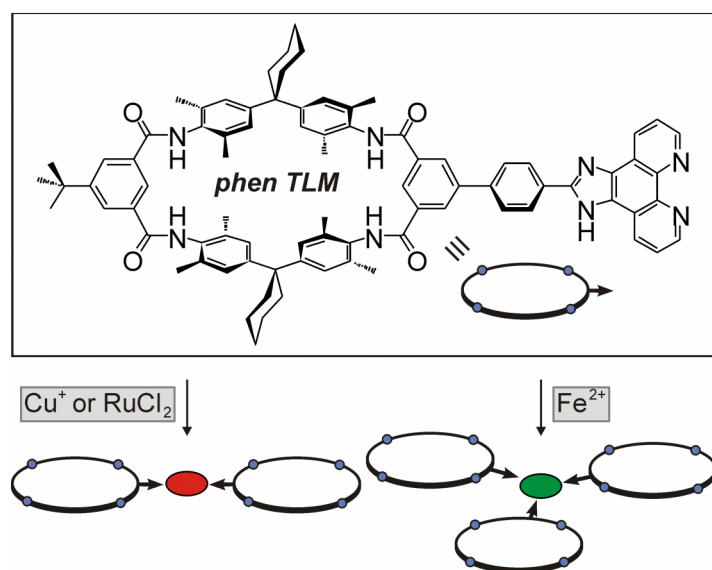


Figure 38. The structure of the phenanthroline-TLM used for the synthesis of di- and trivalent hosts through metal coordination chemistry.

tries were formed if Cu^{I} and RuCl_2 cores were used. On the other hand, a trivalent complex is obtained from Fe^{II} . Depending on the nature of the metal ion, the complexes' properties can be tuned with respect to valency (e. g. phen-TLM + Cu^{I} : divalent, phen-TLM + Fe^{II} : trivalent) and lability against TLM ligand exchange (e. g. Cu^{I} : slow, but reversible exchange, $\text{Ru}^{\text{II}}\text{Cl}_2$: kinetically inert).

phenanthroline substituted imidazolated phenanthroline compound. The desired phenanthroline-substituted TLM was obtained by using the Suzuki coupling of a 4-formyl-phenyl pinacol boronic acid ester leading to an aldehyde moiety and subsequently an imidazole formation with 1,10-phenanthroline-5,6-dione.

The phenanthroline TLM is able to form multivalent metal complexes with metal centers such as Cu^{I} , Ru^{II} or Fe^{II} . On the one hand, divalent metallo-supramolecules with different coordination geometries

[†] Dzyuba, E. V.; Baytekin, B.; Sattler, D.; Schalley, C. A. *European Journal of Organic Chemistry*. The original article will be online available at [http://onlinelibrary.wiley.com/journal/10.1002/\(ISSN\)1099-0690](http://onlinelibrary.wiley.com/journal/10.1002/(ISSN)1099-0690). Please contact the corresponding author (Egor V. Dzyuba) for reprint or pdf request.

4.3. Synthesis of Multivalent Host and Guest Molecules for the Investigation in Multivalency and Cooperativity

Abstract: In order to obtain more insights into multivalency effects in synthetic supramolecular systems, the “toolbox” approach that was used to implement Vögtle/Hunter-type TLM and diverse dicarbonyl guest compounds (mostly the diamide axle centerpiece) was applied. In addition to the multivalent hosts through metal coordination chemistry shown in chapter 4.2, hosts were obtained by connecting TLMs through appropriate linker molecules such as 2,2'-bipyridine, different ethynyl-substituted benzenes, styrene, CH₂ chains etc. Convenient multivalent guests are presented here. However, binding studies using NMR or ITC that have to be performed leading to all relevant thermodynamics were not successful so far mostly due to the rather bad solubility of the multivalent hosts. NMR dilution and NMR displacement experiments mentioned in this thesis e. g. using monovalent squaraine axle were also performed but the evaluation of the obtained data proved to be complicated due to strong broadening and overlapping of the signals in the ¹H NMR spectra. However, further investigations have to be performed. In addition, some compounds were synthesized for the investigation of multivalency and cooperativity using gold surfaces or nanoparticles.

Introduction: This chapter summarizes the results obtained from the synthesis of the multivalent hosts and guests bearing Vögtle/Hunter-type TLM's and dicarbonyl guest compounds, their characterization and the evaluation of their binding behavior performed during this thesis (with the exception of those described in chapter 4.2). All compounds shown here are based on previous work from Schalley *et al.*^[1] as mentioned in chapter 2. Mainly, the diamide moiety was implemented into the multivalent guest molecules.

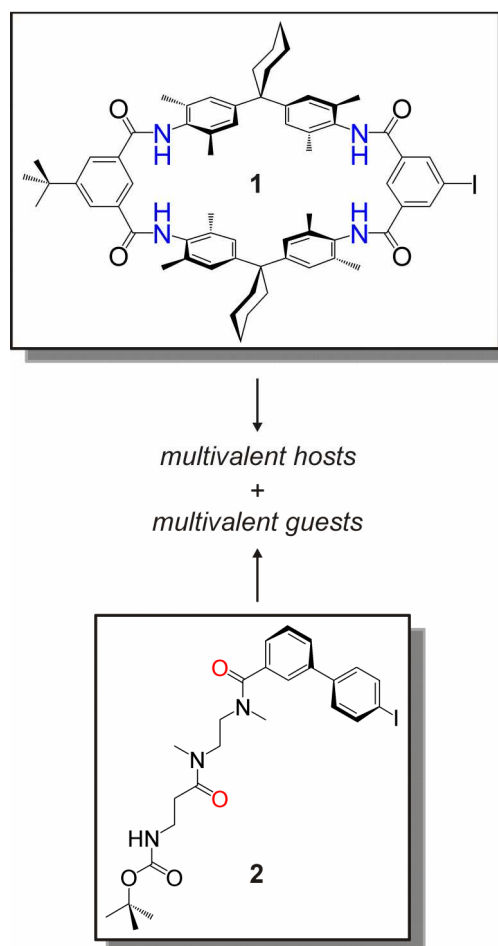


Figure 39. The structures of the iodo-substituted TLM **1** and the diamide axle **2** those were used for the construction of a “toolbox” of multivalent hosts and guests using Sonogashira coupling.

Result and Discussion: During the first project described here, the “toolbox” approach was used and several di- and trivalent hosts and guest were synthesized in addition to the compounds described earlier.^[1] As starting material, only two simple building blocks were used: The iodo-substituted TLM **1**^[1a] and a iodo-substituted axle centerpiece **2**^[1c] (Figure 39), that was first synthesized by Brusilowskij using a four-step procedure.^[1c] Both compounds can be connected through linker moieties to multivalent host and/or guest molecules by using Sonogashira coupling^[2]. Although iodo, bromo, triflate and chloro groups were also used as coupling reagents, the previous studies showed only iodo to be suitable enough, even if TLM's were applied in the Sonogashira coupling.^[1a]

Initially, Baytekin developed the “toolbox” approach for the synthesis of multivalent hosts^[1b] and guests and Brusilowskij was able to isolate first di- and trivalent host and guest molecules.^[1c] This research was continued and the compounds **4**, **6**, **9** and **11** shown in Figures 40 and 41 were obtained in good to satisfying yields by coupling of the linker molecules **3**, **5** and **7** to TLM **1** or diamide axle **2**. Besides numerous possible catalysts exist, $(\text{Ph}_3\text{P})_2\text{PdCl}_2$ and CuI under the presence of co-ligand PPh_3 , and NEt_3 as base were used. This protocol is known to be successful for the synthesis of the trivalent host **8**^[1a] shown here for completeness. It should be noted that for the synthesis of the di- and trivalent guests shown in Figure 41 different Sonogashira conditions were applied since neither the use of $(\text{Ph}_3\text{P})_2\text{PdCl}_2/\text{CuI}/\text{PPh}_3$ nor $\text{Pd}_2(\text{dba})_3/\text{AsPh}_3$ ^[1c] resulted in the desired products. The reactions proceeded only under conditions shown in Figure 41 in adequate yield.

The approach described here uses different ethynyl-substituted spacers that differ in the number of these groups and their positions to each other. Thus, the multivalent interactions can be investigated under the focus of the number of binding sites and their spatial arrangement in respect to each other. However, ^1H NMR titrations and ITC experiments are not applicable here so far as the solubility of the components in non-competitive solvents differs completely from those monovalent hosts and guests described in chapter 4.1. Therefore, the behavior of the pseudorotaxanes resulted from this “toolbox” is initially under study^[3] using two methods: (i) ^1H NMR dilution experiments that are required for cases where the single components are not soluble but the complex is. Using this approach, the complex can be prepared from its components in 1:1 ratio in known concentration. After addition of known amounts of pure solvent, a dethreading process should be observable because of the dilution. This method is somehow similar to a reversible ^1H NMR titration. (ii) ^1H NMR displacement experiments can be used here as well. This approach was described in chapter 3.4 using a monovalent squaraine axle.

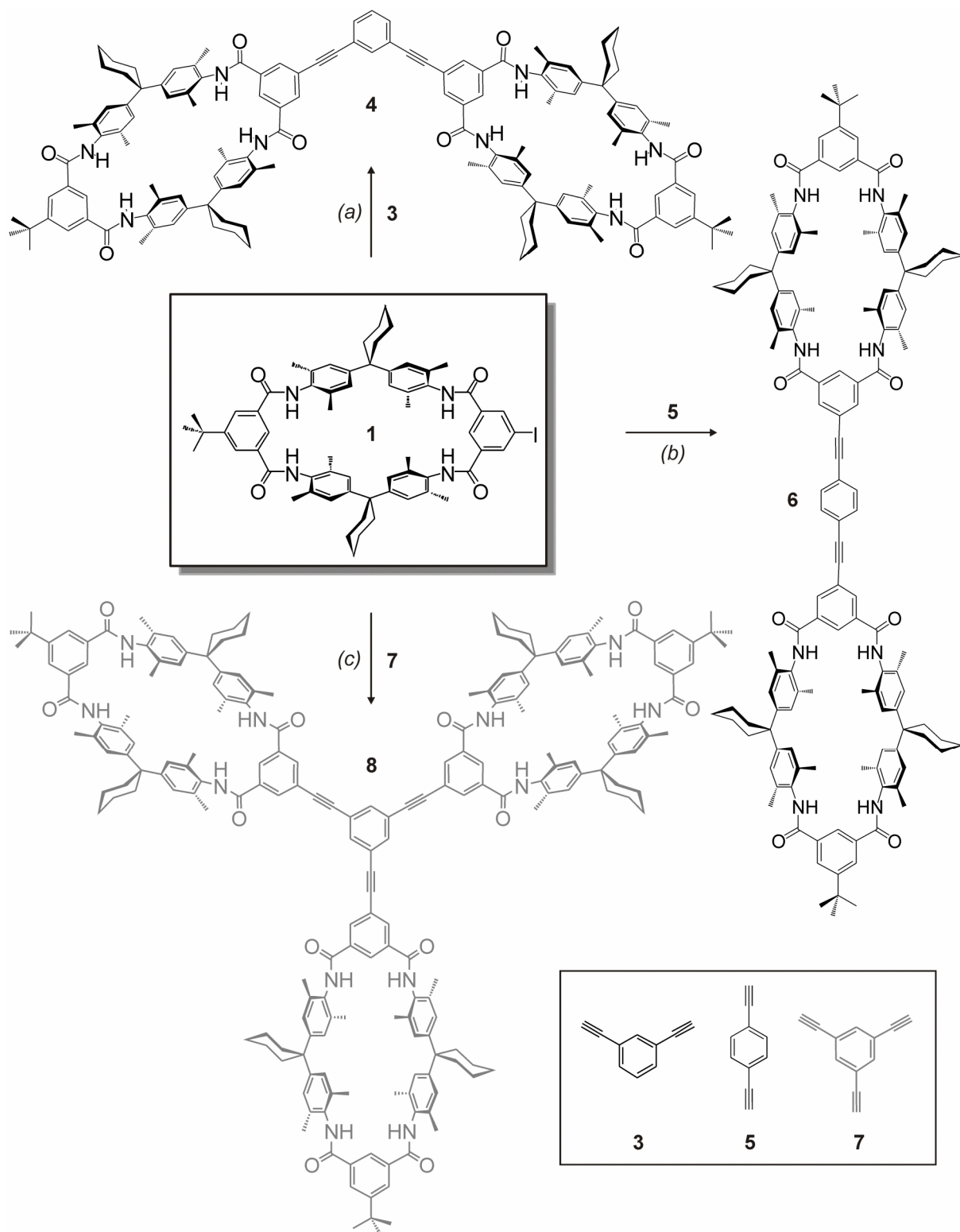


Figure 40. Synthesis of a series of di- and trivalent hosts starting from the iodo-substituted TLM 1: (a), (b), (c) $(\text{Ph}_3\text{P})_2\text{PdCl}_2$, CuI, PPh_3 , NEt_3 , DMF, 25 °C, 24 hours, 90% (**3**), 78% (**5**), 40% (**8**). The trivalent host grey-colored was reported previously^[1a] and is shown here only for sake of completeness.

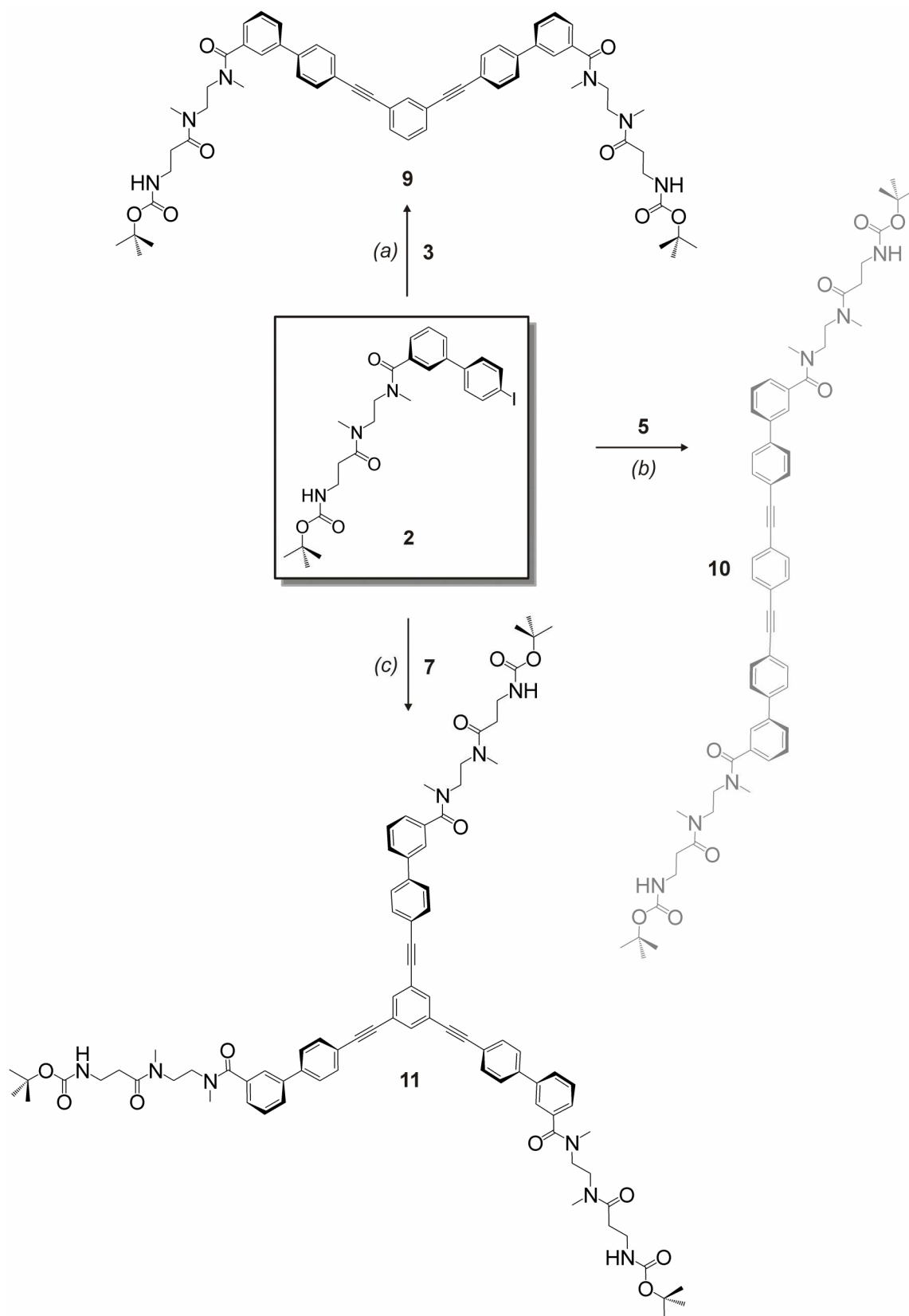


Figure 41. Synthesis of a series of multivalent guests starting from the axle **2**: (a), (b), (c) $\text{Pd}_2(\text{dba})_3$, CuI , PPh_3 , NEt_3 , DMF , $70\text{ }^\circ\text{C}$, 3 days, 32% (**9**), 37% (**10**), 24% (**11**). The divalent guest grey-colored was reported previously^[1c] and is shown here only for sake of completeness (dba = dibenzylideneacetone).

In the next study, the “toolbox” approach was applied to different 2,2'-bipyridines (Figure 42). It is preferable to study this system as the coordination of Pt^{II}/Pd^{II} or Fe^{II}/Ru^{II} at the bipyridine core leads to tetra- and hexavalent host molecules. Besides tetravalent hosts were obtained through complexation of their pyridine units to Pd^{II} in early studies,^[1a] the synthesis of multivalent hosts containing TLM's through metal coordination is limited to the di- and trivalent complexes shown in chapter 4.2. Especially the hexavalent molecules are difficult to achieve by using covalent coupling even though these compounds would lead to a significant impact to this research.

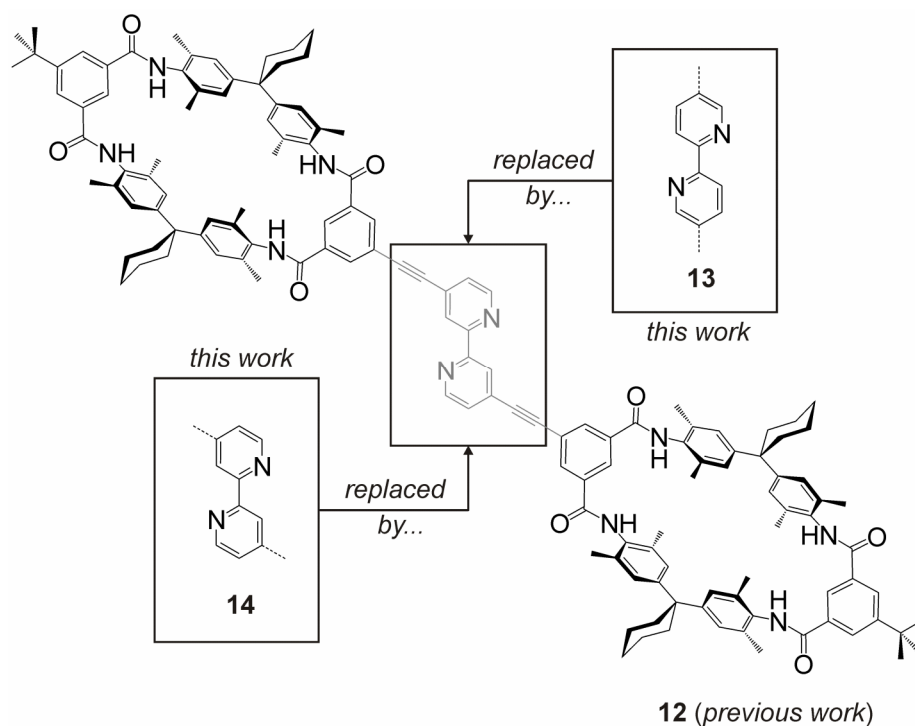


Figure 42. The divalent host consisting of the 2,2'-bipyridine, disubstituted with two TLM's at the 4,4'-positions *via* ethynyl linkers, was synthesized previously by Brusilowskij using Sonogashira coupling^[1c]. The diethynylsubstituted 2,2'-bipyridine skeleton was replaced by other different 2,2'-bipyridine cores in this work.

In order to synthesize the divalent host molecules **13** and **14** using Suzuki coupling (Figures 42 and 43), separate reactions of TLM **15** with either 5,5'- or 4,4'-dibromo-2,2'-bipyridine **16** or **17** were investigated. The divalent host **13** was obtained after chromatographic workup in a satisfying yield of 46%. In contrast, no desired product **14** could be detected as confirmed by NMR and ESI MS in case of the Suzuki coupling at the 4,4'-position at the bipyridine skeleton. In order to obtain this compound using another synthetic pathway, bromo-substituted TLM **18** was used in the Suzuki coupling with pyridine derivative **19**. The resulted TLM **20** should be able to undergo a nickel-catalyzed Negishi homocoupling to the desired host **14**. However, no successful separation of the precursor **18** from the

product **20** was achieved using chromatographic workup procedures. This was clearly confirmed by ESI MS (by spraying a sample from CH₂Cl₂/MeOH 1:1 v/v), where **18** appears as H⁺-H₂O ion at *m/z* 1023, as H⁺ adduct at *m/z* 1041, as Na⁺ adduct at *m/z* 1063 and as K⁺ adduct at *m/z* 1079 (Figure 50). In contrast, peaks for the ions of **20** are visible at *m/z* 1119 (H⁺ adduct), at *m/z* 1141 (Na⁺ adduct) and at *m/z* 1157 (K⁺ adduct). As no **14** was synthesized, neither directly by coupling of **17** to **19** nor *via* **22**, no further synthesis was performed (e.g. Negishi coupling).

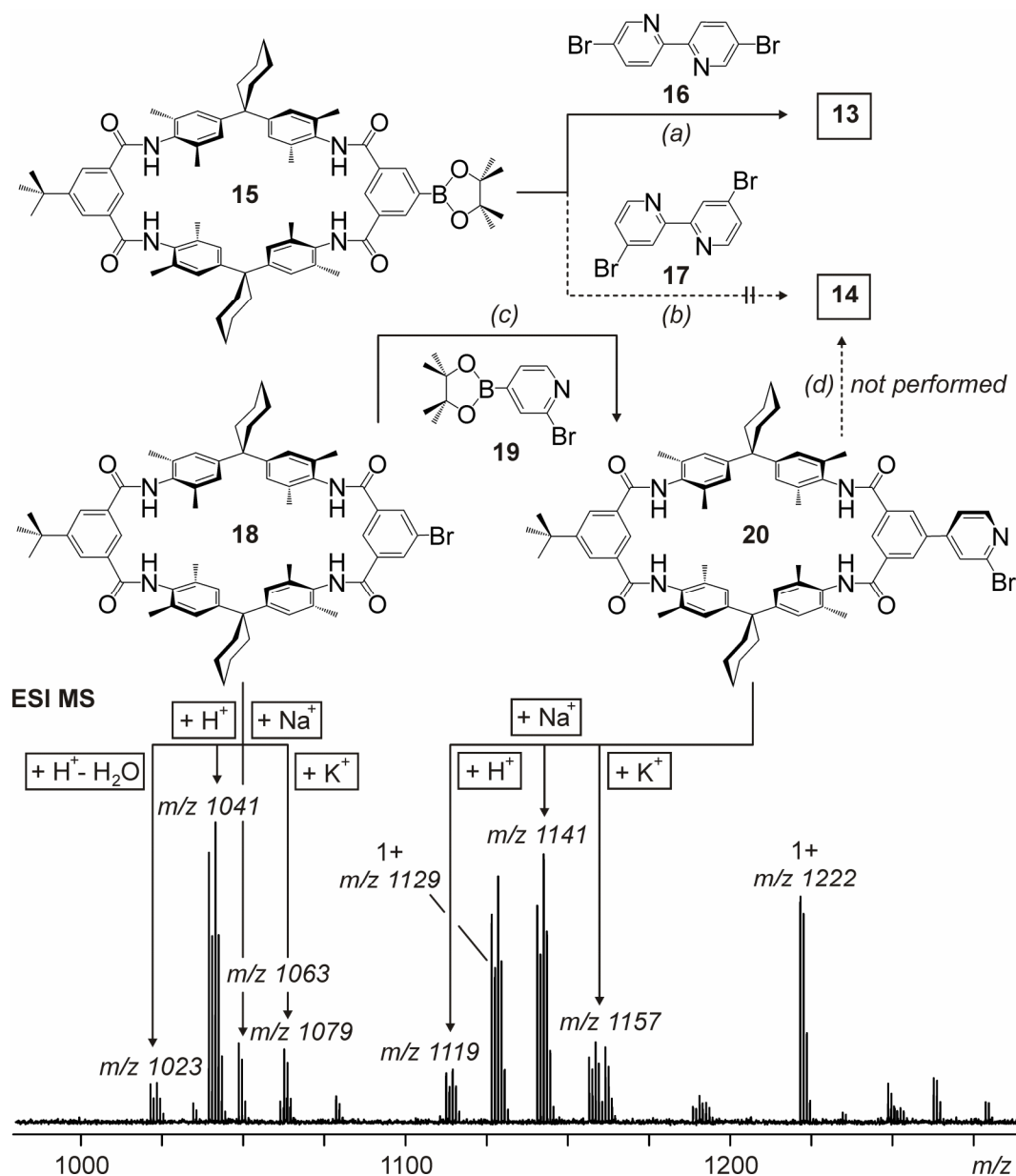


Figure 43. Experiments for the synthesis of **13** and **14**: (a) Pd(PPh₃)₄, Cs₂CO₃, DMF/toluene 1:1 v/v, 125 °C, 2 days, 46%. (b) Pd(PPh₃)₄, Cs₂CO₃, DMF/toluene 1:1 v/v, 125 °C, 2 days. (c) Pd₂(dba)₃, PPh₃, Cs₂CO₃, DMF/toluene 1:1 v/v, 125 °C, 24 hours. (d) NiCl₂ • 6H₂O, PPh₃, Zn, DMF, 60 °C^[4]. The Suzuki coupling of **18** to **20** resulted in a chromatographically inseparable mixture of these both TLM's as clearly confirmed by ESI MS shown here.

For the first time ever, it was possible to introduce the diketopiperazine station into a multivalent guest (Figure 44) by the reaction of two equivalents of monomethylated diketopiperazine **21** and 1,6-diiodohexane **22**.^[5] The resulting molecule **23** should be able to thread into the divalent host **12** described above.

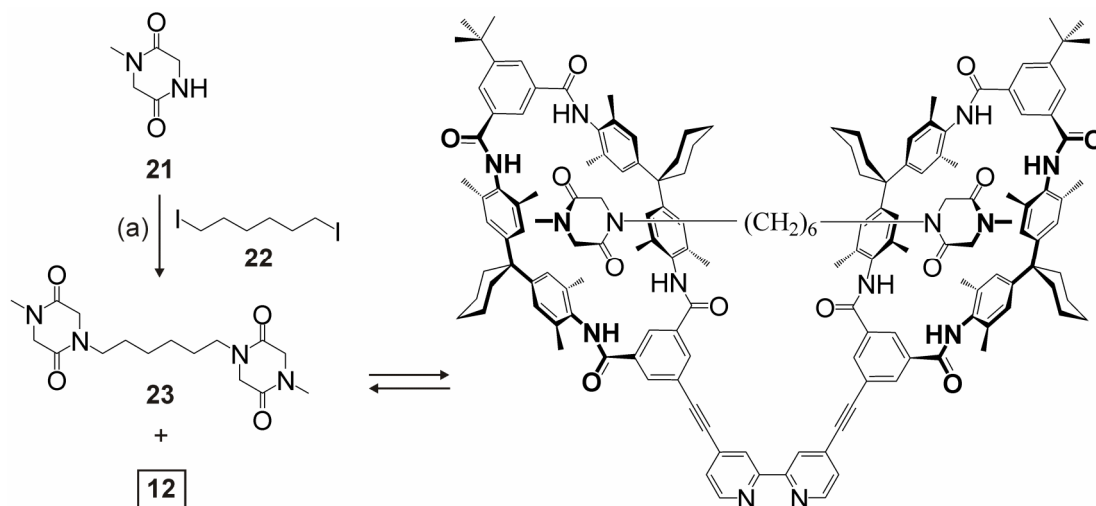


Figure 44. Synthesis of the divalent guest **23** bearing two diketopiperazine binding stations: (a) NaH (60 wt%), DMF, 0 °C, 2 hours, 25 °C, 18 hours, 53%. Compound **21** was synthesized using literature-known protocol.^[6] This guest should be able to form a host-guest complex with **12** as shown here. Until now no further investigations were performed.

Further studies deal with the synthesis of divalent host and guest molecules shown in Figure 45. Two different host molecules were designed for this system. On the one hand, the host **24** bears a rigid styrol moiety, which connects two TLMs in one molecule. On the other hand, the second host **25** contains a flexible alkyl chain of six CH₂ groups between the two TLMs. The guest **26** is also flexible, because it bears an alkyl chain of 18 CH₂ groups in between the diamide stations. For both divalent [2]pseudorotaxanes resulted from **24** or **25** with **26**, the MM2 force field method implemented into CaChe 5.0^[7] leads to reasonable calculated structures (Figure 46). Additional end-capped substitution with phenyl ethynyl moieties would allow the use of “click chemistry” for the stoppering reaction if one would like to synthesize divalent [2]rotaxanes. Further aim of this project is to evaluate wherever a linker (flexible vs. rigid) plays an important role in the threading process.

The synthesis of the host **24** and **25** is shown in Figure 47. Starting from the bromo-substituted TLM **18**^[1a] a phenyl vinyl moiety was introduced resulting in the TLM **28** through Suzuki coupling with pinacol ester **27**. Subsequently, TLM **28** was applied in a ruthenium-catalyzed metathesis reaction with itself to the desired host **24**. Besides other catalysts such as Grubbs Ind or IInd Generation are often applied in metathesis reactions,^[8] the use of the Grubbs-Hoveyda IInd Generation **GH II Gen** catalyst gives the best yield (56%) of **24**.

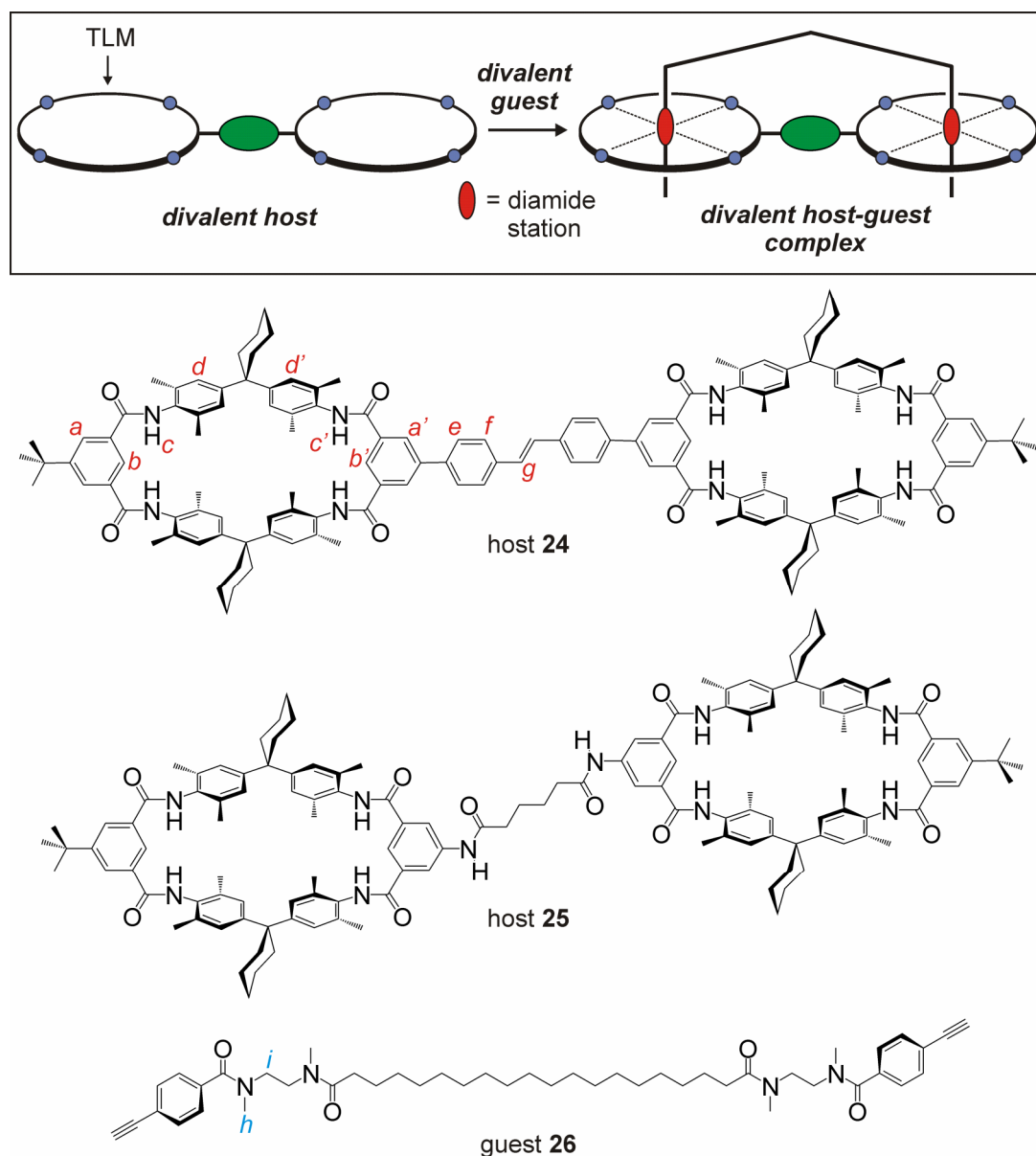


Figure 45. Schematic representation of the aim of this project using divalent hosts **24** and **25**, and appropriate guest **26**.

The other host **25** was obtained after the reaction of amino substituted TLM **29**^[1b] and adipoyl chloride **30** in a yield of 43%. In addition, the synthesis procedure for the guest **26** is shown in Figure 47 and starts with the mono Boc-protected diamide **31**^[9], which reacts with 11-undecenoyl chloride **32** yielding the compound **33** in 92% yield. Subsequently, a “self-metathesis” was performed using **GH II Gen** as described for the host **24** and the divalent axle centerpiece **34** resulted in a satisfactory yield of 43%. In order to obtain the desired guest molecule **26**, three successively consecutive reaction steps were applied. First, the double bond was reduced using standard hydrogenation procedure. After this, the Boc groups were removed under acidic conditions. As the last step, acid **35** was introduced into the axle. As the hydrogenation normally proceeds with a nearly quantitative yield and the

cleavage of two Boc groups results here in a diamine moiety that is hard clean by column chromatography alone, the chromatographic work up was performed after the amide coupling reaction. As coupling reagents, CDMT and NMM^[10] were used and the guest **26** resulted in a yield of 22% over three steps.

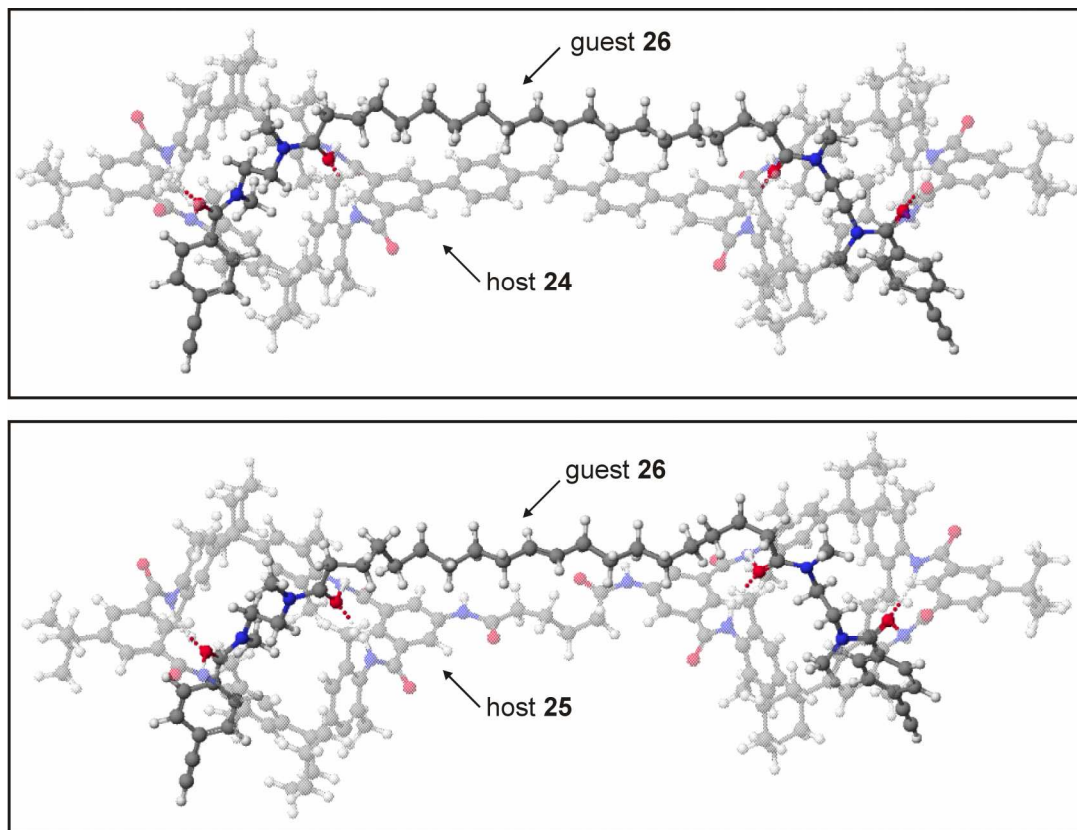


Figure 46. MM2-calculated structures of the host-guest complexes resulted from **30** and **32** (top) and **31** and **32** (bottom).

Additional confirmation of **24** and **25** provide NMR and ESI MS (Figure 48). The ¹H NMR of **24** shows all signals as expected in the aromatic region. No signals for the amide protons *c* and *c'* are visible because of the solvent mixture CD₂Cl₂/CD₃OD 6:1 v/v (H/D exchange of TLM-amide-NH with CD₃OD). The addition of CD₃OD is necessary; otherwise an aggregation would occur resulting in strong signal broadening that would complicate peak assignment. A peak for the double bond proton *g* occurs at 7.26 ppm indicating that only a double bond with TLM's *trans* is formed since a *cis* double bond would give a signal below 7.0 ppm.^[8] ESI MS confirms the formation of the hosts **24** and **25**. Spraying from CH₂Cl₂/MeOH 1:1 v/v with addition of NEt₃ (because ionization turned out to be significantly easier, when NEt₃ were added which forms a complex with the TLM's in high abundances)^[1a], only ions [M+H]⁺, [M+Na]⁺ and [M+HNEt₃]⁺ of either **24** (*m/z* = 2099, 2121 and 2200, respectively) or **25** (*m/z* = 2063, 2085 and 2164, respectively) occur.

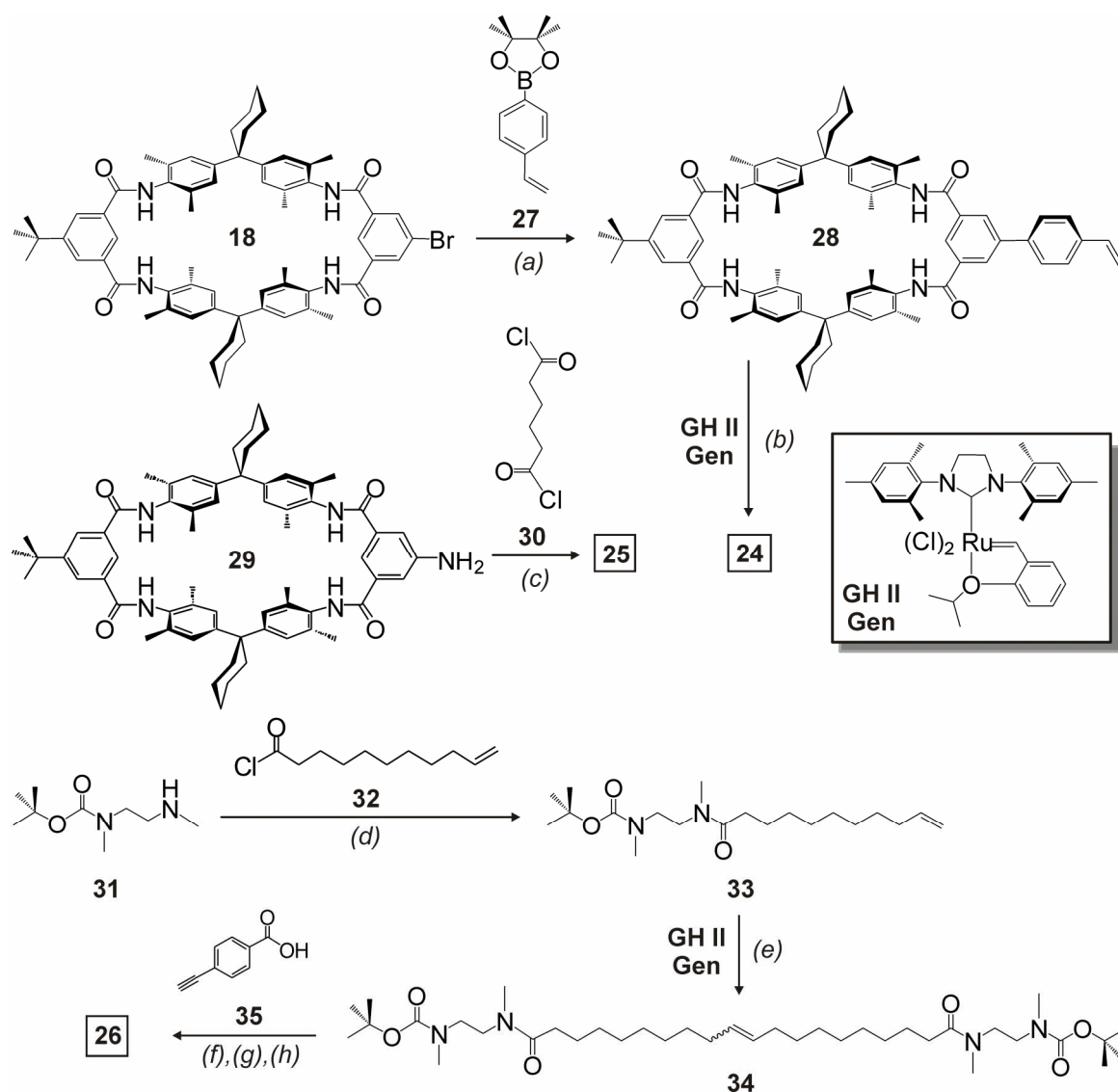


Figure 47. Synthesis of **24**, **25** and **26**: (a) $\text{Pd}(\text{PPh}_3)_4$, Cs_2CO_3 , DMF/toluene 1:1 v/v, 125 °C, 2 days, 72%. (b) **GH II Gen**, CH_2Cl_2 , 25 °C, 3 days, then 40 °C, 18 hours, 56%. (c) NEt_3 , CH_2Cl_2 , 40 °C, 18 hours, 43%. (d) NEt_3 , CH_2Cl_2 , 25 °C, 24 hours, 92%. (e) **GH II Gen**, CH_2Cl_2 , 25 °C, 3 days, then 40 °C, 6 hours, 43%. (f) H_2 , Pd/C, EtOH, 25 °C, 3 days. (g) TFA, CH_2Cl_2 , 0 °C, 1 hour, 25 °C, 24 hours. (h) CDMT, NMM, $\text{CH}_2\text{Cl}_2/\text{MeCN}$ 2:1 v/v, 0 °C, 2 hours, 25 °C, 2 days, 22% over three steps (TFA = trifluoroacetic acid, CDMT = 2-chloro-4,6-dimethoxy-1,3,5-triazine, NMM = N-methylmorpholine).

The partial ^1H NMR spectra of compound **34** and the guest **26** suggest some characteristics of these divalent guests. In comparison to **24**, the signal for the double bond (Figure 48) occurs here as a multiplet indicating that this double bond in the center of **34** is a mixture of *cis*,*trans*-isomers that are typically formed after a metathesis reaction.^[8] Figure 48 shows the aliphatic region of the ^1H NMR spectra of guest **26**. As explained in chapter 4.1 for monovalent diamide axes, the diamide station show a strong preference for *cis*/*trans*-isomerization. This is clearly illustrated here since multiplets (for the CH_2 groups and three (or more) singulets, some of them broader, for the CH_3 groups are visible.

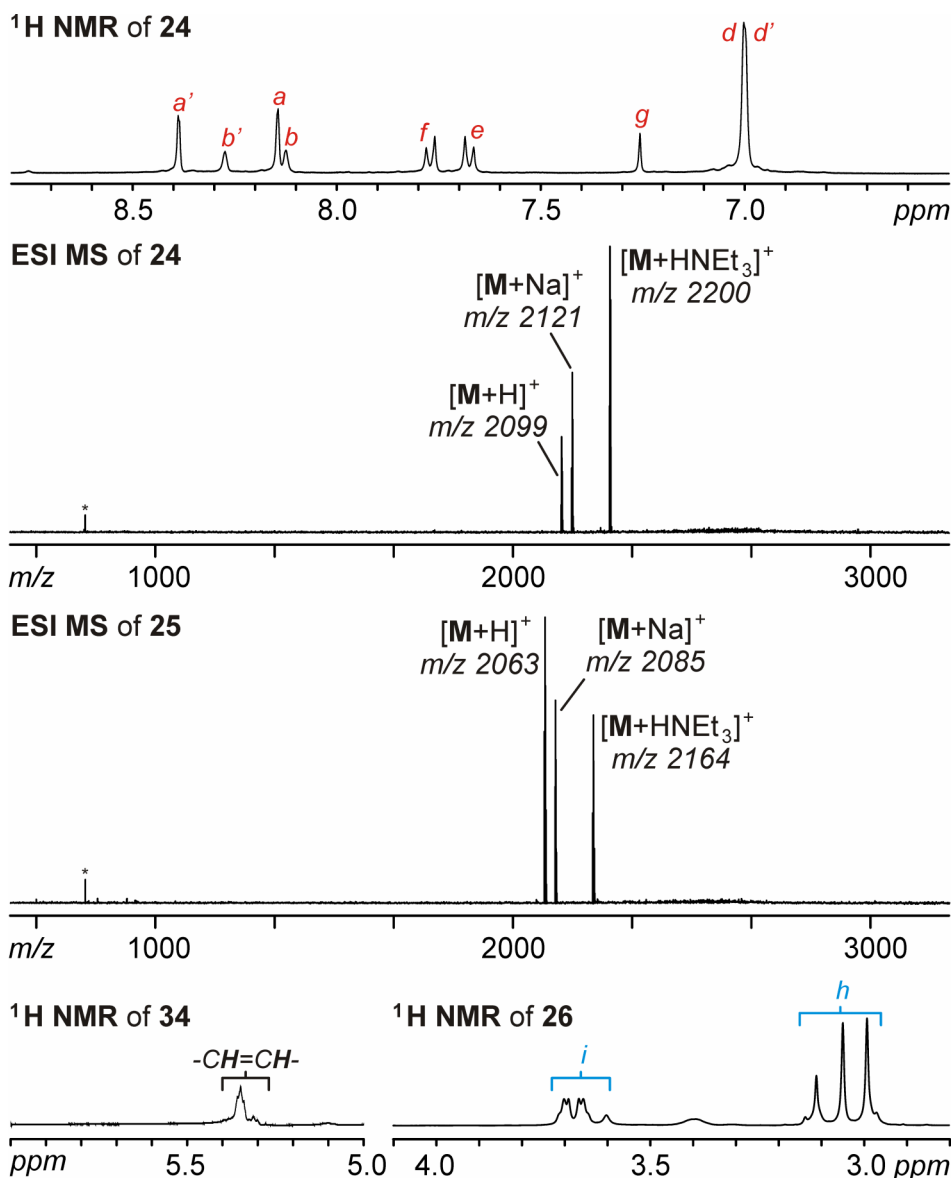


Figure 48. Aromatic region of the ^1H NMR spectrum of host **24** (500 MHz, $\text{CD}_2\text{Cl}_2/\text{CD}_3\text{OD}$ 2:1 v/v), ESI MS spectra of **24** and **25**, and aliphatic region of the ^1H NMR spectra of compound **34** (400 MHz, CDCl_3) and guest **26** (500 MHz, CDCl_3). See Figure 45 for signal assignment.

Multivalent studies can also be performed at surfaces and/or nanoparticles using different analytical methods (see chapter 3.5). Taking this into account, the Vögtle/Hunter-type TLM and the different dicarbonyl compounds shown previously were decorated with sulfur-containing substituents, e. g. lipoic acid derivatives. This approach allows the investigation of mono- and multivalent binding processes using single molecule force spectroscopy (SMFS). Herein, PEG polymers terminated with the binding stations were isolated and a TLM containing two lipoic acid esters was obtained. Moreover, different TLMs and [2]rotaxanes were synthesized for the Layer-by-layer deposition of supramolecular architectures on gold nanoparticles.

Initially, Hunter/Vögtle-type TLM was decorated with two lipoic acid units by using an ester coupling protocol. This approach allows the deposition of the TLMs on a gold surface (Figure 49). PEG polymers that are often used for SMFS were separately substituted with three different dicarbonyl moieties and used as guest molecules. They are able to bind to the TLM as described in chapters 2 and 3.1. The polymer **36** bears the diamide station, **37** has the diketopiperazine moiety as the binding motif and **38** is end-capped with benzochinone moiety.^[11] Attaching these polymers separately on a gold-coated AFM tip allows to measure the forces that are necessary for the disruption of the host-guest complex formed between the TLM-decorated surface and PEG-decorated AFM tip (Figure 49). This schematic representation is limited to the monovalent case, but the surface bears more than one TLM and also the AFM tip should be able to bind more than polymer molecules. Thus, this project allows the evaluation of multivalency on surfaces.

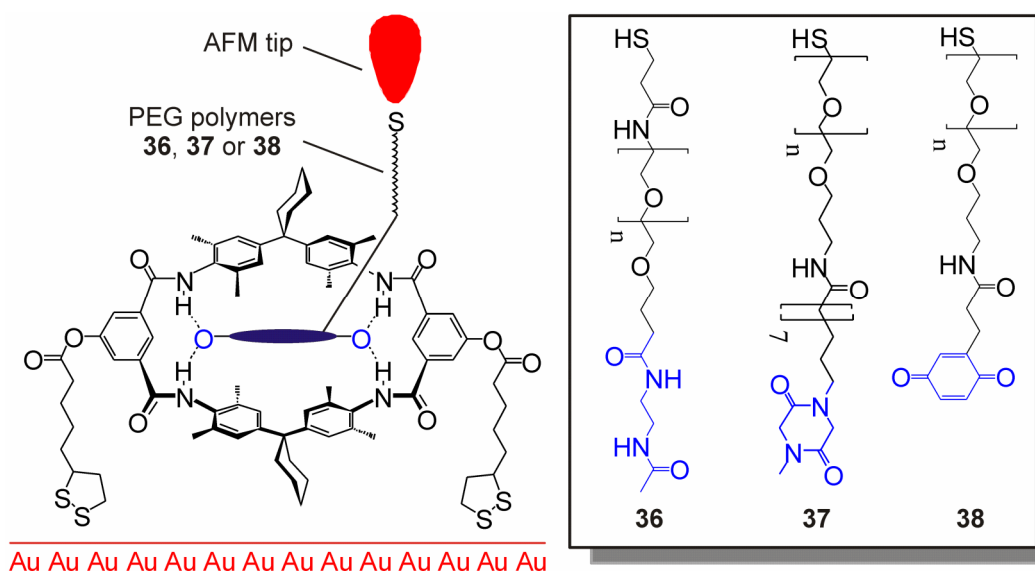


Figure 49. Principle of the SMFS investigations of a host-guest system consisting of lipoic acid-substituted TLM and different dicarbonyl-decorated PEG polymers **36** - **38** ($M_w \sim 10,000$ Da).

The synthesis of all compounds used here is shown in Figure 50. The polymer **36** was obtained from the PEG polymer **39** and mono-acetyl protected ethylene diamine **40** using EDC and HOBt as amide coupling reagents. Because such polymers are challenging to isolate using common work up procedures such as column chromatography, a dialysis was performed after the reaction had taken place in order to separate all precursors from the desired polymer. Similar approaches were applied to the polymers **37** and **38**. Here, the binding stations were introduced into the PEG polymer **41** using the acids **42** and **43**^[12]. All polymers initially were used in the SMFS analysis without further purification.^[13] In addition, the dihydroxy-substituted TLM **44**^[14] and lipoic acid **45** reacted to the desired TLM **46** under the influence of PyBOP and *i*Pr₂NEt in a good yield of 58%.

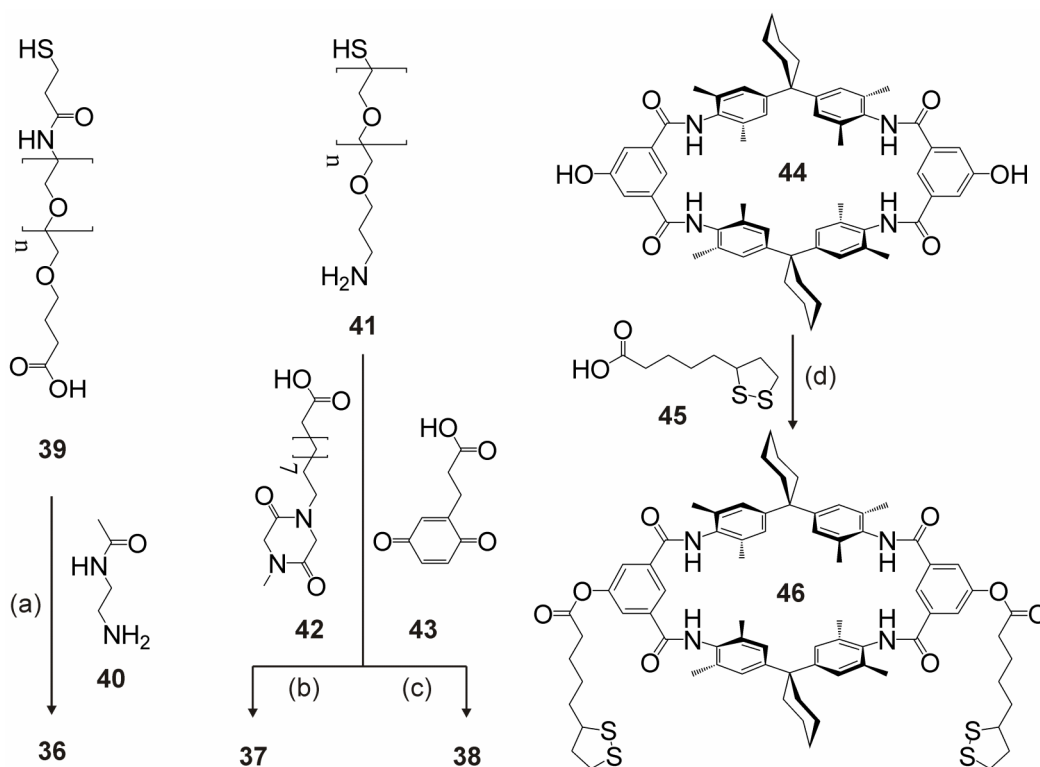


Figure 50. Synthesis of the lipoic acid-decorated TLM **46** and the PEG polymers **36**, **37** and **38**: (a) EDC, HOBT, 25 °C, 7 days, 97%. (b) EDC, HOBT, 25 °C, 7 days, 92%. (c) EDC, HOBT, 25 °C, 7 days, 58%. (d) PyBOP, *i*Pr₂NEt, CH₂Cl₂/MeCN 4:1 v/v, 25 °C, 18 hours, 58% (EDC = 1-Ethyl-3-(3-dimethylaminopropyl)carbodiimide, HOBT = N-Hydroxybenzotriazole).

Gold nanoparticles decorated with supramolecules can be also suitable for the investigation of multivalency. For this, compounds **48** and **52** were prepared (Figure 51).^[15] The [2]rotaxane **48** resulted from [2]rotaxane **47**^[14] by esterification with lipoic acid **45**. It acts as a control compound. In order to obtain multivalent gold nanoparticles, the axle **52** was synthesized. First, an amide coupling between the amine **49** and the acid **50** resulted in the compound **51** in a good yield. This compound bears a Boc protecting group and was then deprotected under acidic conditions using TFA. In the last step, the desired axle **52** was obtained by reaction with lipoic acid **45**. This system is advantageous as the nanoparticle can act as a stopper group and a multivalent pseudorotaxane would result.^[16] The termination with an ethynyl substituent allows then the attachment of a second stopper using e.g. “click chemistry”.

Conclusions: In conclusion, several multivalent hosts and guests were synthesized by using different coupling methods Suzuki, Sonogashira or amide/ester coupling. They differ in the number of their binding sites and their geometry, and allow therefore a thorough study of multivalency effects in synthetic supramolecular systems. However, bad solubility and data that are challenging to interpret because of broadening or overlapping of the signals prevent

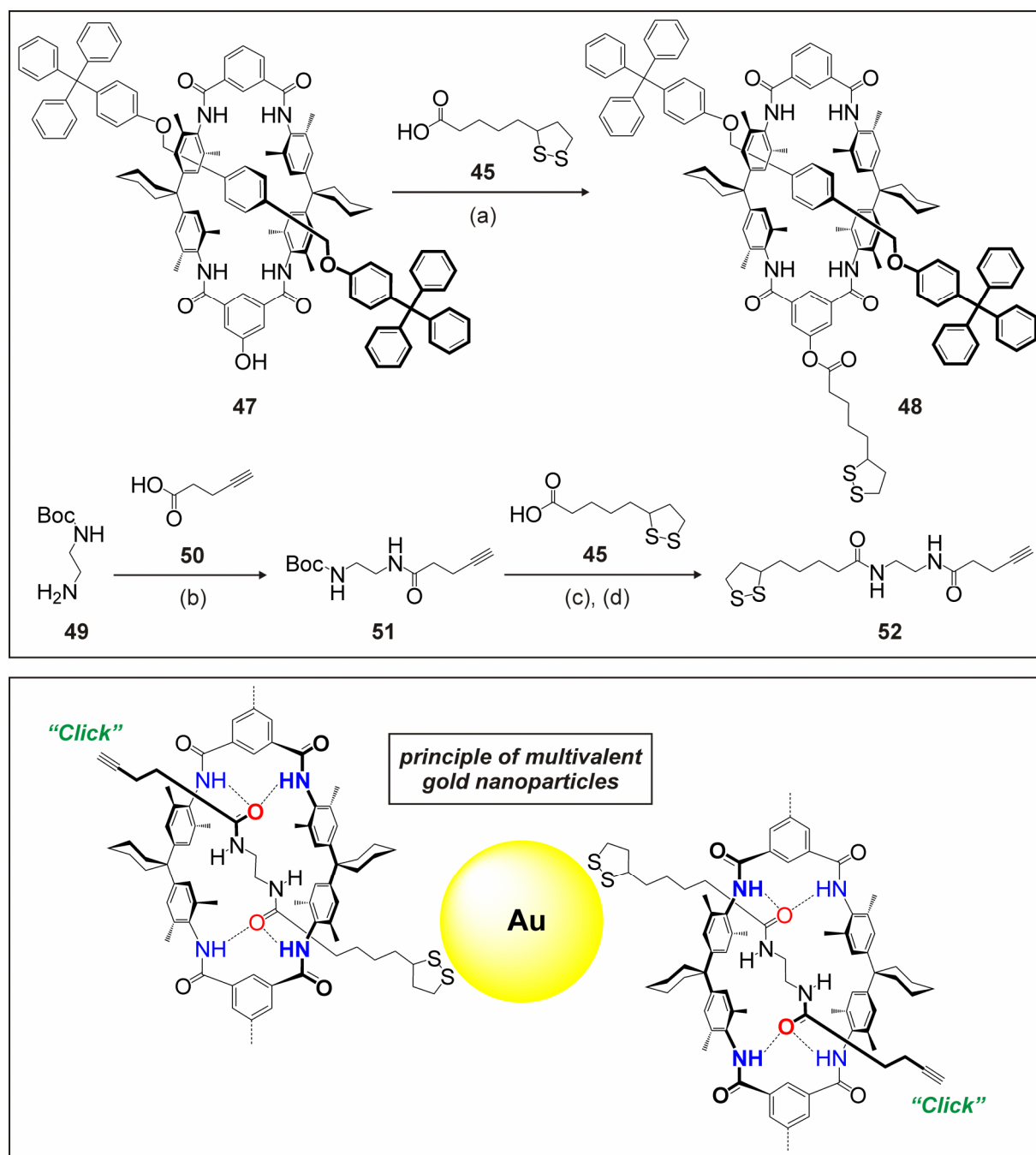


Figure 51. Synthesis of the [2]rotaxane **48** and the diamide axle **52**: (a) PyBOP, *i*Pr₂NEt, CH₂Cl₂/MeCN 4:1 v/v, 25 °C, 18 h, 71%. (b) CDMT, NMM, CH₂Cl₂, 25 °C, 24 hours, 82%. (c) TFA, CH₂Cl₂, 0 °C, 1 hour. (d) PyBOP, *i*Pr₂NEt, CH₂Cl₂/MeCN 4:1 v/v, 25 °C, 3 days, 38% (two steps). Moreover, the principle of multivalent gold nanoparticles is shown (e. g. the divalent case). Such structures can be obtained either by first forming a pseudorotaxane in solution and then deposition on the gold nanoparticle by formation of two Au-S bonds or first deposition of **52** and then forming the pseudorotaxane.

an evaluation of their binding behavior so far. The bad solubility can for example be demonstrated on the experiments to obtain the Cu⁺ complex of **13** by stirring two equivalents with Cu(MeCN)₄(PF₆) in CD₂Cl₂/CD₃CN 2:1 at 25 °C for 7 days (~ 3 mM). Regrettably, the desired complex could not be synthesized by this method. This was confirmed by NMR (no signal

shifting of the bipyridine moiety to the lower field of the ^1H NMR spectrum as expected) and ESI MS (no complex detected, not even in 1:1 ratio). In addition, no clear solution after stirring for 7 days could be obtained. These observations can be only explained by a poor solubility of **13** in the solvents applied here.

Moreover, the synthesis of different TLM's and axle compounds for surfaces was described; most of them are recently under study. For example, a lipoic acid-decorated TLM was designed and synthesized for SMFS evaluation of differently substituted PEG polymers. First AFM and SMFS measurements were performed and the data obtained therein are under evaluation.^[17] They should add new insights into the surface-based studies in the field of e. g. multivalency and cooperativity. Moreover, it would have an impact on the design of multivalent guest molecules for the Hunter/Vögtle-type TLM because the SMFS study described here would focus on the different properties of the binding stations.

Experimental section: Reagents were purchased from Aldrich, ACROS, Lancaster, or Fluka and used without further purification. All reactions were carried out under a protecting atmosphere of argon. Yields refer to chromatographically and spectroscopically homogeneous materials. Solvents were dried and distilled prior to use by usual laboratory methods. Thin-layer chromatography (TLC) was performed on precoated silica gel 60/F254 plates (Merck KGaA). Silica gel (0.04-0.063 mm; Merck) or activated neutral alumina (Macherey-Nagel) were used for column chromatography.

NMR spectroscopy: ^1H and ^{13}C spectra were obtained on Bruker ECX 400 (^1H : 400 MHz; ^{13}C : 101 MHz), Jeol ECP 500 (^1H : 500 MHz; ^{13}C : 125 MHz) or Bruker AVANCE III 700 (^1H : 700 MHz; ^{13}C : 220 MHz) instruments at 298 K. All chemical shifts are reported in ppm with signals of solvent protons taken as internal standards; coupling constants are in Hz. The following abbreviations were used to indicate NMR-multiplicities: s (singlet), d (doublet), t (triplet), q (quartet), m (multiplet), br (broad).

Mass spectrometry: ESI-TOF mass spectra were obtained on an Agilent 6210 ESI-TOF, Agilent Technologies, Santa Clara, CA, USA. The solvent flow rate was adjusted to 4 $\mu\text{L}/\text{min}$ and the spray voltage set to 4 kV. The drying gas flow rate was adjusted to 15 psi (1 bar). ESI-FT-ICR mass spectra were obtained on an Ionspec QFT-7, Varian Inc., Lake Forest, CA, USA, equipped with a 7 T magnet and a micromass Z-spray ESI source, Waters Co., Saint-Quentin, France. The solvent flow rate was adjusted to 4 $\mu\text{L}/\text{min}$ and the spray voltage set to 3.8 kV. All other parameters were optimized for a maximum abundance of the $[\text{M}+\text{H}]^+$, $[\text{M}+\text{Na}]^+$ or $[\text{M}+\text{K}]^+$ ions.

Divalent host 4: TLM **1** (200.0 mg, 0.184 mmol) and 1,3-diethynyl benzene **3** (11.3 mg, 0.09 mmol) were dissolved in DMF (10 mL) and NEt₃ (3 mL). The solution was degassed for 1 h and protected from light. Afterwards, PPh₃ (5.4 mg, 18 μmol), (Ph₃P)₂PdCl₂ (6.3 mg, 9 μmol) and Cul (1.8 mg, 9 μmol) were added. The resulting mixture was stirred at room temperature for 24 hours. The solvents were evaporated under reduced pressure and the desired product **4** was obtained after chromatographic work-up (silica gel, CH₂Cl₂/EtOAc 12:1 to 4:1 v/v) from the third fraction as a slightly brown solid (159.0 mg, 90%). ¹H NMR (500 MHz, CDCl₃/CD₃OD 10:1 v/v): δ = 1.32 (s, 18H; C(CH₃)₃), 1.38 (br, 8H; CH₂), 1.53 (br, 16H; CH₂), 2.06 (br, 24H; ArCH₃), 2.20 (br, 16H; CH₂), 6.85 (2 s, 16H; ArH), 7.28 (br, 2H; ArH), 7.42 (br, 1H; ArH), 7.58 (s, 1H; ArH), 8.01 (s, 2H; ArH), 8.09 (s, 4H; ArH), 8.17 ppm (br, 6H; ArH); ¹³C NMR (125 MHz, CDCl₃/CD₃OD 10:1 v/v): δ = 18.3, 22.7, 26.1, 25.0, 29.4, 30.8, 44.9, 88.1, 90.1, 121.9, 123.8, 124.6, 125.9, 126.0, 128.2, 128.6, 131.0, 131.1, 133.6, 133.9, 134.7, 134.8, 147.7, 147.9, 153.1, 165.6, 166.6 ppm; ESI MS: *m/z* (%): 2146.3 (100) [M+HNEt₃]⁺; HRMS (FT-ICR-ESI⁺): *m/z* calcd. for C₁₄₄H₁₆₂N₉O₈⁺: 2146.2579 [M+HNEt₃]⁺; observed: 2146.2570 (The ionization turned out to be significantly easier, when NEt₃ were added which forms a complex with the macrocycle in high abundances, see ref. [1a]).

Divalent host 5: TLM **1** (200.0 mg, 0.184 mmol) and 1,4-diethynyl benzene **5** (11.3 mg, 0.09 mmol) were dissolved in DMF (10 mL) and NEt₃ (3 mL). The solution was degassed for 1 h and protected from light. Afterwards, PPh₃ (5.4 mg, 18 μmol), (Ph₃P)₂PdCl₂ (6.3 mg, 9 μmol) and Cul (1.8 mg, 9 μmol) were added. The resulting mixture was stirred at room temperature for 24 hours. The solvents were evaporated under reduced pressure and the desired product **6** was obtained after chromatographic work-up (silica gel, CH₂Cl₂/EtOAc 12:1 to 6:1 v/v) from the third fraction as an yellow solid (129.0 mg, 78%). ¹H NMR (500 MHz, CDCl₃/CD₃OD 10:1 v/v): δ = 1.30 (s, 18H; C(CH₃)₃), 1.41 (br, 8H; CH₂), 1.61 (br, 16H; CH₂), 2.08 (br s, 24H; ArCH₃), 2.23 (br, 16H; CH₂), 6.90 (2 s, 16H; ArH), 7.43 (br, 4H; ArH), 7.75 (s, 2H; ArH), 8.08 (s, 4H; ArH), 8.17 (s, 4H; ArH), 8.31 ppm (s, 2H; ArH); ¹³C NMR (125 MHz, CDCl₃/CD₃OD 10:1 v/v): δ = 18.1, 22.7, 26.4, 24.8, 29.3, 30.9, 44.9, 87.7, 92.4, 122.0, 122.4, 123.7, 124.2, 124.9, 125.1, 126.3, 128.6, 128.9, 131.0, 131.3, 133.7, 134.1, 134.5, 134.8, 147.4, 148.0, 153.3, 165.4, 165.9 ppm; ESI MS: *m/z* (%): 2146.3 (100) [M+HNEt₃]⁺; HRMS (FT-ICR-ESI⁺): *m/z* calcd. for C₁₄₄H₁₆₂N₉O₈⁺: 2146.2579 [M+HNEt₃]⁺; observed: 2146.2581.

Divalent guest 9: Compound **2** (150 mg, 0.270 mmol) and 1,3-diethynyl benzene **3** (15.3 mg, 0.12 mmol) were dissolved in DMF (3 mL) and NEt₃ (2 mL). The solution was degassed for 1 h and protected from light. Afterwards, PPh₃ (15.6 mg, 52 μmol), Pd₂(dba)₃ (23.8 mg, 26 μmol) and Cul (5.2 mg, 26 μmol) were added. The resulting mixture was stirred at 70 °C for 3 d. The solvents were evaporated under reduced pressure and the desired product **9** was obtained after chromatographic work-up (silica gel, CH₂Cl₂/MeOH 30:1 v/v)

from the third fraction as a brown solid (39.0 mg, 32%). ^1H NMR (400 MHz, CD_2Cl_2): δ = 1.38 (s, 18H; $\text{C}(\text{CH}_3)_3$), 2.44 - 2.66 (m, 4H; CH_2), 3.01, 3.05, 3.10 (3 s, 12H; CH_3), 3.30 - 3.46 (m, 4H; CH_2), 3.65 - 3.70 (m, 8H; CH_2), 5.35 (br, 2H; NH), 7.34 - 7.40 (m, 4H; ArH), 7.47 - 7.54 (m, 4H; ArH), 7.63 - 7.70 ppm (m, 12H; ArH); ^{13}C NMR (125 MHz, CD_2Cl_2): δ = 28.2, 29.8, 33.0, 33.7, 35.6, 36.5, 38.0, 44.6, 49.7, 78.7, 89.4, 89.8, 122.4, 122.5, 123.7, 125.4, 126.1, 127.1, 127.2, 127.9, 128.8, 129.0, 131.5, 132.2, 134.5, 137.5, 140.4, 155.8, 171.1, 172.4 ppm; ESI MS: m/z (%): 1023.5 (100) $[\text{M}+\text{Na}]^+$; HRMS (TOF-ESI $^+$): m/z calcd. for $\text{C}_{60}\text{H}_{68}\text{N}_6\text{O}_8\text{Na}^+$: 1023.4991 $[\text{M}+\text{Na}]^+$; observed: 1023.4958.

Trivalent guest 11: Compound **2** (150 mg, 0.270 mmol) and 1,3,5-triethynyl benzene **7** (12.3 mg, 0.8 mmol) were dissolved in DMF (3 mL) and NEt_3 (2 mL). The solution was degassed for 1 h and protected from light. Afterwards, PPh_3 (15.6 mg, 52 μmol), $\text{Pd}_2(\text{dba})_3$ (23.8 mg, 26 μmol) and CuI (5.2 mg, 26 μmol) were added. The resulting mixture was stirred at 70 $^\circ\text{C}$ for 3 d. The solvents were evaporated under reduced pressure and the desired product **11** was obtained after chromatographic work-up (silica gel, $\text{CH}_2\text{Cl}_2/\text{MeOH}$ 18:1 v/v) from the third fraction as a slightly yellow solid (29.0 mg, 24%). ^1H NMR (400 MHz, CD_2Cl_2): δ = 1.38 (s, 27H; $\text{C}(\text{CH}_3)_3$), 2.44 - 2.66 (m, 6H; CH_2), 3.01, 3.04, 3.10 (3 s, 18H; CH_3), 3.32 - 3.43 (m, 6H; CH_2), 3.62 - 3.70 (m, 12H; CH_2), 5.35 (br, 3H; NH), 7.31 - 7.37 (m, 4H; ArH), 7.47 - 7.53 (m, 4H; ArH), 7.63 - 7.71 ppm (m, 19H; ArH); ^{13}C NMR (125 MHz, CD_2Cl_2): δ = 27.5, 29.1, 33.0, 34.9, 35.8, 37.3, 44.0, 44.3, 48.0, 78.0, 87.9, 89.8, 121.4, 121.5, 123.5, 124.7, 125.4, 126.5, 127.2, 128.4, 131.6, 133.4, 136.3, 136.8, 139.7, 139.9, 155.2, 170.5, 171.7 ppm; ESI MS: m/z (%): 1485.7 (100) $[\text{M}+\text{Na}]^+$; HRMS (TOF-ESI $^+$): m/z calcd. for $\text{C}_{87}\text{H}_{99}\text{N}_9\text{O}_{12}\text{Na}^+$: 1485.7338 $[\text{M}+\text{Na}]^+$; observed: 1485.7329.

Divalent host 13: 5,5'-Dibromo-2,2'-bipyridine **16** (18 mg, 57 μmol), $\text{Pd}(\text{PPh}_3)_4$ (4.5 mg, 3.8 μmol) and Cs_2CO_3 (60 mg, 0.183 mmol) were placed in DMF/toluene (15 mL). The mixture was reached to 100 $^\circ\text{C}$ and stirred at this temperature for 30 minutes. After that, TLM **15** (137 mg, 0.126 mmol), dissolved in DMF/toluene (5 mL), was added drop by drop and the whole mixture stirred at 125 $^\circ\text{C}$ for additional two days. After cooling down to room temperature, the solvents were evaporated under reduced pressure and residue chromatographed at neutral alumina eluting with $\text{CH}_2\text{Cl}_2/\text{MeOH}$ 49:1 v/v. The desired product **13** was isolated from the third fraction after evaporating the solvent as a yellow solid (52 mg, 46%). ^1H NMR (400 MHz, CDCl_3 + 2 drops CD_3OD): δ = 1.29 (s, 18H; $\text{C}(\text{CH}_3)_3$), 1.39 - 1.50 (br, 24H; CH_2), 2.16 (s, 24H; Ar CH_3), 2.19 (s, 24H; Ar CH_3), 2.29 (br, 16H; CH_2), 7.01 (br, 16H; ArH), 8.10 (br, 2H; ArH), 8.30 (s, 4H; ArH), 8.42 (s, 4H; ArH), 8.50 - 8.64 (m, 4H; ArH), 8.69 (s, 2H; ArH), 8.94 ppm (s, 2H; ArH); ^{13}C NMR (101 MHz, CDCl_3 + 2 drops CD_3OD): δ = 13.5, 19.3, 22.7, 26.3, 27.5, 31.3, 34.8, 35.1, 41.2, 44.4, 51.0, 125.7, 125.8, 128.7, 130.1, 132.1, 134.0, 134.9,

134.9, 135.0, 135.3, 152.4, 166.7, 167.5, 179.4 ppm; ESI MS: m/z (%): 2075.2 (100) $[M+H]^+$; HRMS (FT-ICR-ESI⁺): calcd. for $C_{138}H_{149}N_{10}O_8^+$: 2075.1587 $[M+H]^+$; observed: 2075.1579.

Divalent guest 23: N-Methyl piperazine-2,5-dione **21** (200 mg, 1.56 mmol) was dissolved in DMF (4 mL) and treated with NaH (72 mg, 1.87 mmol, 60 wt%). After vigorous stirring at room temperature for 2 hours, 1,6-diiodohexane **22** (250 mg, 0.74 mmol) in DMF (1 mL) was added drop by drop. The resulted mixture was stirred for further 18 hours and then the solvent was evaporated under reduced pressure. The product **23** was obtained after column chromatography on silica gel eluting with $CH_2Cl_2/MeOH$ 30:1 v/v from the second fraction as a white powder (132 mg, 53%). ¹H NMR (400 MHz, CD_2Cl_2/CD_3OD 3:1 v/v): δ = 1.23 - 1.27 (m, 4H; CH_2), 1.45 - 1.53 (m, 4H; CH_2), 2.87 (s, 6H; CH_3), 3.29 (t, ³ J = 7.4 Hz, 4H; CH_2), 3.88 (s, 4H; CH_2), 3.90 ppm (s, 4H; CH_2); ¹³C NMR (101 MHz, CD_2Cl_2/CD_3OD 3:1 v/v): δ = 26.7, 26.8, 33.4, 33.8, 45.1, 46.3, 50.0, 51.8, 52.1, 164.2, 164.6 ppm; ESI MS: m/z (%): 361.2 (100) $[M+Na]^+$; HRMS (TOF-ESI⁺): calcd. for $C_{16}H_{26}N_4O_4Na^+$: 361.1846 $[M+Na]^+$; observed: 361.1845.

TLM 28: TLM **18** (125.0 mg, 0.120 mmol), boron ester **27** (35.2 mg, 0.153 mmol), $Pd(PPh_3)_4$ (4.4 mg, 0.038 mmol) and Cs_2CO_3 (59.7 mg, 0.183 mmol) were placed in a mixture of DMF and toluene (20 mL, 1:1 v/v) and stirred at 125 °C for 2 days. After cooling down to room temperature, the solvents were evaporated under reduced pressure. The product **28** was obtained after column chromatography (silica gel, $CH_2Cl_2/EtOAc$ 9:1 v/v) from the first band as a white solid (92.0 mg, 72%). ¹H NMR (500 MHz, $CDCl_3/CD_3OD$ 6:1 v/v): δ = 1.37 (s, 9H; $C(CH_3)_3$), 1.48 (br, 4H; CH_2), 1.60 (br, 8H; CH_2), 2.14 (s, 12H; $ArCH_3$), 2.15 (s, 12H; $ArCH_3$), 2.29 (br, 8H; CH_2), 5.26 (d, ³ J = 11.1 Hz, 1H; CH_2), 5.78 (d, ³ J = 17.9 Hz, 1H; CH_2), 6.69 - 6.75 (m, 1H; CH), 6.95 (s, 8H; ArH), 7.49 (d, ³ J = 8.0 Hz, 2H; ArH), 7.67 (d, ³ J = 8.0 Hz, 2H; ArH), 8.10 (s, 1H; ArH), 8.16 (s, 2H; ArH), 8.23 (s, 1H; ArH), 8.35 ppm (s, 2H; ArH); ¹³C NMR (125 MHz, $CDCl_3/CD_3OD$ 6:1 v/v): δ = 18.2, 22.7, 26.5, 30.8, 34.1, 36.2, 44.9, 114.1, 126.0, 126.1, 126.6, 127.0, 128.5, 128.6, 129.2, 130.8, 131.0, 131.2, 131.9, 133.9, 134.7, 134.8, 134.9, 135.9, 137.3, 138.2, 142.2, 147.7, 167.8 ppm; ESI MS: m/z (%): 1164.7 (100) $[M+HNEt_3]^+$; HRMS (FT-ICR-ESI⁺): m/z calcd. for $C_{78}H_{94}N_5O_4^+$: 1164.7300 $[M+HNEt_3]^+$; observed: 1164.7305.

Divalent host 24: TLM **28** (60.0 mg, 0.056 mmol) was dissolved in CH_2Cl_2 (3 mL) and treated with Grubbs-Hoveyda IInd generation catalyst (**GH II Gen**, 1.7 mg, 0.003 mmol). The reaction mixture was stirred at room temperature for 3 days and further refluxed for 18 hours. After cooling down to room temperature, the solvent was evaporated under reduced pressure. The product **24** was obtained after purification (preparative TLC, $CH_2Cl_2/EtOAc$ 9:1 v/v) from the third band as a white solid (65.8 mg, 56%). ¹H NMR (500 MHz, CD_2Cl_2/CD_3OD

2:1 v/v): δ = 1.41 (s, 18H; C(CH₃)₃), 1.52 (br, 8H; CH₂), 1.64 (br, 16H; CH₂), 2.18 (s, 24H; ArCH₃), 2.20 (s, 24H; ArCH₃), 2.33 (br, 18H; CH₂), 7.01 (s, 16H; ArH), 7.26 (s, 2H; CH), 7.68 (d, ³J = 8.6 Hz, 4H; ArH), 7.77 (d, ³J = 8.6 Hz, 4H; ArH), 8.13 (s, 2H; ArH), 8.15 (s, 4H; ArH), 8.31 (s, 2H; ArH), 8.41 ppm (s, 4H; ArH); ¹³C NMR (220 MHz, CDCl₃/CD₃OD 6:1 v/v): δ = 18.7, 23.5, 26.8, 30.1, 31.3, 35.6, 35.8, 45.8, 124.4, 126.0, 126.8, 127.7, 127.9, 128.8, 129.0, 129.7, 132.1, 132.2, 134.8, 135.7, 135.8, 137.8, 138.9, 142.7, 148.6, 148.7, 153.9, 167.0, 167.4 ppm; ESI MS: *m/z* (%): 2200.3 (100) [M+HNEt₃]⁺; HRMS (FT-ICR-ESI⁺): *m/z* calcd. for C₁₄₈H₁₆₈N₉O₈⁺: 2200.3043 [M+HNEt₃]⁺; observed: 2200.3051.

Divalent host 25: TLM **29** (100 mg, 0.102 mmol) was dissolved in CH₂Cl₂ (10 mL) containing NEt₃ (0.2 mL) und treated with adipoyl chloride **30** (8.9 mg, 0.049 mmol) drop by drop. The reaction mixture was then stirred under reflux for 18 hours. After cooling down to room temperature, the solvent was evaporated under reduced pressure. The product **25** was obtained after purification (preparative TLC, CH₂Cl₂/EtOAc 1:3 v/v) from the second band as an yellow solid (43.5 mg, 43%). ¹H NMR (500 MHz, CDCl₃/CD₃OD 6:1 v/v): δ = 1.29 (s, 18H; C(CH₃)₃), 1.40 (br, 8H; CH₂), 1.52 (br, 16H; CH₂), 2.02 (s, 24H; ArCH₃), 2.05 (s, 24H; ArCH₃), 2.21 (br, 16H; CH₂), 2.35 (br, 4H; CH₂), 3.99 (br, 4H; CH₂), 6.86 (br, 16H; ArH), 7.92 (s, 2H; ArH), 8.05 - 8.11 ppm (m, 10H; ArH); ¹³C NMR (220 MHz, CDCl₃/CD₃OD 6:1 v/v): δ = 18.4, 22.5, 22.9, 29.2, 29.6, 31.0, 31.8, 35.2, 36.6, 46.5, 122.2, 122.7, 123.7, 126.2, 128.6, 131.4, 134.1, 135.0, 135.1, 148.0, 153.2, 163.2, 167.0 ppm; ESI MS: *m/z* (%): 2063.2 (100) [M+H]⁺; HRMS (FT-ICR-ESI⁺): *m/z* calcd. for C₁₃₄H₁₅₃N₁₀O₁₀⁺: 2063.1798 [M+HNEt₃]⁺; found: 2063.1838.

Compound 33: N-Boc-N,N'-dimethylethylene diamine **31** (2.73 g, 14.5 mmol) was dissolved in CH₂Cl₂ (120 mL) containing NEt₃ (4.5 mL). 11-Undecenoyl chloride **32** (3.61 g, 17.3 mmol) was added drop by drop and the reaction mixture stirred at room temperature for 24 hours and after this washed with saturated sodium bicarbonate solution (3x), and brine (2x), dried over MgSO₄ and evaporated to dryness. The product **33** was obtained after column chromatography (silica gel, CH₂Cl₂/MeOH 20:1 v/v) from the first band as a slightly yellow oil (4.7 g, 92%). ¹H NMR (400 MHz, CDCl₃): δ = 1.28 (br, 10H; CH₂), 1.42 (s, 9H; C(CH₃)₃), 1.57 - 1.63 (m, 2H; CH₂), 2.01 (q, ³J = 21.1 Hz, 2H; CH₂), 2.23 - 2.33 (m, 2H; CH₂), 2.86 (br, 3H; CH₃), 2.93 (s, 3H; CH₃), 3.00 (s, 3H; CH₃), 3.29 - 3.36 (m, 2H; CH₂), 3.43 - 3.52 (m, 2H; CH₂), 4.89 - 4.99 (m, 2H; CH₂), 5.74 - 5.84 ppm (m, 1H; CH); ¹³C NMR (101 MHz, CDCl₃): δ = 25.1, 27.5, 28.5, 28.5, 28.5, 28.5, 29.0, 29.2, 29.4, 29.5, 29.5, 29.6, 29.6, 33.7, 33.7, 33.9, 34.8, 114.2, 126.1, 139.3, 179.4 ppm; ESI MS: *m/z* (%): 377.3 (100) [M+Na]⁺; HRMS (TOF-ESI⁺): *m/z* calcd. for C₂₀H₃₈N₂O₃Na⁺: 377.2775 [M+Na]⁺; found: 377.2763.

Compound 34: Compound **33** (706 mg, 2.0 mmol) and **GH II Gen** (60 mg, 0.07 mmol) were stirred in CH₂Cl₂ (20 mL) 3 days at room temperature and afterwards refluxed for 6 hours. After cooling down to room temperature, the solvent was evaporated under reduced pressure and the residue purified by column chromatography (silica gel) eluting first with CH₂Cl₂/EtOAc 2:1 v/v. After the first two bands have passed through the column, the product **34** was obtained from the third band eluting with CH₂Cl₂/MeOH 13:1 v/v as a slightly brown oil (645 mg, 43%). ¹H NMR (400 MHz, CDCl₃): δ = 1.25 (br, 20H; CH₂), 1.43 (s, 18H; C(CH₃)₃), 1.52 - 1.62 (m, 4H; CH₂), 1.87 - 1.97 (m, 4H; CH₂), 2.24 (q, ³J = 29.1 Hz, 4H; CH₂), 2.84 (br, 6H; CH₃), 2.91 (s, 3H; CH₃), 2.98 (s, 3H; CH₃), 3.27 - 3.34 (m, 4H; CH₂), 3.37 - 3.49 (m, 4H; CH₂), 5.29 - 5.36 (m, 2H; CH); ¹³C NMR (101 MHz, CDCl₃): δ = 25.0, 27.3, 27.5, 28.5, 28.5, 28.6, 29.2, 29.5, 29.5, 29.6, 29.6, 29.7, 32.7, 32.8, 33.7, 34.8, 47.4, 130.4, 173.5, 179.4 ppm; ESI MS: *m/z* (%): 703.5 (100) [M+Na]⁺; HRMS (TOF-ESI⁺): *m/z* calcd. for C₃₈H₇₂N₄O₆Na⁺: 703.5344 [M+Na]⁺; found: 703.5356.

Divalent guest 26: Compound **34** (645 mg, 0.86 mmol) was dissolved in EtOH (20 mL), treated with Pd on C (~ 2 g) and hydrogenated under stirring at room temperature under normal pressure (balloon filled with H₂) for 3 days. After that, the reaction mixture was filtered over Celite® and evaporated to dryness. The residue was redissolved in CH₂Cl₂ (20 mL) and cooled down to 0 °C. TFA (2.5 mL) was added drop by drop and the reaction mixture stirred at 0 °C for 1 hour and at room temperature for additional 24 hours. After that, aqueous saturated sodium bicarbonate solution was added carefully and the residue transferred to a separating funnel. The organic phase was separated, dried over Na₂SO₄ and the solvent was evaporated. In a separate reaction flask, 4-ethynyl benzoic acid **35** (535 mg, 2.5 mmol), CDMT (308 mg, 1.75 mmol) and NMM (0.2 mL) were stirred for 2 h at 0 °C in MeCN (10 mL). The residue obtained after deprotection of the two Boc group, work up and evaporating the solvent was redissolved in CH₂Cl₂ (20 mL) and added via dropping funnel to the solution of the acid **35** and CDMT. After the addition of further NMM (0.4 mL), the reaction mixture was stirred for 2 days at room temperature. The solvents were evaporated under reduced pressure and the residue was redissolved CH₂Cl₂ (20 mL). The organic phase was washed with water (30 mL), hydrochloric acid (1 M, 2 x 30 mL), aqueous saturated sodium bicarbonate solution (2 x 30 mL), water (30 mL), and brine (2 x 30 mL), dried over Na₂SO₄ and the solvent was evaporated. The desired guest **26** was obtained after column chromatography (silica gel, CH₂Cl₂/MeOH 20:1 v/v) from the second band as a white solid (142 mg, 22% over three steps). ¹H NMR (500 MHz, CD₂Cl₂): δ = 1.21 (br, 28H; CH₂), 1.56 (br, 4H; CH₂), 2.24 (t, ³J = 15.4 Hz, 4H; CH₂), 2.99 (s, 6H; CH₃), 3.05 (s, 6H; CH₃), 3.11 (s, 2H; C≡CH), 3.60 - 3.70 (m, 8H; CH₂), 7.32 (d, ³J = 8.2 Hz, 4H; ArH), 7.47 ppm (d, ³J = 7.9 Hz, 4H; ArH); ¹³C NMR (125 MHz, CD₂Cl₂): δ = 24.9, 29.4 - 29.6 (7 signals), 33.5, 35.5, 37.8, 44.2, 44.7, 78.4, 82.9, 123.3, 127.0, 132.0, 136.4, 170.7, 173.9 ppm; ESI MS: *m/z* (%): 761.5

(100) $[M+Na]^+$; HRMS (TOF-ESI⁺): calcd. für $C_{46}H_{66}N_4O_4Na^+$: 761.4982 $[M+Na]^+$; observed: 761.5016.

PEG polymer 36: PEG polymer **39** (50 mg, $M_w \sim 10,000$ Da) and N-acetylene diamine **40** (51 mg, 0.5 mmol) were dissolved in DMF (3 mL) and cooled down to 0 °C. A solution of EDC (0.1 mL, 0.57 mmol) and HOBt (27 mg, 0.2 mmol) in DMF (2 mL) was added drop by drop and the resulting reaction mixture stirred after warming to room temperature for 7 days. The solvent was evaporated under reduced pressure and the residue purified using dialysis (tubes for $M_w > 10,000$ Da, solvent: water/MeOH 1:3 v/v).

PEG polymer 37: PEG polymer **41** (25 mg, $M_w \sim 10,000$ Da) and acid **42** (78 mg, 0.25 mmol) were dissolved in DMF (3 mL) and cooled down to 0 °C. A solution of EDC (0.1 mL, 0.57 mmol) and HOBt (27 mg, 0.2 mmol) in DMF (2 mL) was added drop by drop and the resulting reaction mixture stirred after warming to room temperature for 7 days. The solvent was evaporated under reduced pressure and the residue purified using dialysis (tubes for $M_w > 10,000$ Da, solvent: water/MeOH 1:3 v/v).

PEG polymer 38: PEG polymer **41** (50 mg, $M_w \sim 10,000$ Da) and acid **43** (90 mg, 0.5 mmol, see ref. 8) were dissolved in DMF (3 mL) and cooled down to 0 °C. A solution of EDC (0.1 mL, 0.57 mmol) and HOBt (27 mg, 0.2 mmol) in DMF (2 mL) was added drop by drop and the resulting reaction mixture stirred after warming to room temperature for 7 days. The solvent was evaporated under reduced pressure and the residue purified using dialysis (tubes for $M_w > 10,000$ Da, solvent: water/MeOH 1:3 v/v).

Compound 42: N-methyl piperazine-2,5-dione **21** (200 mg, 1.56 mmol) was dissolved in DMF (4 mL) and treated with NaH (144 mg, 3.74 mmol, 60 wt%). After vigorous stirring at room temperature for 2 hours, 11-bromo undecanoic acid (459 mg, 1.73 mmol) in DMF (1 mL) was added drop by drop. The resulted mixture was stirred for further 18 hours and then the solvent was evaporated under reduced pressure. The acid **42** was obtained after column chromatography on silica gel eluting with $CH_2Cl_2/MeOH$ 20:1 v/v from the second fraction as a white powder (85 mg, 17%). ¹H NMR (400 MHz, DMF-D₇): δ = 1.28 - 1.55 (m, 16H; CH₂), 2.26 (t, ³J = 6.6 Hz, 2H; CH₂), 2.89 (s, 3H; CH₃), 3.35 (t, ³J = 6.8 Hz, 2H; CH₂), 3.98 ppm (s, 4H; CH₂); ¹³C NMR (101 MHz, DMF-D₇): δ = 26.8, 27.0, 27.2, 27.3, 29.3, 29.6, 30.0, 32.8, 33.1, 34.3, 45.7, 45.9, 50.0, 52.0, 164.1, 164.5, 175.0 ppm; TOF-MS (ESI⁺): m/z (%): 335.2 (100) $[M+Na]^+$; HRMS (ESI⁺): calcd. for $C_{16}H_{28}N_2O_4Na^+$: 335.1941 $[M+Na]^+$; observed: 335.1948.

TLM 44: TLM **44** (114.4 mg, 0.122 mmol), lipoic acid **45** (75.6 mg, 0.366 mmol, mixture of R/S isomers) and PyBOP (190.6 mg, 0.366 mmol) were dissolved in CH_2Cl_2 (20

mL) and MeCN (5 mL). After cooling down to 0 °C, *i*Pr₂NEt (2 mL) were added drop by drop. The reaction mixture was warmed up to room temperature and stirred for further 18 hours. The solvents were evaporated under reduced pressure and the residue taken up in CH₂Cl₂ (20 mL). The organic phase was washed with aqueous saturated sodium bicarbonate solution (20 mL) and brine (20 mL), dried over Na₂SO₄ and evaporated to dryness. The desired TLM **44** was isolated after column chromatography (silica gel, CH₂Cl₂/EtOAc 4:1 v/v) from the first band as a yellow solid (91 mg, 58%). ¹H NMR (700 MHz, CD₂Cl₂/CD₃OD 10:1 v/v): δ = 1.51 (br, 4H; CH₂), 1.63 (s, 8H; CH₂), 1.72 - 1.87 (m, 8H; CH₂), 1.88 - 1.92 (m, 4H; CH₂), 2.12 (s, 24H; ArCH₃), 2.32 (s, 8H; CH₂), 2.42 - 2.47 (m, 4H; CH₂), 2.62 (t, ³J = 7.3 Hz, 4H; CH₂), 3.07 (m, 2H; CH₂), 3.14 - 3.17 (m, 2H; CH₂), 3.56 - 3.61 (m, 2H; CH), 6.99 (s, 8H; ArH), 7.81 (s, 4H; ArH), 8.19 ppm (s, 2H; ArH); ¹³C NMR (220 MHz, CD₂Cl₂/CD₃OD 10:1 v/v): δ = 18.7, 23.5, 25.0, 26.8, 29.1, 31.5, 34.4, 35.0, 35.7, 39.0, 40.7, 45.7, 56.7, 56.8, 120.1, 120.4, 124.5, 125.0, 125.7, 125.8, 125.8, 126.8, 129.4, 129.5, 131.9, 135.6, 136.7, 148.7, 152.2, 165.9, 172.7 ppm; ESI MS: m/z (%): 1313.6 (100) [M+H]⁺; HRMS (FT-ICR-ESI⁺): calcd. for C₇₆H₈₉N₄O₈S₄⁺: 1313.5556 [M+H]⁺; observed: 1313.5531.

Rotaxane 48: Rotaxane **47** (215 mg, 0.127 mmol), lipoic acid **45** (76 mg, 0.366 mmol, mixture of R/S isomers) and PyBOP (191 mg, 0.366 mmol) were dissolved in CH₂Cl₂/MeCN 4:1 v/v (25 mL) and cooled down to 0 °C. After addition of *i*Pr₂NEt (0.1 mL), the mixture was warmed to room temperature and stirred for further 18 hours. The solvents were evaporated under reduced pressure and the residue taken up in CH₂Cl₂ (20 mL). The organic phase was washed with aqueous saturated sodium bicarbonate solution (20 mL) and brine, dried over Na₂SO₄ and evaporated to dryness. The desired product **48** was isolated after column chromatography over silica gel eluting with CH₂Cl₂/EtOAc 9:1 v/v from the first band as a yellow solid (162 mg, 71%). ¹H NMR (400 MHz, CDCl₃/CD₃OD 2:1 v/v): δ = 1.45 (br, 4H; CH₂), 1.57 (br, 8H; CH₂), 1.62 - 1.71 (m, 4H; CH₂), 1.84 (s, 24H; ArCH₃), 2.26 (br, 8H; CH₂), 2.34 - 2.42 (m, 2H; CH₂), 2.53 (t, ³J = 7.3 Hz, 2H; CH₂), 2.97 - 3.10 (m, 2H; CH₂), 3.23 - 3.24 (m, 2H; CH₂), 3.45 - 3.53 (m, 1H; CH), 4.16 (s, 4H; CH₂), 6.18 (br, 4H; ArH), 6.38 (d, ³J = 8.8 Hz, 4H; ArH), 6.98 - 7.00 (m, 12H; ArH), 7.07 - 7.16 (m, 30H; ArH), 7.52 (t, ³J = 7.7 Hz, 1H; ArH), 7.65 (s, 1H; ArH), 7.68 (s, 2H; ArH), 7.76 (s, 1H; ArH), 8.00 ppm (dd, ³J = 7.7 Hz, ⁴J = 1.2 Hz, 2H; ArH); ¹³C NMR (101 MHz, CDCl₃/CD₃OD 2:1 v/v): δ = 17.9, 22.4, 23.9, 25.7, 28.1, 34.0, 35.0, 37.9, 39.7, 44.7, 49.8, 63.8, 69.4, 89.1, 112.9, 124.5, 125.5, 126.1, 126.9, 130.4, 130.6, 131.9, 133.9, 134.5, 135.5, 140.0, 146.2, 151.3, 155.5, 165.1, 166.2, 171.5, 215.1 ppm; ESI MS: m/z (%): 1906.9 (100) [M+Na]⁺; HRMS (TOF-ESI⁺): calcd. for C₁₂₆H₁₂₂N₄O₈S₂Na⁺: 1906.8634 [M+Na]⁺; observed: 1906.8695.

Compound 51: Acid **50** (332 mg, 3.38 mmol), NMM (0.4 mL) and CDMT (694 mg, 3.95 mmol) were dissolved in CH₂Cl₂ (40 mL) and cooled down to 0 °C. After that, a solution

of NMM (0.4 mL) and amine **49** (620 mg, 3.87 mmol) in CH₂Cl₂ (5 mL) were added drop by drop. The reaction mixture was warmed to room temperature and stirred for further 18 hours. The solvents were evaporated under reduced pressure and the residue was redissolved in CH₂Cl₂ (20 mL). The organic phase was washed with water (50 mL), hydrochloric acid (1 M, 2 x 50 mL), aqueous saturated sodium bicarbonate solution (2 x 50 mL), water (50 mL), and brine (2 x 50 mL), dried over Na₂SO₄ and the solvent was evaporated. The product **51** was obtained without further purification as a yellow solid (709 mg, 84%). ¹H NMR (400 MHz, CDCl₃): δ = 1.41 (s, 9H; C(CH₃)₃), 1.98 (t, ³J = 2.6 Hz, 1H; C≡CH), 2.36 - 2.40 (m, 2H; CH₂), 2.47 - 2.52 (m, 2H; CH₂), 3.22 - 3.37 (m, 4H, CH₂), 5.12 (br, 1H; NH), 6.54 ppm (s, 1H; NH); ¹³C NMR (101 MHz, CDCl₃): δ = 14.8, 28.3, 35.2, 40.1, 40.5, 69.2, 82.9, 89.5, 144.8, 171.6 ppm; ESI MS: m/z (%): 263.1 (100) [M+Na]⁺; HRMS (TOF-ESI⁺): calcd. for C₁₂H₂₀N₄O₂N₃Na⁺: 263.1372 [M+Na]⁺; observed: 263.1350.

Axle 52: Compound **51** (620 mg, 2.50 mmol) was dissolved in CH₂Cl₂ (20 mL) and cooled down to 0 °C. After TFA (2 mL) was added drop by drop, the reaction mixture was stirred at this temperature for one hour. The organic phase was then washed with aqueous saturated sodium bicarbonate solution (2 x 50 mL), dried over Na₂SO₄ and evaporated to dryness. The residue was redissolved in CH₂Cl₂ (20 mL). After addition of lipoic acid **45** (1 g, 5.00 mmol) and PyBOP (2.6 g, 5.00 mmol), the solution was cooled down to 0 °C. iPr₂NEt (5 mL) was added drop by drop, the residue warmed up to room temperature and stirred for 3 days. After that, the organic phase was washed with water (50 mL), hydrochloric acid (1 M, 2 x 50 mL), aqueous saturated sodium bicarbonate solution (2 x 50 mL), water (50 mL), and brine (2 x 50 mL), dried over Na₂SO₄ and the solvent was evaporated. The axle **52** was isolated after column chromatography over silica gel eluting with CH₂Cl₂/EtOAc 1:1 from the third fraction (308 mg, 38% over two steps). ¹H NMR (400 MHz, DMSO-D₆): δ = 1.33 (q, ³J = 7.8 Hz, 2H; CH₂), 1.46 - 1.70 (m, 4H; CH₂), 1.82 - 1.90 (m, 1H; CH₂), 2.05 (t, ³J = 7.4 Hz, 2H; CH₂), 2.23 - 2.26 (m, 2H; CH₂), 2.32 - 2.38 (m, 3H; CH₂), 2.76 (t, ³J = 2.7 Hz, 1H; C≡CH), 3.06 - 3.08 (m, 4H; CH₂), 3.10 - 3.22 (m, 2H; CH₂), 3.57 - 3.64 (m, 1H; CH), 7.80 (s, 1H; NH), 7.90 ppm (s, 1H; NH); ¹³C NMR (100 MHz, DMSO-D₆): δ = 14.1, 24.9, 28.2, 34.1, 34.2, 35.2, 38.0, 49.8, 56.0, 71.2, 83.6, 89.1, 170.3, 172.0 ppm; ESI MS: m/z (%): 351.1 (100) [M+Na]⁺; HRMS (TOF-ESI⁺): calcd. for C₁₅H₂₄N₂O₂S₂Na⁺: 351.1177 [M+Na]⁺; observed: 351.1173.

-
- [1] (a) Baytekin, B.; Zhu, S. S.; Brusilowskij, B.; Illigen, J.; Ranta, J.; Huuskonen, J.; Rissanen, K.; Kaufmann, L.; Schalley, C. A. *Chem.-Eur. J.* **2008**, *14*, 10012. (b) Baytekin, B. *An easily accessible toolbox of functionalized macrocycles and rotaxanes and a (tandem) ESI-FTICR mass spectrometric study on Fréchet-type dendrimers with ammonium cores and hierarchical self-assembly of metallo-supramolecular nano-spheres*, PhD thesis, Freie Universität Berlin,
-

- 2008.** (c) Brusilowskij, B. *Studien zur Entschlüsselung von Komplexität in supramolekularen Architekturen*, PhD thesis, Freie Universität Berlin, **2010**.
- [2] Chinchilla, R.; Nájera, C. *Chem. Rev.* **2007**, *107*, 874.
- [3] Such experiments were performed by Nora L. Löw during her Master thesis.
- [4] Tao, X.-C.; Zhou, W.; Zhang, Y.-P.; Dai, C.-Y.; Shen, D.; Huang, M. *Chin. J. Chem.* **2006**, *24*, 939.
- [5] Ayvalik, G. *Multivalente Gäste mit Diamid- und Glycinanhydridbindungsstellen*, Bachelor thesis, Freie Universität Berlin, **2010**.
- [6] Nabulsi, N. B.; Smith, D. E.; Kilbourn, M. R. *Bioorg. Med. Chem.* **2005**, *13*, 2993.
- [7] *CACHE 5.0 for Windows*; Fujitsu Ltd.: Krakow, Poland, **2001**.
- [8] Grubbs, R. H. *Handbook of Metathesis*, Wiley-VCH, Germany, **2003**.
- [9] Kleemann, H.-W.; Heitsch, H.; Henning, R.; Kramer, W.; Kocher, W.; Lerch, U.; Linz, W.; Nickel, W.-U.; Ruppert, D.; Urbach, H.; Utz, R.; Wagner, A.; Weck, R.; Wiegand, F. *J. Med. Chem.* **1992**, *35*, 559.
- [10] (a) Garrett, C. E.; Jiang, X.; Prasad, K.; Repic, O. *Tetrahedron Lett.* **2002**, *43*, 4161. (b) Brinas, R. P.; Troxler, T.; Hochstrasser, R. M.; Vinogradov, S. A. *J. Am. Chem. Soc.* **2005**, *127*, 11851.
- [11] Kaufmann, L.; *Organokatalytische Beschleunigung von Diels-Alder-Reaktionen*, Master thesis, Universität Bonn, **2009**.
- [12] Eipert, E.; Maichle-Mössmer, C.; Maier, M. E. *J. Org. Chem.* **2002**, *67*, 8692-8695.
- [13] After the dialysis the residue was analyzed using ^1H NMR (700 MHz, D_2O) where new signal appeared in comparison to the used PEG polymers **39** and **41**. However, the use of FT ICR ESI MS (where peaks with distances of m/z 15 would appear, shifted for the desired polymers **36** - **38** compared to **39** or **41**) was not possible due to problems with the instrument.
- [14] Felder, T. *Von Rotaxanen als potentiellen Enzym-Mimetika zu massenspektrometrischen Untersuchungen von Makromolekülen in der hochverdünnten Gasphase*, PhD thesis, Universität Bonn, **2007**.
- [15] Kayikci, P. *Schwefelhaltige Tetralactam-Makrozyklen zur Anbringung an eine Gold-Oberfläche sowie Synthese modifizierter PEG-Polymere für SFMS*, Bachelor thesis, Freie Universität Berlin, **2010**.
- [16] (a) Dzyuba, E. V. *Acridiniumsalze mit Ankergruppen an der 10-Position*, Diploma thesis, Humboldt-Universität zu Berlin, **2008**. (b) Duo, Y.; Jacob S.; Abraham, W. *Org. Biomol. Chem.* **2011**, *9*, 3549-3559.
- [17] The characterization of the TLM **46** on the gold surface (by AFM) and the SMFS experiments using PEG polymers **36** - **38** were performed by Manuel Gensler at the Department of Physics, Humboldt-Universität zu Berlin in the research group of Rabe and can be found in his PhD thesis.

4.4. C-H...O Hydrogen Bonds in "Clicked" Diketopiperazine-Based Amide Rotaxanes[†]

Abstract: In this work, two amide [2]rotaxanes are presented, that contain a previously undescribed N,N'-dipropargyl diketopiperazine axle centerpiece as the template for rotaxane construction (Figure 52). Both were synthesized from ethynyl- and azide-substituted precursors in high yields by "click-chemistry" with $(\text{Ph}_3\text{P})_3\text{Cu}(\text{I})\text{Br}$ as the catalyst, which operates in unpolar organic solvents.

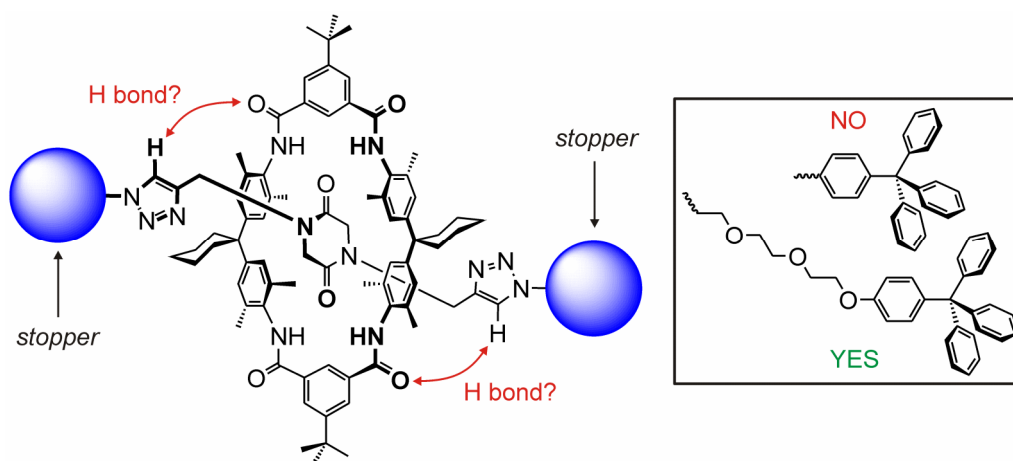


Figure 52. [2]Rotaxanes bearing the diketopiperazine axle centerpiece and two triazole units as additional binding units. Both rotaxanes differ in their stopper units and in the hydrogen bonding network between TLM and axle.

The ability of this axle centerpiece to form host-guest complexes with a TLM was studied by ^1H NMR, where two sets of signals appear, one for the complexed and one for the non-complexed axle. Complex stabilities were determined using a simple integration procedure and are in the range of 10^4 M^{-1} (at -40°C). In addition, a X-ray structure of a host-guest complex bearing a TLM and the desired axle centerpiece was obtained. Moreover, ^1H and $^1\text{H},^1\text{H}$ ROESY NMR spectra provide unambiguously the existence of two different hydrogen bonding motifs depending on the nature of the stoppers in the [2]rotaxanes. One of them involves C-H...O=C hydrogen bonding between the hydrogens located at the triazole rings and the carbonyl groups of inverted TLM amide groups. This motif can be found in the [2]rotaxane bearing sterically less demanding stopper and is controllable and switchable reversibly by competitive anion binding as shown exemplarily for chloride and acetate.

[†] Dzyuba, E. V.; Kaufmann, L.; Löw, N. L.; Meyer, A. K.; Winkler, H. D. F.; Rissanen, K.; Schalley, C. A. *Organic Letters* **2011**, *13*, 4838 - 4841. The original article is online available at <http://dx.doi.org/10.1021/ol201915j>.

4.5. Effects of Subtle Differences in Ligand Constitution and Conformation in Metallo-Supramolecular Self-Assembled Polygons[†]

Abstract: Di- and tetradentate ligands consisting of 3,3'-Bis(pyridin- $[n]$ -ylethynyl)biphenyl ($n = 3, 4$) and the corresponding 2,2'-bipyridines assemble with Pt(dppp)OTf₂ into metallo-supramolecular polygons (Figure 53). Since a slow exchange takes place on Pt^{II} metal center used herein, the equilibrium is observed within a many-hour time scale and larger polygons are formed under kinetic control confirmed by time-dependent ¹H and ³¹P NMR in combination with ESI mass spectrometry.

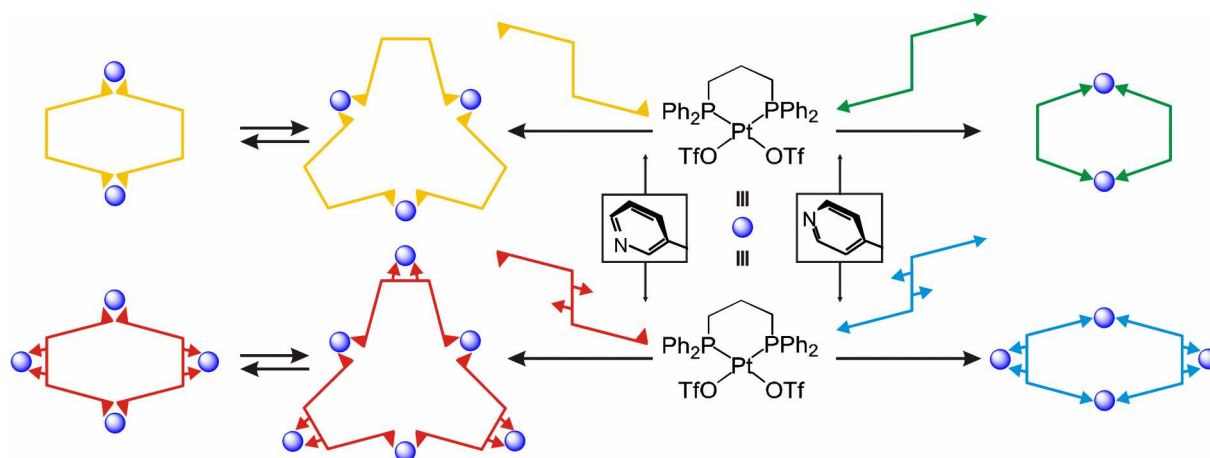


Figure 53. Schematic representation of di- and tetradentate ligands and the Pt^{II}-containing metal center used in this study. At the equilibrium point of the self-assembly reaction, different behavior of the systems can be observed depending of the position of the nitrogen of the pyridine moiety.

A fresh ³¹P NMR and ESI MS were used to follow the assembly processes. If the metal center Pt(dppp)OTf₂ with either the ligand bearing a 2,2'-bipyridine core and the nitrogen of the pyridine moiety *para* to the ethynyl substituent or with the ligand bearing biphenyl core and the nitrogen of the pyridine moiety *para* to the ethynyl substituent was mixed, three different polygons after 10 minutes, two after 5 hours and only one after 24 hours were observed. Surprisingly, the existence of both the smaller and the larger polygons was confirmed if ligands with the nitrogen of the pyridine *meta* to the ethynyl substituent were used and after the equilibrium had reached.

[†] Brusilowskij, B.; Dzyuba, E. V.; Troff, R. W.; Schalley, C. A. *Dalton Transactions* **2011**, *40*, 12089 - 12096. The original article is online available at <http://dx.doi.org/10.1039/C1DT10621J>.

4.6. Thermodynamically controlled Self-Sorting of Heterobimetallic Metallo-Supramolecular Macrocycles: What a Difference a Methylene Groups makes![†]

Abstract: A combination of ³¹P NMR and tandem MS experiments clearly confirms the formation of hetero-bimetallic metallo-supramolecular polygons through thermodynamically controlled self-sorting of a tetradentate ligand by independently mixing of the ligand with differently substituted metal centers (Figure 54).

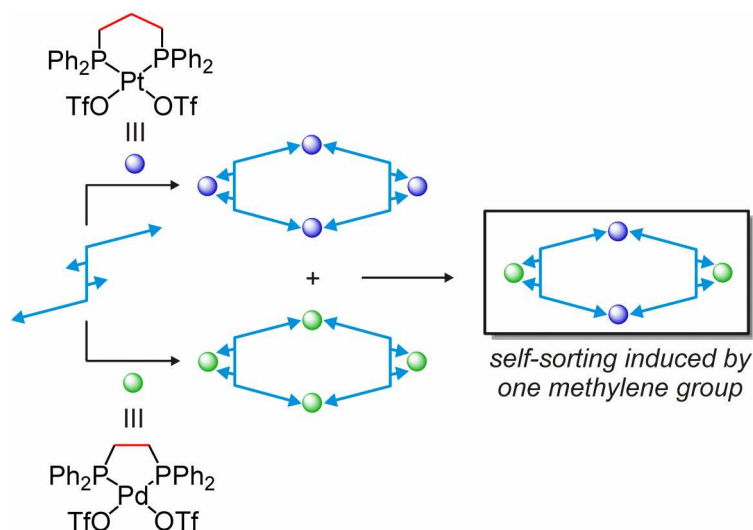


Figure 54. Formation of a hetero-bimetallic metallo-supramolecular macrocycle from homo-monometallic species through self-sorting induced by only one methylene group.

Initial experiments with 1 : 1 mixtures of the ligand and the metal centers show that only the coordination at the bipyridine site occurs if a metal center substituted with dppp was used. In comparison, metal centers with dppe ligands can be occupied by both pyridine and bipyridine. This observation was used for the self-sorting that was confirmed for all of the metallo-macrocycles after 24 h mixing time. No self-sorting was observed in case of coval use of either dppp- or dppe-substituted metal centers. Tandem ESI MS experiments confirmed the compositions of the metallo-supramolecular polygons. The fragmentation patterns provide structural information and the positions of dppp and dppe substituted metal centers can be differentiated.

[†] Brusilowskij, B.; Dzyuba, E. V.; Troff, R. W.; Schalley, C. A. *Chemical Communications* **2011**, *47*, 1830 - 1832. The original article is online available at <http://dx.doi.org/10.1039/C0CC04476H>.

4.7. Gas-phase H/D-exchange experiments in supramolecular chemistry[†]

Abstract: The perspective article focuses on the H/D-exchange reactions in the gas phase for the characterization of synthetic non-covalent complexes, in which hydrogen bond formation plays a crucial role. Until now, such experiments were performed mainly for biomolecular systems. Therefore, examples of synthetic supramolecules (e.g. hydrogen-bonded capsules, host-guest complexes) where gas phase H/D exchange was used for the investigation of structural as well as mechanistic aspects are presented. Intramolecular dynamic features can be analyzed using gas-phase H/D-exchange experiments since hydrogen bonds influence the H/D-exchange rates. For example, the number and position of hydrogen bonds can often be determined, zwitterionic and charge-solvated structures of amino acids and peptides can be distinguished. Beyond structure, dynamic features such as the mobility of building blocks within complexes can be followed if H/D exchange experiments are used in combination with e.g. ion mobility MS.

[†] Winkler, H. D. F.; Dzyuba, E. V.; Schalley, C. A. *New Journal of Chemistry* **2011**, 35, 529 - 541. The original article is online available at <http://dx.doi.org/10.1039/C0NJ00634C>.

4.8. A one-dimensional analogue to the Grotthuss mechanism of proton transport through water: Gas-phase H/D-exchange reactions on resorcinarene and pyrogallarene capsules[†]

Abstract: The H/D exchange behavior of the hydrogen-bonded dimeric resorcinarene (**reso**) and pyrogallarene (**pyro**) capsules with cationic guests such as Cs⁺, tetramethyl ammonium (TMA⁺) and tetraethyl ammonium (TEA⁺) was investigated (Figure 55).

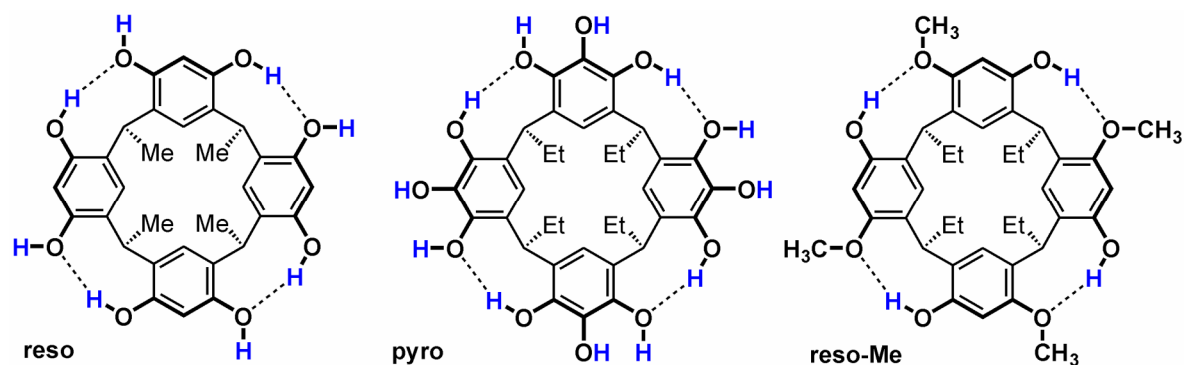


Figure 55. Structures of resorcin[4]arene (**reso**), pyrogall[4]arene (**pyro**) and tetramethylated resorcin[4]arene (**reso-Me**). Labile OH hydrogen atoms are marked in blue.

Initial experiments were done with the monomer/cation complexes. No exchange was observed because neither onium nor relay mechanism lead to a successful H/D exchange. In comparison to the monomers, significant differences occur in the dimer-cation complexes. Cs⁺ binds inside the capsules with an intact seam of hydrogen bonds between. Larger cations such as TMA⁺ or TEA⁺ lead to open capsules with partially disrupted seam and a PacMan-shaped structure is formed. This can be followed by H/D-exchange as only an intact seam of hydrogen bonds in between the two halves of the capsules enable a fast exchange of labile hydrogens through a concerned mechanism. This intact seam can be postulated for **reso** dimers with Cs⁺ while it is disrupted in case of TMA⁺ or TEA⁺ complexes, where more or less no H/D exchange is observed. The same conclusion can be drawn for the **pyro** dimers with one exception: The H/D-exchange even occurs in case of the TMA⁺ or TEA⁺ dimers. This observation can be rationalized in a way that the H/D exchange proceeds in “H-bond cells” between two **pyro**'s followed by a rearrangement of the PacMan-shaped structure.

[†] Winkler, H. D. F.; Dzyuba, E. V.; Sklorz, J. A. W.; Beyeh, N. K.; Rissanen, K.; Schalley, C. A. *Chemical Science* **2011**, *2*, 615 - 624. The original article is online available at <http://dx.doi.org/10.1039/C0SC00539H>.

5 CONCLUSION AND PERSPECTIVES

The results obtained during this thesis allow to draw the following conclusions:

(1) Mono- and multivalent (pseudo)rotaxanes based on the TLM/diamide binding motif:

Initially, the research related to the multivalency and cooperativity started with this binding motif. Both mono- and multivalent supramolecules and their building blocks were synthesized and their binding behavior was studied.

(a) It was possible to obtain a clear picture of the binding properties of differently substituted monovalent diamide guest molecules to a Hunter/Vögtle-type tetralactam macrocycle (TLM).^[1] Here, the binding constants K_a and the binding energies ΔG depend strongly on the substitution at the diamide binding motif. On the one hand, substituents such as simple alkyl chains result in K_a values of 2,000 - 4,000 M^{-1} . On the other hand, displacement of an alkyl chain against a phenyl group substituted at the 4-position of the phenyl ring results in a decrease of the K_a to values that are approximately one order of magnitude lower. The K_a values depend on the substitution at the 4-position of the phenyl ring. While electron-donating groups increase the binding constants K_a up to 700 M^{-1} , electron-withdrawing groups decrease them to $< 100 M^{-1}$.

(b) This study makes sense for several reasons. First of all, the theoretical data that were available for such systems^[2] are nicely confirmed here. In addition, this study has an influence on the research of templates for rotaxane synthesis and focus on the secondary effects that occur in this case. For example, ether linkage between the axle and the stopper is preferable in comparison to ester or amide coupling. This study collects two different methods applied to such pseudorotaxanes: NMR and ITC. Both lead to the thermodynamic values such as binding constants K_a (and binding energies ΔG). Especially the use of ITC is unique because it was possible to apply this technique in our group for the first time ever. Besides the Wiseman's value c (explained in chapter 3.5) is less suitable for some of the ITC data presented here, the correlation between NMR titrations and ITC nicely shows that a good evaluation of the binding behavior of supramolecules is possible even at not perfect c values if additional methods such as NMR titration are used.

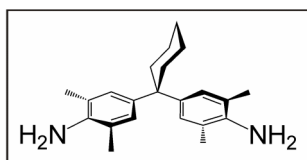
(c) The work of Schalley *et al.* to implement the TLM/diamide binding motif into multivalent host / guest architectures by using the "toolbox" method was continued.^[3] On the

one hand, multivalent metal complexes of phenanthroline- and terpyridine-decorated TLM's were obtained through coordination chemistry of Cu^I , $\text{Ru}^{II}\text{Cl}_2$ and Fe^{II} .^[4] On the other hand, numerous synthesis experiments and binding studies were performed with multivalent hosts and guests covalently connected to a linker centerpiece. For example, the use of iodo-substituted TLM and diamide axle results in various di- and trivalent host and guest molecules after coupling to appropriate linker molecules through Sonogashira coupling.^[5] The number and geometry (e. g. 1,4-benzene linking vs. 1,3) of the binding stations can be varied by changing these linker moieties and such studies would have an impact on the evaluation of the multivalent effects in artificial supramolecules. It was further tried to obtain divalent host molecules with 2,2'-bipyridine cores that might be able to form hexavalent hosts using coordination chemistry of metals such as Ru^{II} and Fe^{II} . One of such host molecules was isolated and fully characterized. In addition, a system consisting of two divalent hosts, one with a rigid linker between the two TLM's and one with a flexible one, and a flexible divalent guest molecule bearing terminal ethynyl groups was designed and synthesized.

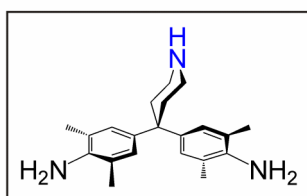
(d) In most of these cases, binding studies (normally using ^1H NMR and ITC) were not successful so far for several reasons. The most severe one is the bad solubility of such systems in non-competitive solvents such as CD_2Cl_2 or CDCl_3 . This is in particular important for the hosts bearing two or more TLMs. Reversible studies where the host-guest complex is formed first (which is often soluble) and then for example dilution experiments that are applied for the determination of the thermodynamic values were also not feasible for a second reason. If following the signals for the protons of the diamide station during e. g. ^1H NMR dilution experiments, strong signal splitting occurs as this station exists as a mixture of *cis/trans* isomers. The same applies to ^1H NMR titration experiment as shown for monovalent diamide guests, but no such analysis was performed for solubility reasons as described above. While the signals for the TLM's protons were examined in case of the monovalent study of diamide guest molecules as described above, the situation here is much more complicated as more signals are visible. To overcome these problems, the use of ITC is required as it would lead to the thermodynamics directly from the heat measured during the binding event, but also no ITC could be performed here for solubility reasons as mentioned above.

(e) The bad solubility of the resulting multivalent hosts (and sometimes guests) has also an influence on their synthesis. For example, problems often occurred in the work-up step using column chromatography or during synthesis as intermediates precipitated out of the reaction mixture. To sort out the solubility problems different strategies were followed. Most of the multivalent diamide guests were terminated with Boc groups in order to solubilize

them in non-competitive solvents. This approach is proved to be successful and even trivalent guest molecules were soluble in e. g. CD_2Cl_2 . In comparison, it is difficult to solubilize the TLM and its corresponding multivalent analogues. Although *t*Bu and cyclohexyl groups were attached such building blocks still aggregate strongly in non-competitive



“normal” Hunter diamine



“modified” Hunter diamine

Figure 56. The Hunter amine moiety usually used and a Hunter moiety with a piperidine group suitable for further modification.

solvents. Tacking this into account, Hunter *et al.*^[6] described a method to displace the cyclohexyl group in the “normal” Hunter diamine moiety against a piperidine (Figure 56). Using alkylation or acylation reactions and attachment of (long) alkyl chains (or other substituents) would increase the solubility of the TLM in non-competitive solvents drastically as indicated by the first results obtained in this study.^[7]

(f) In order to obtain addition informations about the multivalency and cooperativity using mono- or multivalent TLM's the corresponding building blocks were modified with sulfur atoms that allow a deposition of supramolecules at gold surfaces or nanoparticles. By doing so, SMFS would lead to some binding strengths of TLM/dicarbonyl complexes. First experiments were performed and the data obtained therein are used in the theoretical calculations. Moreover, compounds for the preparation of multivalent gold nanoparticles were presented. However, such molecules are still under in-vestigation and to this point no conclusion can be drawn.

(g) Other binding stations that fit preferably into the cavity of a TLM were presented. It was shown that the diketopiperazine binding motif leads to good yields of the corresponding [2]rotaxanes using the “click” reaction for the stoppering.^[8] This motif was further investigated by X-ray and ^1H NMR. It can be quite interesting to interlock the architectures of multivalent supramolecules bearing the diketopiperazine motif mechanically by means of “click chemistry”. For this, it is required to use an azide stopper with a quite rigid (flat aromatic) spacer between the stopper and the azide or rather the resulting triazole moiety. With the flexibility, signal splitting and overlap of signals as observed in [2]rotaxanes described in chapter 4.4 can occur and a binding study using e. g. ^1H NMR (titration) can be complexed. On the other hand, the use of squaraine dyes as binding motif gives rise to other methods for the study of the thermodynamics of the resulting complexes, e. g. UV-Vis or fluorescence titration as this station has completely different fluorescence pro-perties in its complexed state compared to the uncomplexed one. It should be possible to insert both the diketopiperazine and the

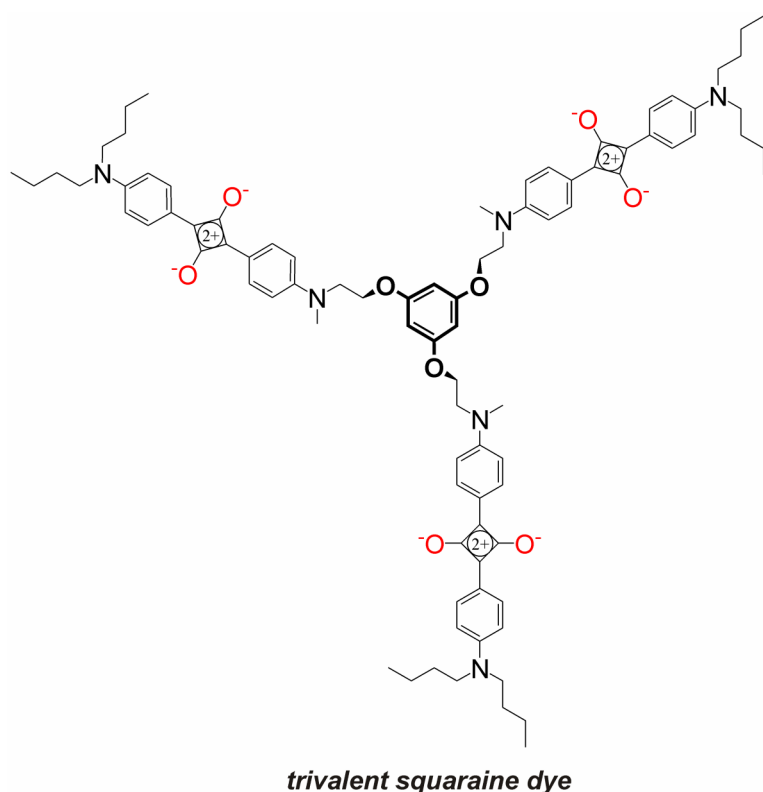


Figure 57. Structure of a molecule bearing three squaraine moieties.^[9]

squaraine into multivalent guests. While this was done for the diketopiperazine during this thesis as shown for the divalent guest suitable for binding to the divalent host bearing a 2,2'-bipyridine core (see chapter 4.3), an exciting compound was reported in the literature bearing three squaraine moieties (Figure 112).^[9] In addition to the use of squaraine dyes as axles of [2]rotaxanes and as markers described in chapter 3.4, this molecule can be used for binding studies to the trivalent host molecule^[3a] shown at the beginning of chapter 4.3.

(h) As shown in chapter 4.2^[4], the use of metal coordination is a good choice as metals and ligand-decorated hosts and/or guests form the desired supramolecules exclusively and more or less quantitatively (if the metal binding is reversible and “error correction” is possible, see chapters 3.1 and 3.2). Classical self-assembly^[10] (and probably also self-sorting) in combination with multivalency helps to obtain even more complex structures. For example, literature-known (2,2'-bipyridine) $M^{II}(\text{OTf})_2$ ($M = \text{Pd}^{II}, \text{Pt}^{II}$)^[11] can be decorated with either the phenanthroline- or bisquinone-substituted TLM (Figure 58) in order to introduce a binding site for guests such as dicarbonyl compounds. Appropriate ligands together with these novel metal corners would lead to metallo-supramolecular polygons similar to the ones described above and add more insights into multivalent binding. One example of this approach is shown in Figure 58. In the first step, the ligand-substituted wheel can coordinate to a metal center, preferably $\text{Pd}^{II}(\text{OTf})_2$ or $\text{Pt}^{II}(\text{OTf})_2$. Subsequent adding of 4,4'-bipyridine (or its derivatives) would result in a self-assembled equilibrium between a square and a triangle. Such equilibria are mentioned in chapter 3.5 and often depend on the ligand and the used solvent system. Besides studying multivalency, it is interesting to observe the switching

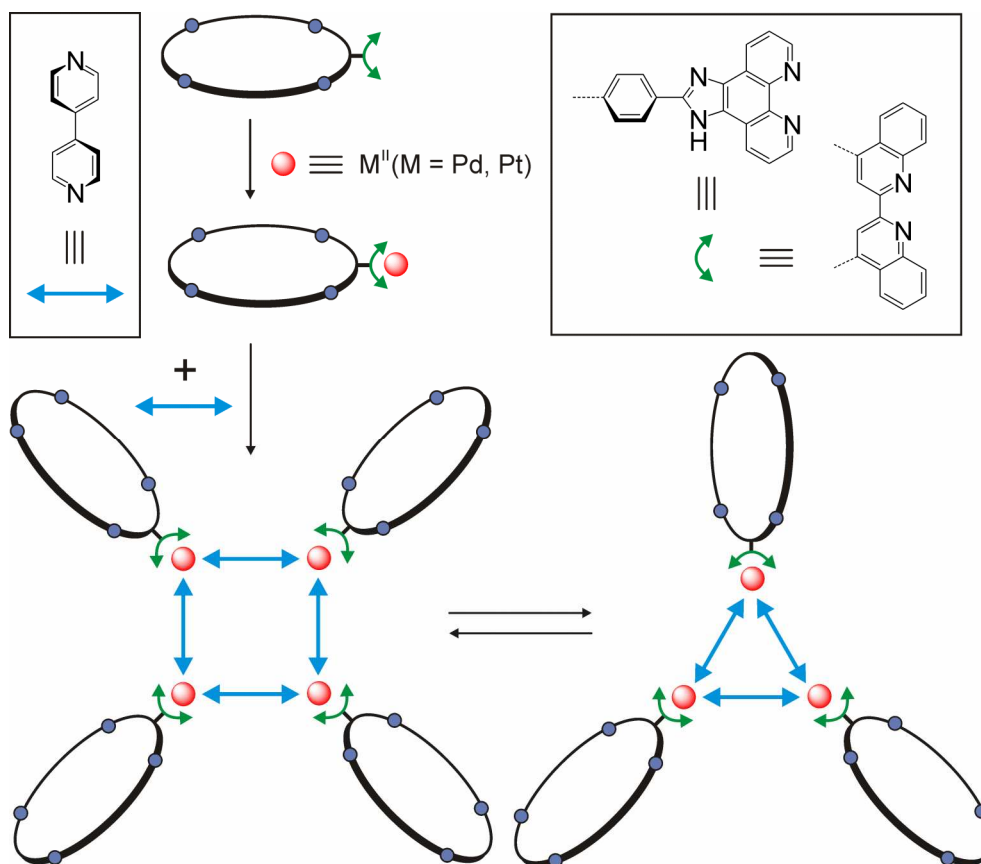


Figure 58. Schematic representation of the structures obtained from the self-assembly-driven reaction of a ligand-substituted TLM, a metal center and 4,4'-bipyridine.

of such reaction equilibrium to either reaction side. In addition, one can also imagine a three-component one-pot reaction (four-component with an appropriate guest for the TLM) to the desired self-assembled metallo-supramolecular polygons. This approach can be used for other ligands instead of 4,4'-bipyridine with different number of pyridine units and different geometries.

(i) Metallo-supramolecular [2]rotaxanes through “second sphere” described by Wisner *et al.*^[12] lead to an additional binding motif (Figure 59) useful for multivalent (pseudo)rotaxane formation. The Pd^{II}Cl₂ core can bind into the cavity of a TLM by forming Cl^{•••}H-N hydrogen bonds with binding constants K_a of approximately 10^3 M^{-1} , a value that is nearly equivalent to the K_a 's observed either for diamide, squaraine or the diketopiperazine binding motif. With the help of the

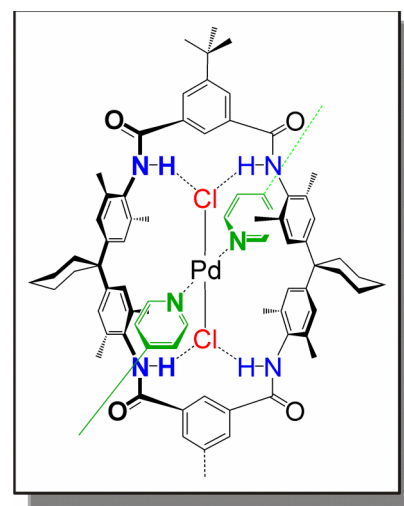


Figure 59. PdCl₂ as the binding station inside the cavity of a TLM. Coordination of suitable pyridine ligands would allow additional studies on multivalency.

“toolbox” approach e. g. using di- and trivalent host molecules with ethynyl phenyl connection between the TLMs described at the beginning of chapter 4.3, similar pyridine-terminated di- and trivalent ligands are reasonable to design and the study of their coordination to the “threaded” PdCl₂ is possible.

(2) Investigations on self-assembly and self-sorting processes of metallo-supramolecular polygons

(a) The studies of self-assembly processes using di- and tetradentate ligands based on pyridine and different metal centers containing either Pd^{II} or Pt^{II} were continued within this thesis. While it was shown that the self-assembly process is fast compared to the NMR time-scale if Pd^{II} metal center is used^[13], the metal center containing Pt^{II} leads to a slow self-assembly process that equilibrates even after 24 hours.^[14] Metallo-supramolecular polygons M₈L₄/M₄L₂ and M₆L₃/M₃L₃ (M = metal center, L = di- or tetradentate ligand) can be observed by ¹H NMR, ³¹P NMR and ESI MS during the self-assembly process. The larger polygons M₈L₄/M₆L₃ formed under kinetic control should assemble over time into the thermodynamically controlled smaller polygons M₄L₂/M₂L₂. However, it was found that this is the case if ligands with pyridine nitrogen *para* to the ethynyl substituent were used. Changing the position to *meta* result in an equilibrium between bigger polygons and smaller species after 24 hours. Consequently, subtle differences in ligand constitution set different products.

(b) The use of metal centers with different ancillary substituents (dppp vs. dppe) results in the observation of self-sorting processes if a tetradentate ligand with pyridine's nitrogen *para* to the ethynyl moiety is applied.^[15] The formation of hetero-bimetallic metallo-supramolecular polygons was yet again confirmed by ¹H NMR, ³¹P NMR and ESI MS. Self-Sorting is instituted here by a combination of the constitution of the ligand and the substituents at the metal centers. The ligand bears a bipyridine moiety that can complex metal ions by “chelating” and two pyridine moieties. If the metal center is substituted with dppp only the complexation to the bipyridine is observed in 1 : 1 ligand/metal center mixtures. In comparison, metal centers substituted with dppe can coordinate both bipyridine and pyridine. This leads to the described hetero-bimetallic polygons consisting of metal centers with distinct positions through self-sorting. No self-sorting was observed in case of the coeval use of either dppp- or dppe-substituted metal centers.

(c) The results obtained here, can be used to develop metallo-supramolecular systems bearing other metal species such as Cu^I or Ru^{II}. For example, it would be interesting

to observe the influence of more or less kinetically inert Ru^{II} towards the self-sorting behavior of the system. In addition, other ligands can be used in order to obtain more complex systems. An approach described by Brusilowskij might be result in novel supramolecular polygons bearing catalytically active metals.^[3a] In principle, numerous remarkable applications are possible as shown for other (non metallo-supramolecular) macrocycles, e.g. recognition of guest molecules or special fluorescence properties.

(3) H/D exchange on self-assembled hydrogen-bridged capsules

(a) During this thesis mass spectrometry was used for the characterization of supramolecular architectures in the gas phase as mentioned for the metallo-supramolecular polygons. It was shown that mass spectrometry is capable of yielding even further insights into the nature of non-covalent architectures as by simple mass measurement alone. However, the exchange behavior of the labile hydrogens of a supramolecule against deuterium leads to significant insights into its hydrogen-bonding patterns. Since a deuterium has one mass more than the hydrogen, this exchange can be followed by mass spectrometry. So far, this method was mostly applied to problems of biomolecules and until now and is quite novel to the research field of supramolecular chemistry as could be shown in the perspective article.^[16]

(b) The investigation of dimeric resorcin[4]arene and pyrogall[4]arene capsules with an encapsulated cation lead to a different exchange behavior depending on the size of the cation inside these complexes. Larger cations expand and interrupt the hydrogen bonding seam between the two halves of the capsule in the PacMan-shaped manner and therefore a slower H/D exchange is observed compared to capsules with smaller cations and intact seam. These results can be explained by a careful mechanistic considerations of the underlying H/D-exchange reactions.^[17] The presented work illustrates the power of H/D-X to yield indirect information on gas-phase structure as well as non-covalent reactivity. Moreover the question if the groththus mechanism of proton transport through water is concerted or not can be answered by taking these experiments into account as only a concerted H/D exchange through the whole seam inbetween the two halves of a capsule is possible.

(c) This method has in principle no limitations if investigating hydrogen-bridged natural or artificial supramolecules in the gas phase. For example, studies of anions encapsulated in resorcinarene or pyrogallarene dimers as described above would nicely complete the study already performed with cationic species. On the other hand, mechanistical

problems of biochemistry and biology that are not solved so far might act as the playground for the H/D-exchange experiments.

-
- [1] Dzyuba, E. V.; Kaufmann, L.; Malberg, F.; Löw, N. L.; Groschke, M.; Brusilowskij, B.; Huuskonen, J.; Rissanen, K.; Kirchner, B.; Schalley, C. A., *submitted*.
 - [2] Kirchner, B.; Spickermann, C.; Reckien, W.; Schalley, C. A. *J. Am. Chem. Soc.* **2010**, *132*, 484.
 - [3] (a) Baytekin, B.; Zhu, S. S.; Brusilowskij, B.; Illigen, J.; Ranta, J.; Huuskonen, J.; Rissanen, K.; Kaufmann, L.; Schalley, C. A. *Chem.-Eur. J.* **2008**, *14*, 10012. (b) Baytekin, B. *An easily accessible toolbox of functionalized macrocycles and rotaxanes and a (tandem) ESI-FTICR mass spectrometric study on Fréchet-type dendrimers with ammonium cores and hierarchical self-assembly of metallo-supramolecular nanospheres*, PhD thesis, Freie Universität Berlin, **2008**. (c) Brusilowskij, B. *Studien zur Entschlüsselung von Komplexität in supramolekularen Architekturen*, PhD thesis, Freie Universität Berlin, **2010**.
 - [4] Dzyuba, E. V.; Baytekin, B.; Sattler, D.; Schalley, C. A. *Eur. J. Org. Chem.* **2011**, ASAP.
 - [5] Löw, N. L.; Dzyuba, E. V.; Brusilowskij, B.; Kaufmann, L.; Franzmann, L.; Maison, W.; Brandt, E.; Aicher, D.; Wiehe, A.; Schalley, C. A., *submitted*.
 - [6] Adams, H.; Hunter, C. A.; Lawson, K. R.; Perkins, J.; Spey, S. E.; Urch, C. J.; Sanderson, J. M. *Chem. Eur. J.* **2001**, *7*, 4863.
 - [7] Tatzke, M. *Synthese substituierter Tetralactam-Amidrotaxane*, Master thesis, Freie Universität Berlin, **2011**.
 - [8] Dzyuba, E. V.; Kaufmann, L.; Löw, N. L.; Meyer, A. K.; Winkler, H. D. F.; Rissanen, K.; Schalley, C. A. *Org. Lett.* **2011**, *13*, 4838.
 - [9] Chithra, P.; Varghese, R.; Divya, K. P.; Ajayaghosh, A. *Chem.-Asian J.* **2008**, *3*, 1365.
 - [10] The term "classical self-assembly" means herein the use of ligand and metal (centers or corner) to obtain 2D- and 3D-metallo-supramolecular polygons (see chapter 3.2).
 - [11] Wehman, P.; Dol, G. C.; Moorman, E. R.; Kamer, P. C. J.; Fraanje, J.; Goubitz, K.; van Leeuwen, P. W. N. M. *Organometallics* **1994**, *13*, 4856.
 - [12] (a) Blight, B. A.; Van Noortwyk, K. A.; Wisner, J. A.; Jennigs, M. C. *Angew. Chem. Int. Ed.* **2005**, *44*, 1499. (b) Blight, B. A.; Wisner, J. A.; Jennigs, M. C. *Chem. Commun.* **2006**, 4593. (c) Blight, B. A.; Wei, X.; Wisner, J. A.; Jennigs, M. C. *Inorg. Chem.* **2007**, *46*, 8445. (d) Blight, B. A.; Wisner, J. A.; Jennigs, M. C. *Inorg. Chem.* **2009**, *48*, 1920.
 - [13] Brusilowskij, B.; Schalley, C. A. *Eur. J. Org. Chem.* **2011**, 469.
 - [14] Brusilowskij, B.; Dzyuba, E. V.; Troff, R. W.; Schalley, C. A. *Dalton Trans.* **2011**, *40*, 12089.
 - [15] Brusilowskij, B.; Dzyuba, E. V.; Troff, R. W.; Schalley, C. A. *Chem. Commun.* **2011**, *47*, 1830.
 - [16] Winkler, H. D. F.; Dzyuba, E. V.; Schalley, C. A. *New J. Chem.* **2011**, *35*, 529.
 - [17] Winkler, H. D. F.; Dzyuba, E. V.; Sklorz, J. A. W.; Beyeh, N. K.; Rissanen, K.; Schalley, C. A. *Chem. Sci.* **2011**, *2*, 615.

6 ACKNOWLEDGMENTS

I am deeply indebted to many people who helped me in various forms in the last years during the work on this thesis. This really was a tough one!

This work could not have been done without the continuous advice and support of my supervisor Prof. Dr. Cristoph Schalley, who guided me through the research with a lot of patience, understanding and encouragement. His insight into organic and supramolecular chemistry has set me on the right track and helped me avoid a lot of obstacles and pitfalls that appeared in the course of the work. For all of this I express my deepest gratitude. I would like to acknowledge Prof. Stefan Hecht, PhD for being my second supervisor, and Prof. Dr. Werner Abraham and Prof. Dr. Jürgen Liebscher for the continuous support at the Humboldt-Universität zu Berlin during my studies of chemistry.

I would like to acknowledge the kind help of my group mates and external cooperation partners ...

...Dr. Bilge Baytekin, Nora Löw, Dr. Boris Brusilowskij, Dr. Wei Jiang, Dr. Sasha Shuxia Zhu, Dr. Thorsten Felder, Karol Nowosinski, Igor Linder, Qi Wang, Zhenhui Qi, Dominik Sattler and Dominik Weimann for numerous collaborations on different synthetical projects related to multivalency research;

...the surface team Johannes Poppenberg, Sebastian Richter and Christoph Traulsen for exchange of chemicals and inspiring discussions on the project related to the surface-deposition of supramolecules, and Maria Tatzke for helping with the synthesis of some of these beasts;

...Lena Kaufmann for a weekend of NMR (titrations), and Annika Meyer and Dr. Henrik Winkler for performing additional experiments on the “click click boom” rotaxanes;

...Dr. Boris Brusilowskij and Ralf Troff for the support in the investigation of self-assembled and self-sorted metallo-supramolecular polygons;

...Dr. Henrik Winkler, Dr. Kodiah Beyeh and Julian Sklorz for helping with the research related to H/D-exchange experiments and in addition Prof. Dr. Kari Rissanen for wonderful X-ray structures;

Acknowledgments

...Prof. Dr. Barbara Kirchner and Friedrich Malberg for DFT calculations of monovalent pseudorotaxanes;

... Prof. Dr. Jürgen Rabe and Manuel Gensler for collaboration on Single Molecule Force Spectroscopy;

...Fabian Klautzsch for numerous ESI MS spectra and help with our “favorite” ITC;

...Sebastian Richter for numerous overnight NMR measurements;

...the Reißig group (Dr. Christian Eidamshaus, Daniel Trawny and Christoph Bentz) and Czekelius group (Roman Rüttinger) for lending me chemicals and sharing measurement time at the 400 MHz NMR with me;

...Nora Löw, Gülsah Ayvalik, Meryem Sezgin, Özlem Dikmen, Piker Kayikci, Luisa Loisky, Sissy Lorenz, Julian Sklorz, Lee Garrett, Matthias Groschke, Matthias Quandt and Nico Rind for helping me with compound synthesis;

...the NMR and MS department, especially Dr. Andreas Schäfer, Dr. Andreas Springer and their co-workers, for numerous NMR and MS measurements;

...Dr. Christian Ortmann and Michael Hau from the TAM Instruments (Waters GmbH) for help with the ITC experiments;

...Andrea Schulz and the people from “Materialverwaltung” for supplying me with chemicals and other useful things.

...Dr. Henrik Winkler for the correction work on this thesis.

Finally, I express my affectionate gratitude to my parents Ekaterina and Vitali Dzyuba, and to my wife Nicole Dzyuba and my daughter Anna Jelena Dzyuba, for their love and patience that enabled me go through this experience.

This work was funded by SFB 765 “multivalency”. I’m deeply indebted to the Studienstiftung des deutschen Volkes e. V. for financial support during my whole research time at the FU Berlin.

7 APPENDIX

7.1. Curriculum Vitae

Der Lebenslauf ist in der Online-Version aus Gründen des Datenschutzes nicht enthalten.

8.1. List of Publications

A. Publications:

- (1.) Dzyuba, E. V.; Kaufmann, L.; Löw, N. L.; Meyer, A. K.; Winkler, H. D. F.; Rissanen, K.; Schalley, C. A. *Organic Letters* **2011**, *13*, 4838 - 4841.

CH...O Hydrogen Bonds in "Clicked" Diketopiperazine-Based Amide Rotaxanes

- (2.) Brusilowskij, B.; Dzyuba, E. V.; Troff, R. W.; Schalley, C. A., *Dalton Transactions* **2011**, *40*, 12089 - 12096.

Effects of subtle differences in ligand constitution and conformation in metallo-supramolecular self-assembled polygons

- (3.) Brusilowskij, B.; Dzyuba, E. V.; Troff, R. W.; Schalley, C. A. *Chemical Communications* **2011**, *47*, 1830 - 1832.

Thermodynamically controlled self-sorting of heterobimetallic metallo-supramolecular macrocycles: What a difference a methylene group makes!

- (4.) Winkler, H. D. F.; Dzyuba, E. V.; Schalley, C. A. *New Journal of Chemistry* **2011**, *35*, 529 - 541.

Gas-phase H/D-exchange experiments in supramolecular chemistry

- (5.) Winkler, H. D. F.; Dzyuba, E. V.; Sklorz, J. A. W.; Beyeh, N. K.; Rissanen, K.; Schalley, C. A. *Chemical Science* **2011**, *2*, 615 - 624.

A one-dimensional analogue to the Grotthuss mechanism of proton transport through water: Gas-phase H/D-exchange reactions on resorcinarene and pyrogallarene capsules

B. Poster presentations:

- (1.) Dzyuba, E. V.; Rind, N.; Schalley, C. A.
JCF Frühjahrssymposium, Essen/GE, 11.-14. Nov **2008**.
Multivalent Oligomacrocyclic Hosts as Key-Compounds for Multiply Interlocked Architectures
- (2.) Brusilowskij, B.; Dzyuba, E. V.; Troff, R. W.; Schalley, C. A.
ISMSC 2009, Maastricht/NL, 21.-25. Jun **2009**.
Proximity Effect vs. Unspecific Dissociation: Studies of Discrete Metallo-Supramolecular Assemblies in the Gas Phase
- (3., 4.) Dzyuba, E. V.; Schalley, C. A.
Doktorandenfahrt SFB 765 "Multivalenz", Rheinsberg/GE, 07.-09. Jul **2009**;
1st International Symposium Research Center (SFB) 765, Berlin/GE, 15. Okt **2010**.
Multivalent Oligomacrocyclic Hosts as Key-Compounds for Multiply Interlocked Architectures
- (5., 6.) Dzyuba, E. V.; Kaufmann, L.; Sattler, D.; Richter, S.; Poppenberg, J.; Löw, N. L.; Sklorz, J. A. W.; Schalley, C. A.
Tag der Chemie 2010, Berlin/GE, 17. Jun **2010**;
CSI Meeting, Berlin/GE, 11. Nov **2011**.
Synthesis of [2]Rotaxanes under Click-Chemistry Conditions and Their Possible Application as Anion Sensors
- (7.) Gensler, M.; Dzyuba, E. V.; Schalley, C. A.; Rabe, J. P.
9th International Symposium on Scanning Probe Microscopy & Optical Tweezers in Life Sciences, Berlin/GE, 07. Okt **2010**.
Analysis of Host-Guest Interactions Using Single Molecule Force Spectroscopy
- (8.) Dzyuba, E. V.; Winkler, H. D. F.; Brusilowskij, B.; Troff, R. W.; Schalley, C. A.
ISMSC 2011, Brighton/UK, 03.-07. Jul **2010**.
Behavior of Supramolecules in the Gas Phase: From H/D Exchange to IRMPD Fragmentation Reactions

C. Oral presentations

(1-.5.) Doktorandenforum Natur + Wissenschaft der Studienstiftung des deutschen Volkes, Köln/GE, 07.-10. Dez **2008**;

Doktorandenforum Natur + Wissenschaft der Studienstiftung des deutschen Volkes, Berlin/GE, 02.-05. Apr **2009**;

G4 Meeting (Schalley / Lützen / Albrecht), Bonn/GE, 04.-06. Nov **2009**;

Doktorandenforum Natur + Wissenschaft der Studienstiftung des deutschen Volkes, Düsseldorf/GE, 22.-25. Apr **2010**;

G4 Meeting (Schalley / Lützen / Albrecht), Burg Bischofstein/GE, 21.-24. Sep **2010**.

Multivalency as Ordering Principle in the Self-Assembly of Supramolecular Architectures

(6.) TAM Usermeeting 2009, ICT Pfinztal, Karlsruhe/GE, 02. Jul **2009**.

Multivalency in Supramolecular Chemistry: Binding studies using Isothermal Titration Calorimetry

(7.) SFB 765-Ringvorlesung, Berlin/GE, 11. Feb **2011**.

ITC - Theory, Trends & Applications

(8.) 1. Berliner Chemie Symposium, Berlin/GE, 07. Apr **2011**.

Pd- and Ru-catalyzed Synthesis of Multivalent Molecules: A Toolbox for Supramolecular Assemblies